

**FINAL REPORT**  
**PRODUCTION OF SSM/I DATA SETS**

**By: Frank J. Wentz**

**Prepared for:**  
**National Aeronautics and Space Administration**  
**Marshall Space Flight Center**  
**Huntsville, Alabama**  
**Under Contract NAS8-38075**

**Prepared by:**

**Remote Sensing Systems**

**1101 COLLEGE AVE., SUITE 220, SANTA ROSA, CA 95404**

**(707) 545-2904**

## ABSTRACT

This Final Report is a summary of the work that was performed under Contract NAS8-38075 between NASA Marshall Space Flight Center and Remote Sensing Systems from September 1989 to September 1992. The primary accomplishment was the delivery of SSM/I data tapes containing sensor and geophysical products. In all, 515 tapes (80 gigabytes) were delivered. These tapes contained the F08 SSM/I data for the period from July 1988 through December 1991 and the F10 SSM/I data for the period from December 1990 through December 1991. For the F08 SSM/I, a data inventory was compiled and an engineering assessment was done. Ephemeris tables for the F08 and F10 spacecrafts were computed. Scientific studies on the oceanic wind vector and water vapor field were published, and color atlases of monthly ocean products were produced. This investigation was part of NASA's WETNET program.

## TABLE OF CONTENTS

1. Introduction .....	1
2. Delivery of SSM/I Data Tapes .....	1
3. Inventory of the F08 Data and Erroneous Data Periods .....	1
4. Engineering Assessment of SSM/I Operation .....	2
5. Geolocation Processing and Ephemeris Tables .....	4
6. Evaluation of NOAA's Level 1B SSM/I Product .....	5
7. Analysis of SSM/I Wind Speed and Wind Direction Signal .....	5
8. Analysis of SSM/I Water Vapor Product .....	6
9. Atlas of Monthly Ocean Products .....	6
10. Geophysical Software .....	6
11. Participation in WETNET, HDAAWG, and SSM/I Pathfinder .....	8
12. Documentation .....	9
Appendix A. User's Manual SSM/I Antenna Temperature Tapes .....	A1
Appendix B. Report Documentation Page: NASA Form 1626 .....	B1

## 1. INTRODUCTION

This Final Report provides a summary of the work that was performed under Contract NAS8-38075 between NASA and Remote Sensing Systems (RSS). The period of performance for this contract was September 1989 to September 1992. A detailed description of the investigation can be found in a series of reports and scientific papers that were delivered during the course of the contract. These documents are listed below on page 9 and are cross-referenced throughout this summary. The principal document (Document 1) is included herein as Appendix A.

The main thrust of this effort was the delivery of quality controlled SSM/I data products, both Level-1 sensor data and Level-2 geophysical products. This required an extensive data processing effort in conjunction with a thorough engineering assessment of the SSM/I in-orbit operation. The production of accurate geophysical products required scientific investigations of the oceanic wind field and columnar water vapor. One particularly interesting finding was that the microwave emission from the ocean depends on the wind direction relative to the observation direction. With respect to water vapor, comparisons with radiosondes and ECMWF fields indicated that the SSM/I water vapor is an extremely accurate parameter that may be of considerable use to climate change studies.

During this investigation, we have had the good fortune to interact with a large number of colleagues in associated disciplines via the WETNET workshops, E-mail, and the many phone calls about SSM/I. We consider this interaction to be an important element of this investigation.

## 2. DELIVERY OF SSM/I DATA TAPES

During the course of this contract, RSS delivered 336 F08 SSM/I antenna temperature ( $T_A$ ) tapes and 94 F10  $T_A$  tapes to Marshall Space Flight Center (MSFC). A duplicate set of  $T_A$  tapes was also delivered to the National Snow and Ice Data Center (NSIDC). The F08 tapes covered the period from July 1988 through December 1991, and the F10 tapes covered the period from December 1990 through December 1991. Approximately 6000 DEF tapes from NOAA/NESDIS were ingested in order to produce the 430  $T_A$  tapes.

In addition to the  $T_A$  tapes, RSS delivered 84 F08 SSM/I geophysical tapes to MSFC. A duplicate set of 84 geophysical tapes was also delivered to the NASA Ocean Data System (NODS) at the Jet Propulsion Laboratory (JPL). These tapes covered the period from July 1988 through December 1991. Software for reading the tapes was also provided along with comprehensive User Manuals (Documents 1 and 2).

## 3. INVENTORY OF THE F08 DATA AND ERRONEOUS DATA PERIODS

We compiled and delivered an inventory of all F08 SSM/I data (Document 4). This inventory is a collection of figures that show time periods of missing data and erroneous data. There is one figure for each semimonthly period from July 1987 through December 1991. The figures show the differences between a 90-second average of the individual  $T_A$ 's minus an average  $1^\circ$  latitude by  $1^\circ$  longitude  $T_A$  map for the previous semimonthly period. There are 16 horizontal lines in each figure, and each line corresponds to a Greenwich day. The 90-second  $T_A$  differences are shown as points along the horizontal lines.

Under normal conditions, the points lie near the horizontal lines, with an occasional small outlier. Storms, coast lines, and varying sea ice can cause larger differences, but only for a short period of time. The periods of erroneous data are shown as clusters of widely varying points. In addition to revealing periods of erroneous data, the figures provide a complete inventory of the SSM/I data set. They can be used to find periods of missing data. These data gaps are shown by the absence of plotted points.

We visually inspected all of the figures in the F08 inventory and identified the begin and end times for the periods of erroneous data. A small ASCII data file called BADLOC containing these times was delivered on a 3.5" inch diskette. The time windows for erroneous data are somewhat larger than the clusters of data outliers shown in the figures in order to ensure that all the erroneous data are excluded. The problem of erroneous data was particularly bad during the second half of 1988. Then, in January 1989 and thereafter the frequency of erroneous data greatly reduced. After 1988, there are, on the average, about one or two erroneous data periods each month.

There appears to be two types of erroneous data. First, the observation time is sometimes in error, and as a result the geolocation routine mislocates the observations. In this case the  $T_A$  values are correct but the latitudes and longitudes are in error. The second type of erroneous data is the occurrence of corrupt  $T_A$  values that are obviously incorrect. The cause of the corrupt  $T_A$ 's is still not known. Both types of erroneous data usually occur over a complete DEF data file and hence are detected using the above procedure. When doing statistical analyses of the SSM/I data, it is very important to exclude these time periods of erroneous data. Otherwise, the statistics can be significantly distorted.

#### 4. ENGINEERING ASSESSMENT OF SSM/I OPERATION

The in-orbit operation of the F08 SSM/I from July 1987 through December 1991 was analyzed in detail. Time series of the following radiometer parameters were produced:

1. Thermistor readings of the warm load and radiometer receivers.
2. The rms variation of the SSM/I cold-space observations
3. The rms variation of the SSM/I warm-load observations
4. The radiometer noise temperature
5. The radiometer gain

The time series are shown by a collection of color-coded figures, with different colors showing the 7 SSM/I channels. In addition to these figures, logs were maintained of the automatic gain control settings and the number of anomalous  $T_A$  observations.

The time series show the stability (and in some cases the instability) of the SSM/I channels. For example, the figure of thermistor readings shows a very large heating cycle with a peak between 30K and 60K above normal, depending on component, every winter due to increased solar illumination on the SSM/I.

During the first heating cycle in December 1987, the 85V temperature resolution begins to degrade. After the heating cycle is over, the 85V channel continues to degrade. After April 1988, the noise in the 85V channel exceeds 20 K. Between May 1988 and January 1989, there are time windows in which the noise subsides. The possibility exists that useful information can be obtained from the 85V channel during these time windows. After January 1989, the noise becomes very large, and the channel is not usable.

The 85H channel shows a slight degradation in the temperature resolution during the first heating cycle, but then recovers. The second heating cycle in December 1988 seems to cause a small but permanent degradation in the 85H channel. Then, the third heating cycle in December 1989 seriously damages the 85H channel, and the noise increases to between 5 and 10 K. Curiously, during the fourth heating cycle in December 1990, the 85H channel temporarily recovers, but after January 1991 the noise becomes very large, exceeding 20 K.

The other channels also experience a small increase in noise during the heating cycles. Fortunately, the lower frequency channels are not permanently affected by the heating, and noise level returns to normal after the heating cycle is over. We also verified that the radiometer noise computed from the cold and warm counts is in good agreement with that computed from the radiometer noise temperature and bandwidth.

In addition to analyzing the time series for radiometer noise, we also investigated the variation of the radiometer gain with time. Under normal operating conditions, the variation in the radiometer gain  $G_r$  is primarily due to changes in the temperature of the receiver. The large heating cycle experienced by the F08 SSM/I provided a means to investigate the variation of  $G_r$  with temperature. The gain of the 19V and 19H channels showed little dependence on temperature, while the gain of the 22V channel increased with increasing temperature. In contrast, the gain of the 37V and 37H channels decreased with increasing temperature. The 85V and 85H gains also decreased with temperature, and then tended to zero during the degradation phase.

The dependence of  $G_r$  on temperature is one of the primary reasons for doing an external calibration each scan. The temperature variation experienced during a single orbit will produce changes in  $G_r$ . Unless frequent calibrations are performed, the changing gain will introduce errors in the computation of the antenna temperatures. We verified that the derivative of  $G_r$  with respect to temperature found during the winter heating cycle (i.e., long-time scale) is the same as that obtained from an analysis of the gain versus temperature variation experienced within individual orbits (short-time scale).

We monitored changes in the automatic gain control (AGC) setting during the 1987-1991 period. The purpose of the AGC is to compensate for the  $G_r$  variation so that the counts stay within the range of the digital converter. There are 16 AGC settings, and each setting adds 0.5 dB attenuation. The AGC system seemed to function properly.

As part of the engineering assessment, we also found a systematic error in the SSM/I  $T_A$ 's near one edge of the swath. The  $T_A$ 's show a roll-off of about 1 K near the scan edge. One explanation for this is that the feedhorn begins to partially see the cold-sky reflector near the end of the Earth-viewing scan. A correction table was produced in order to remove this systematic error.

The engineering assessment is further described in Document 1.

## 5. GEOLOCATION PROCESSING AND EPHEMERIS TABLES

While processing the 1988 SSM/I data, we found a number of problems with the spacecraft and Earth locations that were being computed at Fleet Numeric Oceanography Center (FNOC). The cell latitudes and longitudes on the DEF tapes produced by FNOC were sometimes in error due to the following problems:

1. There are some algorithm errors in the FNOC data processing software.
2. The satellite ephemeris is sometimes incorrect due to spacecraft tracking errors and orbit prediction errors. This problem is particularly severe during periods of increased solar activity.
3. The boresight nadir angle and the alignment of the SSM/I instrument relative to the spacecraft are slightly misspecified.

There have been a number of FNOC algorithm errors. Sometimes the wrong Julian day is assigned to the orbit. Occasionally, the time for the spacecraft location and the scan time are very different. The two times should be within 60 s of each other, but at the begin and end of an FNOC DEF file, the two times can be as much as 40,000 s apart. The spacecraft longitude is sometimes out-of-bounds. There were also other problems that have now been corrected at FNOC. For example, the ephemeris was not updated frequently enough, and the location of cell 128 was in error.

In response to these problems, we developed our own routine for computing the latitudes and longitudes rather than using the DEF values. The input to our geolocation routine is the satellite ephemeris for a  $\pm 7$  day period centered on the orbit being processed. The ephemeris is first subjected to quality control to remove any data that are clearly erroneous. Next the ephemeris is smoothed to remove the noise. The smoothed ephemeris is then used to compute the SSM/I cell latitudes and longitudes.

This procedure of computing latitude and longitude from a smoothed ephemeris was initiated with the January 1, 1989 F08 T<sub>A</sub> tape. Prior to 1989, the latitudes and longitudes on the T<sub>A</sub> tapes are the same as the values on the DEF tapes. Fortunately, an analysis of the ephemeris prior to 1989 does not show any large errors except for a brief period during the second half of February 1988. For these pre-1989 tapes, subroutine DECODE does the sensor alignment and the cell 128 correction while reading the tape.

Our geolocation routine is free of the algorithm errors listed above except for the Julian day error. As each orbit is processed, we perform a number of cross-checks to verify the Julian day. Usually these cross-checks detect the Julian day error, which can then be corrected. However, a few of the Julian day errors will go undetected, and these 'erroneous' orbits will be written to the T<sub>A</sub> tape. These erroneous orbits are later detected by the quality control routine discussed in Section 3 above.

The third geolocation problem listed above is the misalignment of the SSM/I sensor relative to the spacecraft and the misspecification of the boresight nadir angle. For F10, this problem is corrected by our geolocation routine, and the locations on the T<sub>A</sub> tapes are correct. For F08, part of the correction is done by our geolocation routine and part is done by DECODE, as is explained in Document 1.

An ephemeris table for the F08 spacecraft was produced. This table gives the value of six orbit parameters for every F08 orbit from July 1987 through December 1991. The six orbit parameters are the following:

1. orbit period (seconds)
2. local time of the ascending node (seconds)
3. inclination angle (degrees)
4. major semi-axis (km)
5. eccentricity
6. angle of perigee (degrees)

Figures were produced that show the variation of these six parameters with time. The period  $P$  and the major semi-axis  $a$  show a slow, steady decrease with time. For example, at the beginning of the F08 mission in July 1987 the values for  $P$  and  $a$  were 6118.5 s and 7229.3 km. Four years later, the values are 6111.0 s and 7223.3 km, respectively. The ascending node local time  $t_L$  steadily increases with time. For F08 the change is small, being about 70 s/year. The inclination angle  $\alpha$  is slowly decreasing with time at a rate of about  $-0.01^\circ/\text{year}$  for F08. The eccentricity  $e$  and angle of perigee  $T_0$  are periodic. The period is about 1800 orbits and the amplitude remains constant over time. Note that the period and the major semi-axis are redundant parameters in the sense that they are related by Kepler's third law of motion. The expression  $21.6106 P^{2/3}$  yields values for  $a$  that are within 0.2 km of the values in the orbit parameter table.

## 6. EVALUATION OF NOAA'S LEVEL 1B SSM/I PRODUCT

We obtained NOAA's new Level 1B SSM/I tape product. Unfortunately, there was very little documentation to support the Level 1B product. We compared the Level-1B SSM/I data with the data on the FNOC DEF tapes. The scan times and cell latitude and longitudes were different. Due to the lack of documentation, we were unable to resolve the differences. Also, the Level-1B product contained no information on the satellite location time, and the satellite location vectors were not defined in the documentation. For the Level-1B product, some type of averaging had been done to the hot load thermistor counts. Again, the documentation did not provide any information on how the averaging was done.

## 7. ANALYSIS OF SSM/I WIND SPEED AND WIND DIRECTION SIGNAL

We investigated the possibility of retrieving both wind speed and direction from SSM/I. The SSM/I observations were collocated with buoy reports from the National Data Buoy Center (NDBC). A physically-based algorithm was used to retrieve the wind speed. The rms difference between the SSM/I and buoy wind speed was 1.6 m/s for 3321 comparisons. We found that the SSM/I minus buoy wind speed difference is correlated with wind direction. This correlation is due to a wind direction signal in the brightness temperatures ( $T_B$ ). For moderate wind speeds, the v-pol upwind  $T_B$  is about 2 K higher than the downwind  $T_B$ . For h-pol observations, the  $T_B$  maximum occurs at crosswind rather than upwind and is approximately 3.5 K higher than the minimum at downwind. When this wind direction signal is removed, the rms difference between the SSM/I and buoy winds reduces to 1.3 m/s. The wind direction signal was used to make global, low-resolution maps of the monthly mean oceanic wind vector. Finally, we assessed the wind direction sensing capability of a prospective two-look satellite radiometer. Preliminary computer simulations indicate a direction accuracy of  $15^\circ$ . The results of this investigation have been published in IEEE Geoscience and Remote Sensing (Document 5).



## 8. ANALYSIS OF SSM/I WATER VAPOR PRODUCT

The SSM/I water vapors were evaluated by comparing them to radiosonde observations and to ECMWF fields. The rms difference between the SSM/I columnar water vapor and the radiosonde value is 3 mm for hourly comparisons and 4 mm for monthly comparisons. The SSM/I vapor fields agree with the ECMWF fields over most ocean areas, but there are significant differences in the dry air masses over the eastern tropical oceans, particularly in the southern hemisphere. Radiosonde reports in these areas indicate that the ECMWF vapor fields are too high, and the SSM/I values seem accurate. The results of this investigation have been published in JGR (Document 6).

## 9. ATLAS OF MONTHLY OCEAN PRODUCTS

We produced a 4.5 year data set of ocean products derived from the F08 SSM/I. The data set covers the period from July 1987 through December 1991. The products include the near-surface wind speed  $W$ , the columnar atmospheric water vapor  $V$ , and the columnar atmospheric liquid water  $L$  (combination of cloud and rain water). The ocean products have been averaged into monthly  $1^\circ$ -latitude by  $1^\circ$ -longitude bins. These monthly averages are put on a single 6250-bpi, 2400-ft tape, called the "Monthly Ocean Tape". This tape contains 53 files, which correspond to each month from July 1987 through December 1991, except that December 1987 is missing because the SSM/I was turned off. Note that in July 1987 and January 1988, the SSM/I was turned off part of the time. The operation period for July 1987 is from July 9 through July 31. The operation period for January 1988 is from January 13 through January 31. Also, starting on December 19, 1991, the Fleet Numerical Oceanography Center (FNOC) began limited processing of the F08 SSM/I data. Typically, only one orbit per day of F08 data is now being processed. The monthly ocean products are further described in Document 3.

We collaborated with other investigators to merge the monthly SSM/I ocean products with the monthly mean distributions of the GEOSAT sea surface height, the AVHRR sea surface temperature, and the ECMWF surface wind components. Atlases that show these products as global colored maps were produced for 1987, 1988, and 1989 (Documents 7, 8, and 9).

## 10. GEOPHYSICAL SOFTWARE

The software for computing geophysical parameters (wind speed, water vapor, and liquid water) from the SSM/I  $T_A$ 's was delivered. This software is a set of Fortran-callable routines. The software computes wind speed  $W$ , water vapor  $V$ , and liquid water  $L$  by solving the following three equations in three unknowns:

$$T_{B22v} = F_{22v}(W, V, L)$$

$$T_{B37v} = F_{37v}(W, V, L)$$

$$T_{B37h} = F_{37h}(W, V, L)$$

where  $T_{B22v}$ ,  $T_{B37v}$ , and  $T_{B37h}$  are the SSM/I brightness temperature measurements for the following three channels: 22-GHz v-pol, 37-GHz v-pol, and 37-GHz h-pol. The unknowns are wind speed  $W$  (m/s), columnar water vapor  $V$  (g/cm<sup>2</sup>), and columnar liquid water  $L$  (mg/cm<sup>2</sup>). The brightness temperature model functions for the three channels are denoted by  $F_{22v}$ ,  $F_{37v}$ , and  $F_{37h}$ . These  $T_B$  functions have the form

$$F(W, V, L) = T_{Bu} + \tau[ET_s + (1 - E)(1 + \omega W)(T_{Bd} + \tau T_{Bc})]$$

where the channel subscript is now implicit. The quantities  $T_{Bu}$  and  $T_{Bd}$  are the upwelling and downwelling brightness temperatures due solely to the atmospheric emission and absorption. The quantity  $T_{Bc}$  is the brightness temperature of cold space and equals 2.8 K at 37 GHz. The emissivity of the sea surface is denoted by  $E$ . The sea-surface temperature is denoted by  $T_s$  and is in units of Kelvin degrees. The term  $(1 + \omega W)$  accounts for a small increase in the reflected atmospheric radiation due to surface scattering (as opposed to simple reflection). The term  $\tau$  is the atmospheric transmission and is given below as a function of  $V$  and  $L$ .

We assume that there is no significant scattering of radiation by the atmosphere. At 22 and 37 GHz, scattering occurs only when there is appreciable rain or ice in the field of view. The upward and downward atmospheric brightness temperatures for a non-scattering atmosphere are given by

$$T_{Bu} = (1 - \tau)T_u$$

$$T_{Bd} = (1 - \tau)T_d$$

where  $T_u$  and  $T_d$  are the effective air temperatures. If the air temperature  $T_a$  were constant (i.e., a zero lapse rate), then  $T_u$  and  $T_d$  would exactly equal  $T_a$ . In reality the air temperature in the troposphere usually decreases with altitude, and  $T_u$  and  $T_d$  are weighted averages of the air temperature, where the weight is approximately equal to the absorption along the propagation path.

The total absorption along the SSM/I viewing path is equal to  $\ln(1/\tau)$  and is the sum of three components: oxygen, water vapor, and liquid water (i.e., both cloud and rain water). It is convenient to normalize the absorption in terms of a vertically integrated quantity rather than a viewing-path integrated quantity. In this way, the dependence on incidence angle  $\theta_i$  is removed. For incidence angles below  $60^\circ$ , the ratio of the viewing-path length through the troposphere to the height of the troposphere is simply  $\sec \theta_i$ . The total absorption is then given by

$$\ln(1/\tau) = (A_O + A_V + A_L) \sec \theta_i$$

where  $A_O$ ,  $A_V$ , and  $A_L$  are the vertically integrated, or columnar, absorption components due to oxygen, water vapor, and liquid water, respectively. Absorption  $A_V$  is proportional to  $V$  and  $A_L$  is proportional to  $L$ .

Document 5 gives values for  $E$ ,  $\omega$ ,  $T_u$ ,  $T_d$ ,  $A_O$ ,  $A_V$ , and  $A_L$ . Once these values are specified, the  $T_B$  model functions and their first derivatives with respect to  $W$ ,  $V$ , and  $L$  can be computed.

Having specified  $F(W,V,L)$ , the three  $T_B$  model function equations are simultaneously solved by Newton's method. The function  $F(W,V,L)$  is quasi-linear in terms of  $W$ ,  $V$ , and  $L$ , and the following approximation is used:

$$F(W,V,L) \approx F(W_o, V_o, L_o) + (\partial F/\partial W)(W - W_o) + (\partial F/\partial V)(V - V_o) + (\partial F/\partial L)(L - L_o)$$

The terms  $W_o$ ,  $V_o$ , and  $L_o$  are 'first-guess' values. Good choices are 8 m/s, 3 g/cm<sup>2</sup>, and 10 mg/cm<sup>2</sup>, respectively, which represent typical values over the ocean. The final solution is independent of the first guess values, but the number of iterations is minimized by starting with typical values. The derivatives  $\partial F/\partial W$ ,  $\partial F/\partial V$ , and  $\partial F/\partial L$  are found by analyti-

cally differentiating the  $T_B$  model functions evaluated at ( $W_o$ ,  $V_o$ ,  $L_o$ ). The above equation represents three linear equations in three unknowns:  $W$ ,  $V$ , and  $L$ . The system of linear equations is inverted to yield the unknowns.

A second iteration is then done for which the first guess values are replaced by the values coming from the first iteration. This procedure is repeated until the values for  $W$ ,  $V$ , and  $L$  converge. Typically, convergence is obtained after 3 to 5 iterations. If convergence is not obtained in 10 iterations, then the brightness temperatures are flagged as anomalous. For SSM/I, non-convergence occurs very rarely (less than 0.01% of the observations) and indicates either erroneous brightness temperatures or possibly heavy rain.

A full description of the exact algorithm is given in Document 5.

#### **11. PARTICIPATION IN WETNET, HDAAWG, AND SSM/I PATHFINDER**

As part of this contract, Frank J. Wentz actively participated in three NASA programs: WETNET, HDAAWG, and the SSM/I Pathfinder. He was the group leader for the WETNET vapor and clouds groups. Participation in these programs required the preparation of presentations and travel. The following trips were made:

1. A 3-day WETNET meeting at MSFC on 2/21/90 through 2/23/90
2. Annual WETNET meeting in Santa Barbara on 2/19/91 through 2/22/91
3. NOAA Level-1B meeting at GSFC on 2/24/91 through 2/26/91
4. WETNET training session at MSFC on 5/28/91 through 5/30/91
5. Annual WETNET meeting at Tallahassee on 4/20/92 through 4/23/92
6. HDAAWG meeting at MSFC on 6/2/92 through 6/4/92

## 12. DOCUMENTATION

We have delivered comprehensive documentation in support of this investigation. The following is a list of the reports and scientific papers produced under this contract. Many of the analyses and results of this investigation are contained in Document 1, which is included herein as Appendix A.

1. Wentz, F., *Revision 1. User's Manual SSM/I Antenna Temperature Tapes*, Remote Sensing Systems, 70 pp, 1991.
2. Wentz, F., *Revision 1. User's Manual SSM/I Geophysical Tapes*, Remote Sensing Systems, 24 pp, 1992.
3. Wentz, F., *User's Manual SSM/I Monthly Ocean Tape*, Remote Sensing Systems, 3 pp, 1992.
4. Wentz, F. J., *F08 Mislocated Orbits and Out-of-Bounds Data*, Remote Sensing Systems, 108pp, 1992.
5. Wentz, F. J., *Measurement of oceanic wind vector using satellite microwave radiometers*, *IEEE Trans. Geoscience and Remote Sensing*, September 1992.
6. Liu, W. T., W. Tang, and F. J. Wentz, *Precipitable water and surface humidity over global oceans from SSM/I and ECMWF*, *J. Geophysical Research* 97, 2251-2264, 1992.
7. Halpern, D., V. Zlotnicki, J. Newman, O. Brown, and F. Wentz, *An Atlas of Monthly Mean Distributions of GEOSAT Sea Surface Height, SSMI Surface Wind Speed, AVHRR/2 Sea Surface Temperature, and ECMWF Surface Wind Components During 1988*, JPL Publication 91-8, 110 pp, 1991.
8. Halpern, D., V. Zlotnicki, J. Newman, D. Dixon, O. Brown, and F. Wentz, *An Atlas of Monthly Mean Distributions of GEOSAT Sea Surface Height, SSMI Surface Wind Speed, AVHRR/2 Sea Surface Temperature, and ECMWF Surface Wind Components During 1987*, JPL Publication 92-3, 111 pp, 1992.
9. Halpern, D., W. Knauss, O. Brown, and F. Wentz, *An Atlas of Monthly Mean Distributions of SSMI Surface Wind Speed, ARGOS Buoy Drift, AVHRR/2 Sea Surface Temperature, and ECMWF Surface Wind Components During 1989*, JPL Publication 92-17, 112 pp, 1992.

**APPENDIX A**

**User's Manual**

**SSM/I Antenna Temperature Tapes**

**Revision 1**

## ACKNOWLEDGMENTS

The development of the SSM/I data processing system was supported by NASA's Earth Science and Applications Division under contract NAS8-38075. We give thanks to the Department of Defense for making the DMSP data available to the civilian research community. We are also grateful to J. Wilkerson at NOAA/NESDIS for supplying the SSM/I DEF tapes.

## TABLE OF CONTENTS

Section 1.	Introduction . . . . .	1
Section 2.	Sensor Description . . . . .	3
Section 3.	SSM/I DEF Tapes . . . . .	6
Section 4.	Computation of Antenna Temperatures . . . . .	7
Section 5.	Computation of Brightness Temperatures . . . . .	9
Section 6.	Computation of Orbit Parameters and Earth Locations . . . . .	15
Section 7.	Erroneous Data Periods . . . . .	22
Section 8.	Time Series of Radiometer Parameters . . . . .	25
Section 9.	Organization of Antenna Temperature Tapes . . . . .	34
Section 10.	Logical Data Record Format . . . . .	37
Section 11.	Description of Subroutine DECODE . . . . .	40
Section 12.	References . . . . .	50
Appendix A.	List of Erroneous Data Periods for F08 Satellite . . . . .	51
Appendix B.	Listing of Subroutine DECODE, Revision 1 . . . . .	57

## SECTION 1. INTRODUCTION

This document is the first revision of the Special Sensor Microwave/Imager (SSM/I) Antenna Temperature ( $T_A$ ) Tapes User's Manual. The original User's Manual for the SSM/I  $T_A$  tapes was issued on March 25, 1988. This first revision provides the User with more information on the product and implements several improvements and extensions. There are now three SSM/I's in operation. The first was launched on June 19, 1987, aboard the Defense Meteorological Satellite Program (DMSP) F08 satellite. The second was launched on December 1, 1990, on the DMSP F10 satellite. And, the third was launched on November 28, 1991, on the F11 satellite. The Air Force plans to maintain at least two SSM/I's in operation through the end of this decade. We plan to continue providing Users with  $T_A$  tapes for this series of satellites.

The SSM/I  $T_A$  tapes are a well-documented, user-friendly product that contains all the information coming from the SSM/I. Essentially, the tapes contain geolocated antenna temperatures along with the sensor calibration data. For each satellite, there are eight 6250-bpi  $T_A$  tapes per month. Software is provided to convert the antenna temperatures to brightness temperatures ( $T_B$ ). The integrity of the  $T_A$  tapes has been established by wide usage of this product for the last several years.

The Fortran subroutine DECODE provides the interface between the  $T_A$  tapes and the User. The input to DECODE is the string of bytes contained in a single tape block. DECODE organizes the data, converts the bytes to the proper engineering units, and stores the results in a common area accessible to the User. An ASCII file containing the DECODE source code is on the enclosed 3.5" diskette. The diskette also includes the file BADLOC, which is a list of time periods containing erroneous F08 data.

In addition to reading the  $T_A$  tapes, DECODE performs other functions such as a correction for F08 geolocation errors, the computation of incidence angle, and the computation of brightness temperatures. Some of the functions depend on which satellite is being processed. DECODE automatically determines the satellite number and then selects the appropriate procedure. There have been two minor changes in the  $T_A$  tape format (see Section 10). DECODE automatically adjusts to these format changes by looking at the scan time. We advise Users to use DECODE rather than writing their own ingest routine. If the User has some unusual application, we will gladly provide assistance in modifying DECODE to suit the application. However, the Revision-1 DECODE should be sufficient for nearly all applications.

There are several improvements and extensions of the Revision-1 DECODE. These include the following:

1. DECODE is now independent of the byte-ordering of the Fortran compiler. For example, Fortran compilers for many mini-computers use the convention that the most-significant byte in a word is stored first in memory. In contrast, Fortran compilers for PC's and Vax machines use the opposite convention that the least-significant byte is stored first. The original version of DECODE used equivalences to relate bytes to words, and hence it was dependent on the byte-ordering convention. (Users with PC's and Vax machines had to modified DECODE.) Revision-1 DECODE does not use equivalences. Rather, it directly computes the sensor data from the individual bytes and executes properly using either type of compiler.



2. Revision-1 DECODE is setup to process multiple satellites. DECODE automatically determines the satellite number and then selects the appropriate procedures for geolocation error correction, incidence angle computation, and  $T_A$  bias removal. The satellite number is stored in the common area /OUTDAT/ that is accessible to the User.

3. Revision-1 DECODE corrects the geolocation errors for the F08 SSM/I. These corrections include an along-track adjustment, a yaw adjustment, and a correction for cell 128 at the edge of the scan. With these corrections, the location accuracy of the SSM/I cells is probably about 10 km or better. For F10 and subsequent satellites, the cell locations on the  $T_A$  tapes have already been corrected, and no action by DECODE is required.

4. A more exact computation of the incidence angle is done. The incidence angle accuracy is now  $0.03^\circ$  as compared to  $0.1^\circ$  for the original version. For the F08 satellite, the incidence angle is relatively constant, being  $53.1^\circ \pm 0.25^\circ$ . The  $\pm 0.25^\circ$  variation is due to the slight eccentricity ( $\epsilon \approx 0.0015$ ) of the F08 orbit and the oblateness of the Earth. The eccentricity for the F10 orbit is greater ( $\epsilon \approx 0.0085$ ), and as a consequence the incidence angle variation is greater. For F10, the incidence angle ranges from  $52.5^\circ$  to  $54.0^\circ$ . This  $\pm 0.75^\circ$  variation is large enough to introduce an error in some geophysical parameters if it is not taken into account.

5. The F08 antenna temperatures are corrected for an along-scan error that occurs near the edge of the scan where the feedhorn partially sees the cold-sky reflector. There is also an option for adding an offset to the antenna temperatures in order to bring them into agreement with the Wentz [1991] radiative transfer model for the ocean. The  $T_A$  corrections for the F10 SSM/I are currently set to zero. We will provide the Users with the correction coefficients as soon as the  $T_A$  error analysis is completed.

In addition to these DECODE updates, a more complete description of the SSM/I  $T_A$  data set is given herein. We have included new sections on geolocation, erroneous data periods, and radiometer parameters. The table BADLOC that lists periods of erroneous F08 data is provided on the enclosed 3.5" diskette (see Section 7). We also include Figure 9 in Section 8 that shows when the F08 85 GHz channels are usable. For more information on SSM/I, we refer the User to the SSM/I report compiled by Hollinger [1989].

For those Users who are not interested in the details of the SSM/I data processing and sensor performance, we suggest that you at least read Sections 7, 9, and 11. It is important to excluded periods of erroneous data (Section 7), to know the organization of the  $T_A$  tapes (Section 9), and to understand the execution of the subroutine DECODE (Section 11).

## SECTION 2. SENSOR DESCRIPTION

The orbits for F08 and F10 are near-circular, sun-synchronous, and near-polar, with an inclination of  $98.8^\circ$ . The altitude for F08 is  $860 \pm 25$  km, and it is  $805 \pm 72$  km for F10. The variation in altitude is due to the eccentricity of the orbit and the oblateness of the Earth. The F08 and F10 orbital periods are 102 and 101 minutes, respectively. The local time for the ascending equatorial crossing for F08 is 6:12 am. Due to a malfunction during launch, F10 is not exactly sun-synchronous, and its local equatorial crossing time is increasing at a rate of 47 minutes/year. On January 1, 1991, the F10 local equatorial crossing time was 7:39 pm. More information on the orbit parameters is given in Section 6.

The SSM/I consists of 7 separate total-power radiometers, each simultaneously measuring the microwave emission coming from the Earth and the intervening atmosphere. Table 1 gives the frequencies, polarizations, and temporal and spatial resolution of the 7 channels. Dual-polarization measurements are taken at 19.35, 37.0, and 85.5 GHz, and only vertical polarization is observed at the 22.235 GHz water vapor channel.

The SSM/I uses an offset parabolic reflector of dimensions 61 by 66 cm to collect the microwave radiation. The reflector focuses the radiation into a corrugated, broad-band, 7-port feedhorn. The reflector and feedhorn spin as a unit about an axis parallel to nadir. The rotation period is 1.9 s. A cold-space reflector and a hot reference load are attached to the spin axis and do not rotate. The rotating feedhorn observes the fixed cold reflector and hot load once each scan. In this way, calibration observations are taken every scan.

Earth observations are taken during a  $102.4^\circ$  segment of the rotation, as is shown in Figure 1. The  $102.4^\circ$  arc is centered on the spacecraft subtrack and corresponds to a 1400 km wide swath on the Earth's surface. Relative to the spacecraft velocity vector, the F08 SSM/I is looking aft, and the F10 SSM/I is looking forward. The 1400-km swath and the orbit inclination of  $98.8^\circ$  provide complete coverage of the Earth in two to three days, except for two small circular sectors of  $2.4^\circ$  centered on the North and South poles.

During each scan, the 85 GHz channels are sampled 128 times over the  $102.4^\circ$  arc. The integration period for a single sample is 3.89 ms. This sampling scheme results in 128 v-pol footprints and 128 h-pol footprints, each having an effective 3-dB spatial resolution of 15 km. Observations at the lower three frequencies are only taken every other scan. Scans during which the lower channels are sampled are called 'A-scans', and the other scans are called 'B-scans'. During the  $102.4^\circ$  arc of an A-scan, 64 samples of each of the lower channels are taken, with the integration period being 7.95 ms. The spatial resolutions of the samples depends upon the frequency and are given in Table 1. The IF passband for the 19 and 22 GHz channels is 240 MHz. The passband for the 37 GHz channels is 900 MHz, and for the 85 GHz channel it is 1400 MHz.

Table 1. Temporal and Spatial Resolution of SSM/I Channels

Frequency (GHz)	Polarization	Integration Period	3 dB Footprint Size	
			Along-track	Cross-track
19.35	vertical	7.95 ms	69 km	43 km
19.35	horizontal	7.95 ms	69 km	43 km
22.235	vertical	7.95 ms	50 km	40 km
37.0	vertical	7.95 ms	37 km	28 km
37.0	horizontal	7.95 ms	37 km	29 km
85.5	vertical	3.89 ms	15 km	13 km
85.5	horizontal	3.89 ms	15 km	13 km

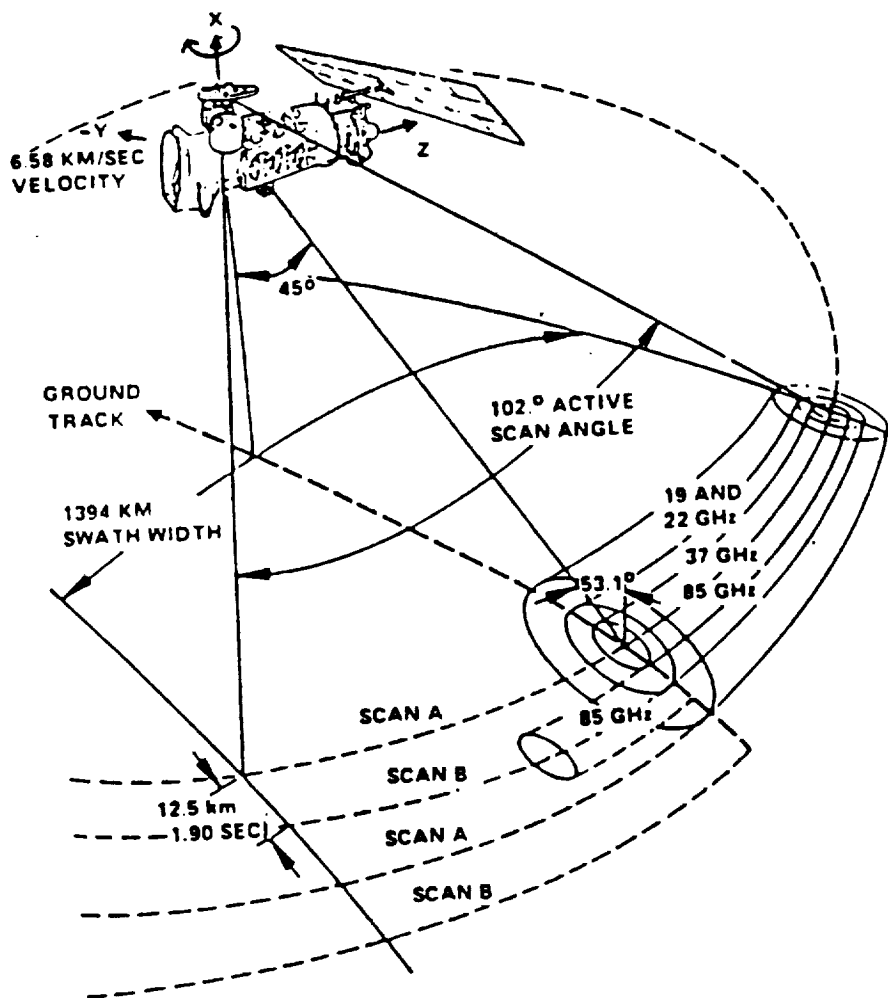


Fig. 1. F08 SSM/I orbit and scan geometry (from Hollinger [1989]).

### SECTION 3. SSM/I DEF TAPES

We obtain the SSM/I data on Date Exchange Format (DEF) tapes. These tapes are originally produced at the Fleet Numerical Oceanography Center (FNOC), and copies are mailed to the National Environmental Satellite, Data, and Information Service (NESDIS). NESDIS then mails us copies of these DEF tapes. There are between 3 and 4 DEF tapes generated each day for each satellite. The large number of tapes is due to an inefficient format. We ingest the daily supply of DEF tapes, organize the data into a chronological, orbit-by-orbit data set, and output the data in a User friendly format onto 6250-bpi tapes. There are 8  $T_A$  tapes per month per satellite. We do not modify the DEF values for antenna temperatures or calibration data. However, we found problems with the cell latitudes and longitudes that are on the DEF tapes. Accordingly, starting with the January 1, 1989  $T_A$  tape, we compute the cell latitudes and longitudes from a smoothed orbit ephemeris rather than using the DEF latitudes and longitudes. Prior to 1989, the  $T_A$  tapes contain the DEF locations. The subroutine DECODE does the necessary location correction for these earlier tapes. Section 6 discusses the problems with the DEF locations and our methods for correcting these problems.

## SECTION 4. COMPUTATION OF ANTENNA TEMPERATURES

In computing the SSM/I antenna temperatures, the basic assumption is that the radiometer output voltage is linearly related to the input power at the mixer/preamplifier. Nonlinear effects such as imperfections in the square-law detector and IF amplifier compression are assumed negligible. Expressing the input power in terms of radiation temperature gives

$$V_i = ck\beta g(T_{Ai} + T_N) \quad (1)$$

where  $V_i$  is the radiometer output voltage,  $T_{Ai}$  (Kelvin) is the radiation temperature entering the feedhorn, and  $T_N$  (Kelvin) is the radiometer noise temperature. The constants are  $c$  = detector constant,  $k$  = Boltzmann constant,  $\beta$  = receiver predetection bandwidth, and  $g$  = receiver gain. The subscript  $i$  denotes either a cold-space observation ( $i = C$ ), a hot-load observation ( $i = H$ ), or an Earth observation ( $i = E$ ). The gain and noise temperature are assumed stable over the period of one scan, which is 1.9 s. That is to say,  $g$  and  $T_N$  are assumed to be the same for the cold-space, hot-load, and Earth observations. The output voltage is converted to counts by applying a scaling factor and a constant offset:

$$C_i = \omega V_i - P \quad (2)$$

Combining (1) and (2) for  $i = C, H$ , and  $E$  gives

$$T_{AE} = A C_E + B \quad (3)$$

$$A = (T_{AH} - T_{AC})/(C_H - C_C) \quad (4)$$

$$B = (T_{AC}C_H - T_{AH}C_C)/(C_H - C_C) \quad (5)$$

Henceforth, the subscript  $E$  on the Earth antenna temperature is dropped, and it is understood that  $T_A$  refers to the Earth observation. For each SSM/I scan, five cold counts and five hot counts are recorded for each channel. (Only 85 GHz observations are taken on the B-scans). The quantities  $C_C$  and  $C_H$  are found by averaging the five individual counts. The cold space antenna temperature  $T_{AC}$  is set to 2.7 K for all channels. The hot reference antenna temperature is found from

$$T_{AH} = T_{oH} + 0.01(T_{oP} - T_{oH}) \quad (6)$$

where  $T_{oH}$  and  $T_{oP}$  are the physical temperatures of the hot load and the radiator plate facing the hot load. The small correction for the radiator plate is to account for radiative coupling between the hot load and the top plate of the rotating drum assembly which faces the hot load. There are three thermistors on the hot load and one on the radiator plate. The temperature  $T_{oH}$  is found by averaging the three thermistor readings. The  $T_A$  tapes contain the values for  $T_A$ ,  $T_{oP}$ ,  $T_{oH}$ ,  $C_C$ , and  $C_H$ . Thus the  $A$  and  $B$  coefficients can be computed, and equation (3) can be inverted to recover the original values for the Earth-viewing counts  $C_E$ .

Starting with the F08 orbit 17057 on October 9, 1990, the FNOC procedure for computing  $T_A$  was slightly modified. Rather than averaging the cold and hot counts for a single scan, the quantities  $C_C$  and  $C_H$  are found by averaging the counts for the last 20 scans (10 A-scans and 10 B-scans). The purpose of this modification is to reduce the noise in  $C_C$  and  $C_H$ . Note that the last 20 scans are used regardless of data gaps. Thus, when

data gaps occur, the time period for this back-averaging will exceed 38 s, and some degradation in the calibration may occur. Also note that the number of scans in the back-average is less than 20 for the first 19 scans in a FNOC DEF file. We need to determine if this change in the calibration procedure produces a discontinuity in the F08 T<sub>A</sub> interannual time series. Any discontinuity will certainly be small ( $\approx 0.1$  K), but climate change studies could still be affected. All F10 data have been processed with the new calibration procedure, and thus there is no discontinuity problem.

## SECTION 5. COMPUTATION OF BRIGHTNESS TEMPERATURES

Antenna temperature is a measure of the radiant power entering the feedhorn. It is computed by integrating over the gain pattern of the parabolic reflector and feedhorn assembly.

$$T_{Ap} = \int d\Omega (G_{vp} T_{Bv} + G_{hp} T_{Bh}) \quad (7)$$

where  $d\Omega$  is the differential solid angle and the integral is over the entire  $4\pi$  steradians of a sphere. The subscript  $p$  equals  $h$  or  $v$  and denotes the feedhorn port. The terms  $G_{vp}$  and  $G_{hp}$  are the antenna gains in the direction  $d\Omega$  for vertically and horizontally polarized radiation received by port  $p$ . The terms  $T_{Bv}$  and  $T_{Bh}$  are the vertically and horizontally polarized brightness temperatures coming from the  $d\Omega$  direction. The polarization is referenced to the Earth's surface. Note that the gains  $G_{vp}$  and  $G_{hp}$  account for both the directional dependence of the antenna pattern and the rotation of the Earth-referenced polarization vector relative to the feedhorn polarization vector.

Before launch, two properties of the antenna gain patterns for each SSM/I channel are measured: 1) the relative antenna gain (both co-pol and cross-pol) in the near-boresight direction and 2) the feedhorn spillover. The near-boresight gains are measured out to  $6^\circ$  for the 19 and 22 GHz channels, out to  $4^\circ$  for the 37 GHz channels, and out to  $3^\circ$  for the 85 GHz channels. The feedhorn spillover is a measure of the power that enters the feedhorn directly from space, as opposed to the primary component of power that enters the feedhorn from the parabolic reflector. The feedhorn spillover is computed by measuring the percentage of the feedhorn gain pattern that is not subtended by the parabolic reflector. It is typically a few percent. Since the brightness temperature of space is much less than the Earth's brightness temperature (2.7 K compared to 150-280 K), the spillover has an appreciable effect.

In order to specify  $G_{vp}$  and  $G_{hp}$  for all directions, we model the antenna gain using the vector Kirchhoff approximation for a circular aperture illuminated by a plane wave, with an amplitude that tapers off according to the SSM/I feedhorn pattern. The effective radius of the aperture is chosen so as to match the SSM/I near-boresight measurements. Thus, the model agrees with the near-boresight and spillover measurements and provide the means to specify the antenna sidelobes that were not measured.

The integral (7) is computed using an ocean brightness temperature model [Wentz, 1991] to compute  $T_{Bv}$  and  $T_{Bh}$  over the entire field of view as seen by the SSM/I at an altitude of 860 km. The ocean environment is assumed uniform over the field of view. For the part of integral that corresponds to cold space,  $T_{Bv}$  and  $T_{Bh}$  are set to 2.7 K. In this way, the antenna temperature is computed for various environmental conditions ranging from clear skies to light rain. An excellent approximation for all environmental conditions is found to be

$$T_{Ap} = Q_{vp} T_{Bvb} + Q_{hp} T_{Bhb} + 2.7 Q_{op} \quad (8)$$

where  $T_{Bvb}$  and  $T_{Bhb}$  are the  $v$ -pol and  $h$ -pol brightness temperatures in the antenna boresight direction (subscript  $b$  denotes boresight) and the  $Q$  terms are functions of the spillover factor  $\delta$  and the cross-polarization factor  $\chi_p$ ,  $p = v$  or  $h$ :



$$Q_{vv} = (1 - \delta)/(1 + \chi_v) \quad (9)$$

$$Q_{hv} = \chi_v(1 - \delta)/(1 + \chi_v) \quad (10)$$

$$Q_{hh} = (1 - \delta)/(1 + \chi_h) \quad (11)$$

$$Q_{vh} = \chi_h(1 - \delta)/(1 + \chi_h) \quad (12)$$

$$Q_{ov} = Q_{oh} = \delta \quad (13)$$

Note that the Q's are normalized such that

$$Q_{vp} + Q_{hp} + Q_{op} = 1 \quad (14)$$

The spillover factor  $\delta$  is given by the integral of the antenna pattern over cold space

$$\delta = \int_{\text{space}} d\Omega (G_{vp} + G_{hp}) \quad (15)$$

The leakage factor  $\chi_p$  is a measure of the amount of radiation entering port p that has a polarization orthogonal to the port-p polarization mode. It is determined by fitting the above approximation (8) for  $T_A$  to the exact integral computation of  $T_A$ . Table 2 gives the values of  $\delta$  and  $\chi_p$  for the seven SSM/I channels. For a given frequency,  $\delta$  is independent of the polarization. Over the considered range of environmental conditions, the error between the  $T_A$  approximation and integral is about 0.1 K. Note that the 0.1 K figure only indicates the accuracy of the linear approximation to the integral, assuming the modeled antenna patterns and a uniform ocean field of view. This does not mean that we know the antenna pattern accurately enough to compute  $T_A$  to an absolute accuracy of 0.1 K.

The  $\delta$  term is computed directly from the antenna patterns and does not depend on the assumed environmental scene. The  $\chi_p$  term does have a small dependence on the choice of scene. For the range of ocean scenes considered (clear skies to light rain), the variation of  $\chi_p$  translates to about a 0.1 K variation in  $T_B$ . Although the value of  $\chi_p$  for land and ice observations differs slightly from the average ocean value given in Table 2, this has negligible effect on the computation of brightness temperature because the  $T_B$  polarization difference for ice and land is small compared to water. As the scene becomes unpolarized, the  $T_B$  computation becomes independent of  $\chi_p$ , as is shown by equation (27) below.

Table 2. Spillover and Polarization Leakage Factors

Frequency (GHz)	Polarization	Spillover, $\delta$	Leakage, $\chi_p$
19.35	vertical	0.03199	0.00379
19.35	horizontal	0.03199	0.00525
22.235	vertical	0.02685	0.00983
37.0	vertical	0.01434	0.02136
37.0	horizontal	0.01434	0.02664
85.5	vertical	0.01186	0.01387
85.5	horizontal	0.01186	0.01967

Before converting the antenna temperatures to brightness temperatures, we make corrections for two types of systematic errors. The first error seems to be due to the feedhorn partially seeing the cold-space reflector at the edge of the Earth-viewing portion of the scan. As a result, there is a systematic rolloff of the  $T_A$  values starting near scan position 100 and reaching a maximum value of about 1 K at the final scan position 128. This error was found by stratifying the SSM/I data according to scan position and then averaging over one year. The results for 1987, 1988, and 1989 are very similar.

The second systematic error is the mean difference between the SSM/I antenna temperature observations and the *Wentz* [1991] radiative transfer model for the ocean and intervening atmosphere. The computation of this error is described in *Wentz* [1991]. The offsets in terms of the observations minus the model are 2.0, 3.5, 1.3, -1.6, and -0.2 K for the 19V, 19H, 22V, 37V, and 37H channels, respectively. These offsets are probably due to a combination of several errors including the following:

1. Errors in specifying antenna parameters  $\delta$  and  $\chi_p$
2. Errors in specifying the emissivity of the hot load
3. Errors in the model formulation for the dielectric constant of sea water
4. Errors in the model formulation for oxygen and water vapor absorption.

Assuming that the along-scan error is due to the feedhorn seeing the cold-space reflector, then the effect can be modeled simply as an error in the spillover term  $1 - \delta$ . According to  $T_A$  equation (8), an error in  $1 - \delta$  produces a multiplicative error in  $T_A$ . It is less clear how to model the offset error because it is probably due to a combination of many effects. Accordingly, we simply assume that it is an additive error, and the following correction is applied to the antenna temperatures.

$$T_{Acor} = \eta T_A - \beta \quad (16)$$

where  $T_A$  is the uncorrected value computed from equation (3),  $T_{Acor}$  is the corrected value,  $\eta$  is the along-scan correction coefficient, and  $\beta$  is the offset listed in the previous paragraph. Figure 2 shows  $\eta$  plotted versus scan position for the 37V channel for the F08 satellite. The 19V, 19H, 22V, and 37H channels show a similar shape for the  $\eta$  curve. The along-scan correction coefficient is normalized such that the value of  $\eta$  average over all scan positions is equal to unity.

Subroutine DECODE performs the along-scan correction if the User has selected the option for computing brightness temperatures (i.e., ITB = 1). However, DECODE does not perform the offset correction. That is to say,  $\beta$  is set to zero in DECODE. Section 11 describes a simple modification to DECODE that will implement the offset correction. Applying the offset matches the observations to the *Wentz* [1991] ocean model. However, this may not be appropriate for land and ice observations.

No error analysis has been done for the 85 GHz channels, and no 85 GHz correction is applied. Also, the error analysis for the F10 satellite has yet to be done, and the current version of DECODE sets  $\eta = 1$  and  $\beta = 0$  for F10. When the F10 error analysis is completed, we will send the Users the  $\eta$  and  $\beta$  values.

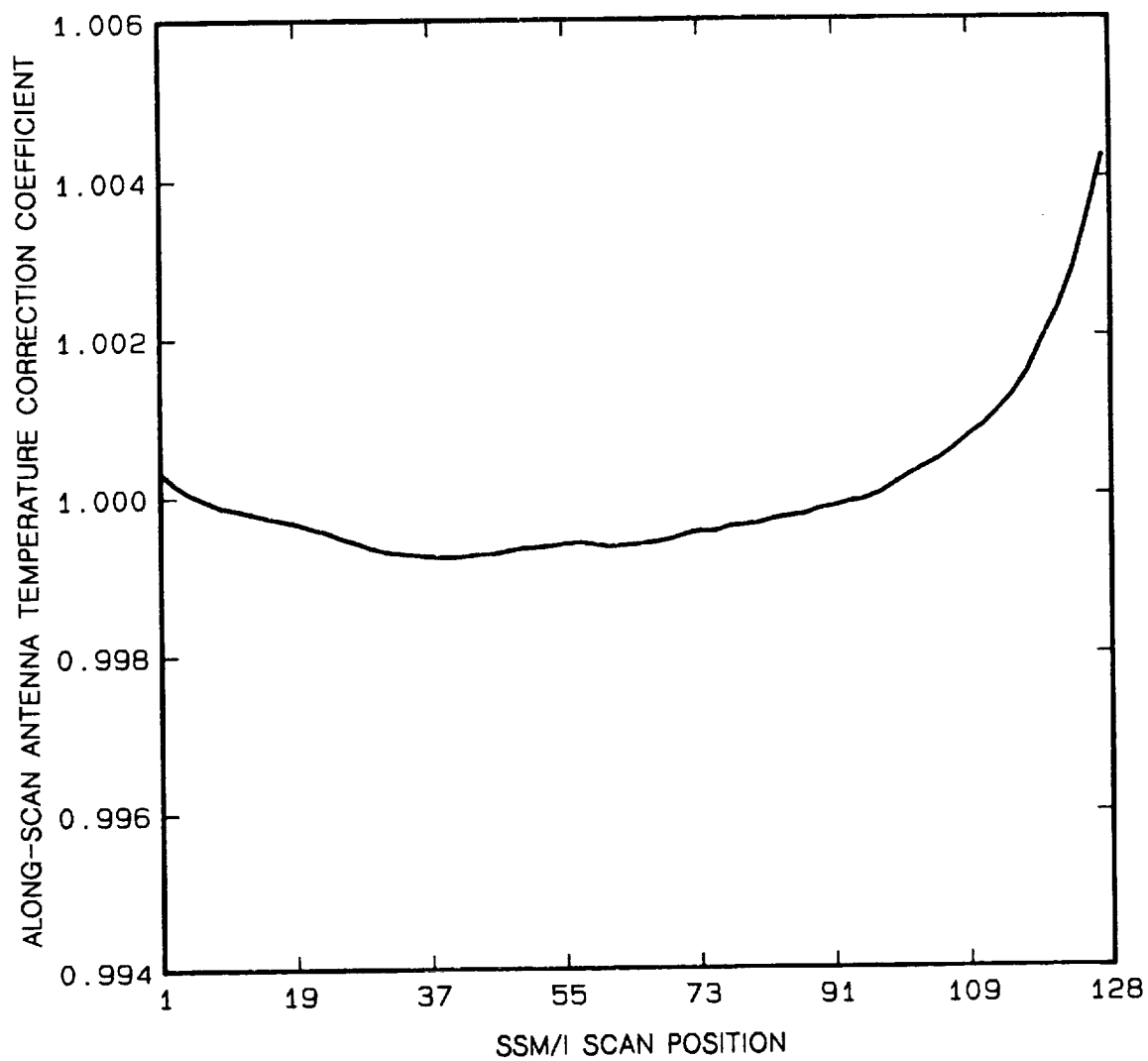


Fig. 2. The F08 along-scan  $T_A$  correction coefficient for the 37 GHz v-pol channel.

After correcting the antenna temperatures, the brightness temperatures are found. At 19, 37 and 85 GHz, dual-polarization antenna temperature measurements are taken.

$$T_{Av} = Q_{vv} T_{Bv} + Q_{hv} T_{Bh} + 2.7 Q_{ov} \quad (17)$$

$$T_{Ah} = Q_{hh} T_{Bh} + Q_{vh} T_{Bv} + 2.7 Q_{oh} \quad (18)$$

where we have dropped the subscript b and it is understood that the brightness temperatures are in the boresight direction. It is also understood that the antenna temperatures  $T_{Av}$  and  $T_{Ah}$  are the corrected values given by equation (16). This system of two linear equations is easily inverted to express brightness temperature in terms of the antenna temperatures:

$$T_{Bv} = A_{vv} T_{Av} + A_{hv} T_{Ah} + 2.7 A_{ov} \quad (19)$$

$$T_{Bh} = A_{hh} T_{Ah} + A_{vh} T_{Av} + 2.7 A_{oh} \quad (20)$$

where the factor of 2.7 is the temperature of cold space. The A coefficients are functions of the spillover factor  $\delta$  and the cross-polarization factor  $\chi_p$ :

$$A_{vv} = (1 + \chi_v) / [(1 - \chi_v \chi_h)(1 - \delta)] \quad (21)$$

$$A_{hv} = -\chi_v(1 + \chi_h) / [(1 - \chi_v \chi_h)(1 - \delta)] \quad (22)$$

$$A_{hh} = (1 + \chi_h) / [(1 - \chi_v \chi_h)(1 - \delta)] \quad (23)$$

$$A_{vh} = -\chi_h(1 + \chi_v) / [(1 - \chi_v \chi_h)(1 - \delta)] \quad (24)$$

$$A_{ov} = A_{oh} = -\delta / (1 - \delta) \quad (25)$$

At 22 GHz, only v-pol antenna temperatures are available. In order to derive an expression giving  $T_B$  as a function of  $T_A$  at 22 GHz, we use the ocean brightness temperature model and the Q coefficients to compute  $T_A$  for a wide range of environmental conditions. A least-squares regression yields the following relationship:

$$T_{Bv} = 1.01993 T_{Av} + 1.994 \quad (26)$$

This proved to be a very accurate fit, with the rms error between the regressed  $T_{Bv}$  value and the actual value being 0.1 K, or less, for the range of antenna temperatures from 176 to 270 K. The reason for the good fit is that the small cross-polarization h-pol leakage is highly correlated with the v-pol radiation. Note that this expression was derived for ocean observations. Over land, the brightness temperature is depolarized. Assuming that  $T_{Bv} = T_{Bh}$ , one can directly invert the  $T_A$  equation, and obtain an alternative expression for  $T_{Bv}$  at 22 GHz.

$$\begin{aligned} T_{Bv} &= T_{Av} / (1 - \delta) - 2.7 \delta / (1 - \delta) \\ &= 1.02759 T_{Av} - 0.074 \end{aligned} \quad (27)$$

Fortunately, these two expressions yield similar values in the 240 K to 300 K range, where they differ by 0.2 K, or less. They intersect at 270 K. Thus, the ocean-derived expression appears to be quite adequate for over land observations. A small error will occur for cases in which the brightness temperatures have relatively low values (below 240 K) and the polarization ratio is markedly different from the ocean polarization ratio.

The above computation of brightness temperature assumes a horizontally-uniform ocean scene. Any horizontal variability will be spatially smoothed by the antenna pattern, and as a result the  $T_B$  computed from the above expressions will be a smoothed representation of the actual brightness temperature field. Image enhancement techniques can be applied to  $T_B$  images to partially restore the actual  $T_B$  contrast. The selection of the appropriate enhancement depends upon the particular application, and we leave this problem to the User.

## SECTION 6. COMPUTATION OF ORBIT PARAMETERS AND EARTH LOCATIONS

The cell latitudes and longitudes on the DEF tapes produced by FNOC are sometimes in error due to the following problems:

1. There are some algorithm errors in the FNOC data processing software.
2. The satellite ephemeris is sometimes incorrect due to spacecraft tracking errors and orbit prediction errors. This problem is particularly severe during periods of increased solar activity.
3. The boresight nadir angle and the alignment of the SSM/I instrument relative to the spacecraft are slightly misspecified.

There have been a number of FNOC algorithm errors. Sometimes the wrong Julian day is assigned to the orbit (see Section 7). Occasionally, the time for the spacecraft location and the scan time are very different. The two times should be within 60 s of each other, but at the begin and end of an FNOC DEF file, the two times can be as much as 40,000 s apart. The spacecraft longitude is sometimes out-of-bounds. There are also other problems that have recently been corrected. For example, the ephemeris was not updated frequently enough, and the location of cell 128 was in error.

In response to these problems, we developed our own routine for computing the latitudes and longitudes rather than using the DEF values. The input to our geolocation routine is the satellite ephemeris for a  $\pm 7$  day period centered on the orbit being processed. The ephemeris is first subjected to quality control to removed any data that are clearly erroneous. Next the ephemeris is smoothed to remove the noise. The smoothed ephemeris is then used to computed the SSM/I cell latitudes and longitudes.

This procedure of computing latitude and longitude from a smoothed ephemeris was initiated with the January 1, 1989 F08 T<sub>A</sub> tape. Prior to 1989, the latitudes and longitudes on the T<sub>A</sub> tapes are the same as the values on the DEF tapes. Fortunately, an analysis of the ephemeris prior to 1989 does not show any large errors except for a brief period during the second half of February 1988. For these pre-1989 tapes, subroutine DECODE does the sensor alignment and the cell 128 correction while reading the tape.

Our geolocation routine is free of the algorithm errors listed above except for the Julian day error. As each orbit is processed, we perform a number of cross-checks to verify the Julian day. Usually these cross-checks detect the Julian day error, which can then be corrected. However, a few of the Julian day errors will go undetected, and these 'erroneous' orbits will be written to the T<sub>A</sub> tape. These erroneous orbits are later detected by the quality control routine discussed in Section 7.

The third geolocation problem listed above is the misalignment of the SSM/I sensor relative to the spacecraft and the misspecification of the boresight nadir angle. For F10, this problem is corrected by our geolocation routine, and the locations on the T<sub>A</sub> tapes are correct. For F08, part of the correction is done by our geolocation routine and part is done by DECODE, as is explained in the next three paragraphs.

The F08 SSM/I requires a yaw adjustment and an along-track adjustment. The yaw correction is done by DECODE. The along-track correction is also done by DECODE for the  $T_A$  tapes prior to 1989. For 1989 and thereafter, the along-track correction is done by our geolocation routine. Hence for the 1989 F08  $T_A$  tapes and thereafter, DECODE only does the yaw correction. DECODE automatically does the necessary corrections based on the scan time and the setting of the User option IADJ (See Section 11).

The F08 yaw adjustment is a  $0.5^\circ$  clockwise rotation (looking down on the satellite) about nadir. For F08  $T_A$  tapes prior to March 1990, the along-track adjustment is a 15-km shift in the direction opposite to the spacecraft velocity vector. Thereafter, the adjustment is a 10-km shift in the same direction. The reason for the change is discussed in the next paragraph. These adjustments were derived by comparing SSM/I images with coastlines and are in good agreement with the corrections found by *Hollinger* [private communication, 1991]. We used 85H images of the South Coast of Australia to determine the along-track error. The residual error after performing these corrections appears to be less than 10 km.

In June 1989, a change was made to the ephemeris computation at FNOC. As a result the original 15-km along-track error was reduced to 10 km. For the  $T_A$  tapes prior to 1989, the 15-km adjustment is applied by subroutine DECODE if the User selects the option IADJ = 1. For the  $T_A$  tapes from January 1989 through February 1990, our geolocation routine applies a 15 km translation when computing latitudes and longitudes. Starting with the March 1, 1990  $T_A$  tape, the geolocation routine applies a 10-km translation rather than a 15-km translation in order to be consistent with the FNOC June 1989 ephemeris update. Unfortunately there is a 9 month lag between the FNOC ephemeris update and our  $T_A$  tape update. (We did not know that the new ephemeris changed the along-track error.) Thus from June 1989 through February 1990, there is a residual 5-km along-track error in the locations on the F08  $T_A$  tapes.

For F10, the necessary adjustments are done by the geolocation routine, and the locations on the  $T_A$  tapes are correct. Two adjustments are done. First, the nadir boresight angle (see equation (45) below) is increased from its prelaunch value of  $44.63^\circ$  to  $45.37^\circ$ . Second, the azimuth start angle (see equation (46) below) is change from its prelaunch value of  $50.9^\circ$  to  $51.1^\circ$ . The change in the azimuth start angle is equivalent to a  $0.2^\circ$  counter-clockwise yaw adjustment. These F10 adjustments were derived by *Hollinger* [private communication, 1991].

In the remainder of this section, we give the formulation for computing the orbit parameters and Earth locations. We use a simple model for the SSM/I orbit. The spacecraft position at time  $t$  is specify by the vector  $R$  that extends from the Earth's center to the spacecraft. This vector is given by its magnitude  $R$  and its three directional components  $R_x$ ,  $R_y$ , and  $R_z$  in a celestial coordinate system that does not rotate with the Earth. The x-axis is defined by the vector pointing from the Earth's center to the celestial position corresponding to the most recent ascending node of the satellite (i.e., the point where the satellite last crossed the equator in the south-to-north direction). The z-axis is defined by the vector pointing from the Earth's center to the North Pole. The y-axis is orthogonal to the x-axis and z-axis. The magnitude  $R$  (km) at time  $t$  is approximated by

$$R = a [1 - \epsilon \cos(T - T_0)] + 1.82 (1 - 2 \sin^2 \alpha \sin^2 \phi) \quad (28)$$

$$\phi = T + 2 \epsilon [\sin(T - T_0) + \sin T_0] \quad (29)$$

$$T = (2\pi/P)(t - t_0) \quad (30)$$

where  $a$  is the major semi-axis (km),  $\epsilon$  is the eccentricity,  $T_0$  is the angle of perigee,  $P$  is the orbit period,  $\alpha$  is the inclination angle, and  $t_0$  is the time of the last ascending node. The second term in (28) with the factor 1.82 km is an empirical adjustment to account for the higher order orbit moments. Except for the empirical adjustment, the above expressions are simply Kepler's equations expanded to first order in  $\epsilon$ . The eccentricity of the SSM/I's orbit is less than 0.01, and the accuracy of this simple model is better than 1 km. In terms of the orbit angle  $\phi$ , the three directional components are

$$R_x = \cos \phi \quad (31)$$

$$R_y = \cos \alpha \sin \phi \quad (32)$$

$$R_z = \sin \alpha \sin \phi \quad (33)$$

The geocentric latitude  $\gamma$  of  $\mathbf{R}$  is

$$\gamma = \arctan[R_z / (R_x^2 + R_y^2)^{1/2}] \quad (34)$$

The azimuth angle  $\psi$  of  $\mathbf{R}$  is defined as the angle between the x-axis and the projection of  $\mathbf{R}$  onto the x-y plane.

$$\psi = \arctan2(R_y, R_x) \quad (35)$$

The spacecraft geodetic latitude and east longitude (in radians) are found from the following:

$$\text{s/c lat} = \arctan[(\rho_e/\rho_p)^2 \tan \gamma] \quad (36)$$

$$\text{s/c lon} = \psi + 2\pi[t_L - \text{mod}(t, 86400)]/86400 \quad (37)$$

where  $\rho_e$  and  $\rho_p$  are the Earth's equatorial and polar radii, which equal 6378.5 and 6356.9 km, respectively. The parameter  $t_L$  is the local time of the ascending node associated with the x-axis. The second term in (37) specifies the longitude of the x-axis and accounts for Earth rotation. The satellite altitude is simply given by

$$\text{s/c alt} = R - \rho \quad (38)$$

$$\rho = \rho_e \rho_p / [(\rho_p \cos \gamma)^2 + (\rho_e \sin \gamma)^2]^{1/2} \quad (39)$$

where  $\rho$  is the Earth's radius along  $\mathbf{R}$ .

The DEF tapes give the spacecraft geodetic latitude, longitude, and altitude at approximately 60 s intervals. For each orbit, the six orbit parameters ( $t_0$ ,  $a$ ,  $t_L$ ,  $\alpha$ ,  $\epsilon$ , and  $T_0$ ) are found by fitting (in a least-squares sense) the above expressions to the DEF latitudes, longitudes, and altitudes. Typical between 1% and 5% of the orbits have a poor quality of fit and are excluded from further processing. The parameters from the remaining orbits are processed by a regression routine that finds either a first-order or a second-order fit versus time to the parameter. First-order fits are used for parameters  $a$ ,  $t_L$ , and  $\alpha$ , and second-order fits are used for the other three parameters. The fits are done over a  $\pm 100$  orbit window centered on the specified orbit. The resulting regressions are used to compute smooth values of the orbit parameters for each orbit, which are stored in an orbit parameter table.



Figures 3 and 4 show the smoothed orbit parameters for the F08 and F10 satellites, respectively. Instead of showing the ascending node time  $t_0$ , we show the period  $P$ , which is the first derivative of  $t_0$ . The figures show the variation of the parameters over 2000 orbits that occurred during the first half of 1991. The dots are the values for the individual orbits that have a good quality of fit, and the solid curves are the regressions.

The period  $P$  and the major semi-axis  $a$  show a slow, steady decrease with time. For example, at the beginning of the F08 mission in July 1987 the values for  $P$  and  $a$  were 6118.5 s and 7229.3 km. Four years later, the values are 6111.0 s and 7223.3 km, respectively. The ascending node local time  $t_L$  steadily increases with time. For F08 the change is small, being about 70 s/year. The F10 ascending node local time is increasing at a much faster rate of 2800 s/year. The inclination angle  $\alpha$  is slowly decreasing with time at a rate of about  $-0.01^\circ/\text{year}$  for F08 and  $-0.05^\circ/\text{year}$  for F10. The eccentricity  $e$  and angle of perigee  $T_0$  are periodic. The period is about 1800 orbits and the amplitude remains constant over time. F10 has a much larger eccentricity than does F08 due to a malfunction that occurred during the F10 launch. (The period and the major semi-axis are redundant parameters in the sense that they are related by Kepler's third law of motion. The expression  $21.6106 P^{2/3}$  yields values for  $a$  that are within 0.2 km of the values in the orbit parameter table.)

To compute the latitudes and longitudes along the SSM/I scan, it is first necessary to specify the spacecraft coordinate system, which is defined by three unit vectors:  $U_1$ ,  $U_2$ , and  $U_3$ . The first vector is the nadir vector. It points from the satellite nadir point on the Earth up toward the satellite. The satellite nadir point is defined such that  $U_1$  is orthogonal to the Earth's surface. Because the Earth is an oblate spheroid,  $U_1$  does not coincide with  $R$  except at the equator. In terms of the  $x,y,z$  coordinate system  $U_1$  is given by

$$U_1 = [\cos \psi \cos(\gamma + \nu\rho/R), \sin \psi \cos(\gamma + \nu\rho/R), \sin(\gamma + \nu\rho/R)] \quad (40)$$

The angle  $\nu$  (radians) is the difference between the geodetic minus geocentric latitude at the satellite nadir point, and  $\rho$  is the Earth's radius at the satellite nadir point. These two quantities depend on the nadir point latitude. For the SSM/I altitude, the difference between the nadir point geocentric latitude and  $\gamma$  is less than  $0.03^\circ$ , and  $\gamma$  can be used in place of the nadir latitude to very accurately approximate  $\nu$  and  $\rho$ .

$$\nu = 1/2 [1 - (\rho_p/\rho_e)^2] \sin 2\gamma \quad (41)$$

The second spacecraft coordinate vector  $U_2$  is the spacecraft bow vector that points approximately in the direction of the spacecraft velocity.  $U_2$  is orthogonal to  $U_1$  and lies in the orbit plane. It is given by

$$U_2 = U_1 \times M / |U_1 \times M| \quad (42)$$

where  $M$  is the vector that is orthogonal to the orbit plane.

$$M = [0, \sin \alpha, -\cos \alpha] \quad (43)$$

The third spacecraft coordinate vector is

$$U_3 = U_1 \times U_2 \quad (44)$$

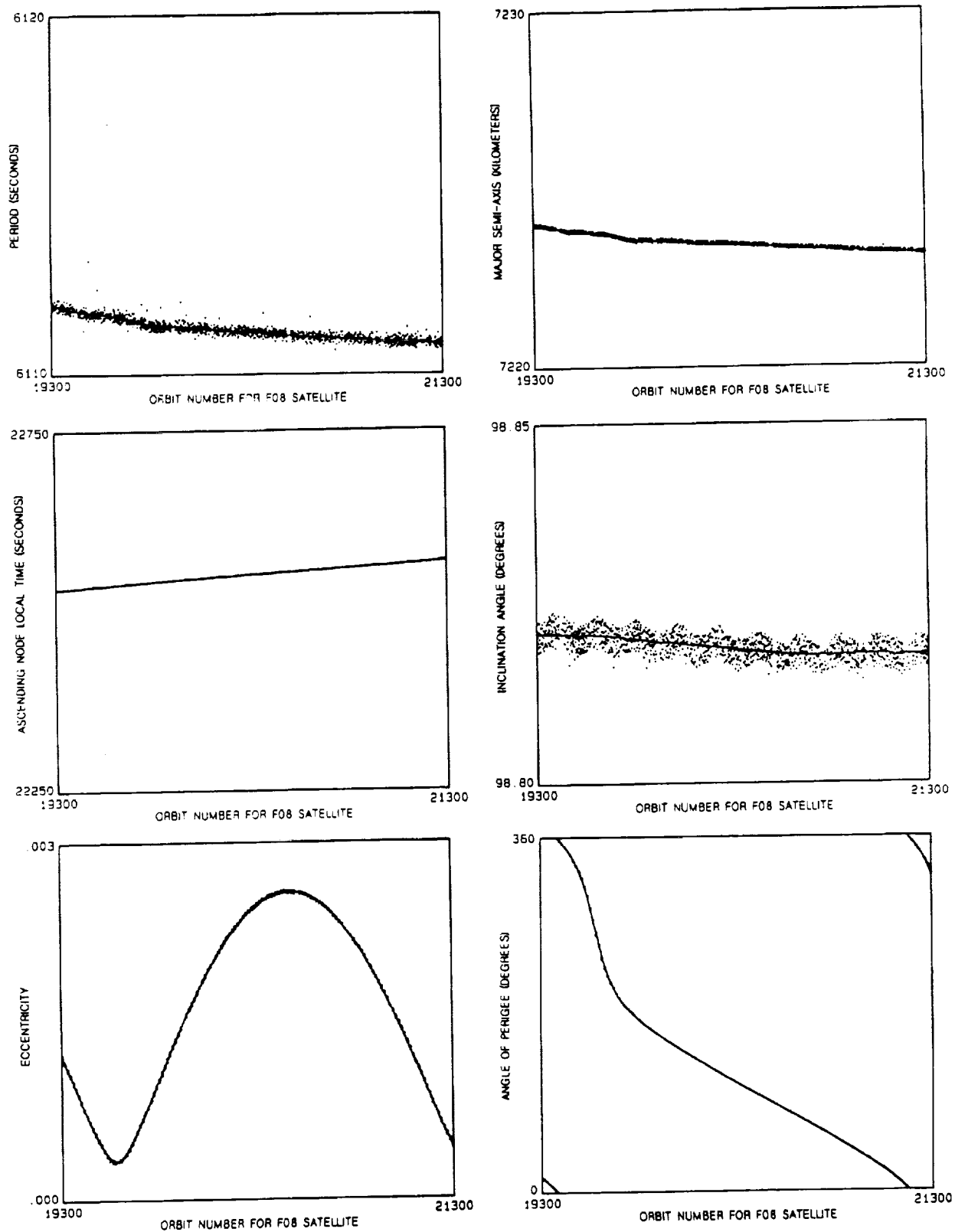


Fig. 3. Orbit parameters for F08 satellite plotted over 2000 orbits.

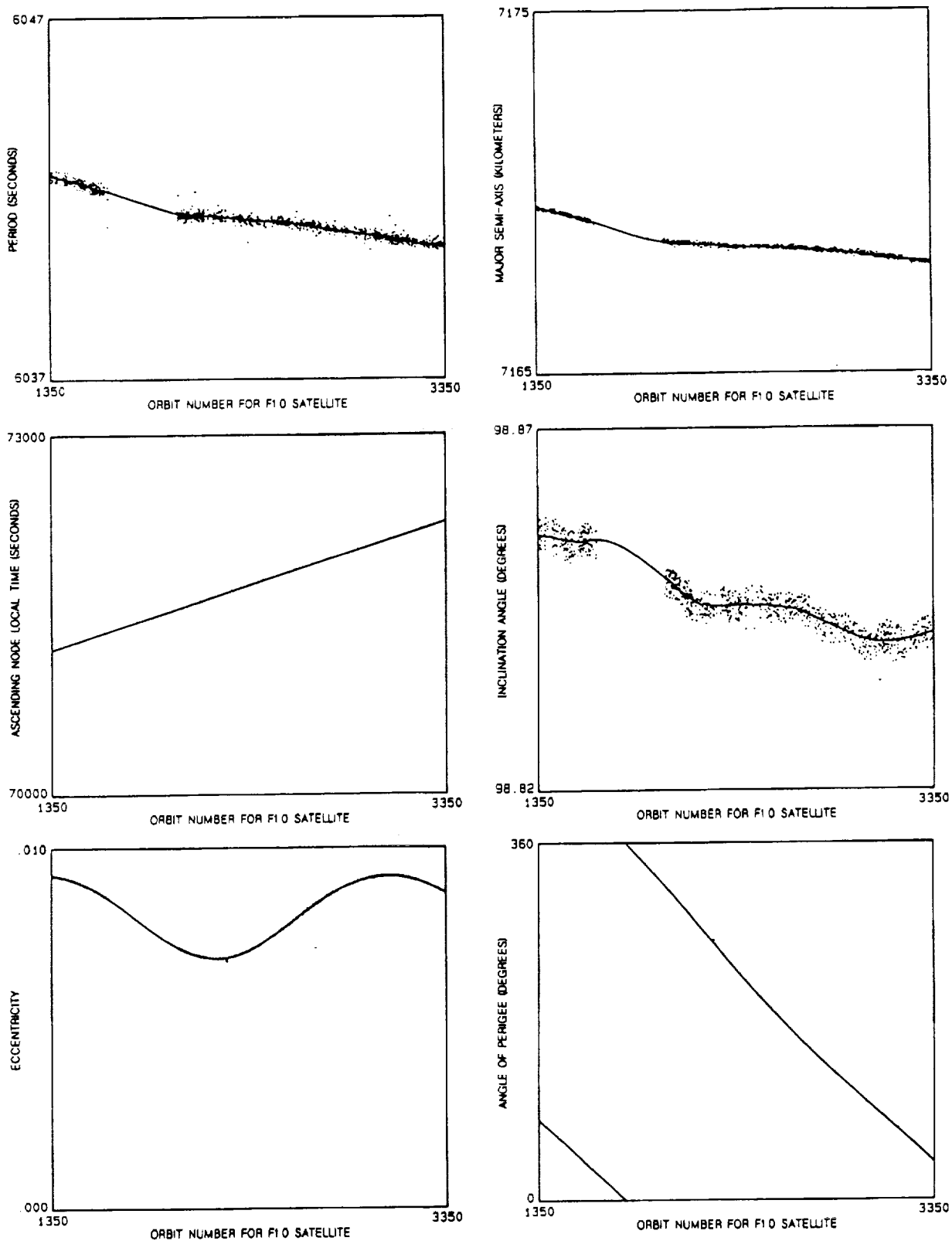


Fig. 4. Orbit parameters for F10 satellite plotted over 2000 orbits.

The antenna boresight unit vector  $\mathbf{B}$  is given by

$$\mathbf{B} = -\cos \theta_n \mathbf{U}_1 + \sin \theta_n (\mathbf{U}_2 \cos \omega + \mathbf{U}_3 \sin \omega) \quad (45)$$

where  $\theta_n$  is the boresight nadir angle and  $\omega$  is the boresight azimuth angle.

$$\omega = \omega_0 - 0.01396(i-1) \quad (46)$$

where  $i$  denotes scan position ( $i = 1$  to 128) and  $\omega_0$  is the azimuth start angle for the first scan position. The factor 0.01396 is in terms of radians and corresponds to  $0.8^\circ$ . The boresight nadir angles for F08 and F10 are  $44.75^\circ$  and  $45.37^\circ$ , respectively. The F08 and F10 azimuth angles  $\omega_0$  are  $230.9^\circ$  and  $51.1^\circ$ , respectively.

Given  $\mathbf{R}$  and  $\mathbf{B}$ , the point where the extended boresight intersects the Earth surface is uniquely determined. Let  $\mathbf{C}$  denote the vector from the center of the Earth to the boresight-Earth intersection point. This vector is given by

$$\mathbf{C} = \mathbf{R} + r\mathbf{B} \quad (47)$$

where  $r$  is the range distance from the satellite to the cell and is given by

$$r = R[b - (b^2 - c)^{1/2}] \quad (48)$$

$$b = [-R_x B_x - R_y B_y - (\rho_e/\rho_p)^2 R_z B_z] / (1 + [(\rho_e/\rho_p)^2 - 1] B_z^2) \quad (49)$$

$$c = (1 - (\rho_e/R)^2 + [(\rho_e/\rho_p)^2 - 1] R_z^2) / (1 + [(\rho_e/\rho_p)^2 - 1] B_z^2) \quad (50)$$

where  $B_x$ ,  $B_y$ , and  $B_z$  are the x, y, and z components of  $\mathbf{B}$ . The geodetic latitudes and east longitudes of the cells are given by

$$\text{cell lat} = \arctan[(\rho_e/\rho_p)^2 C_z / (C_x^2 + C_y^2)^{1/2}] \quad (51)$$

$$\text{cell lon} = \arctan2(C_y, C_x) + 2\pi[t_L - \text{mod}(t, 86400)]/86400 \quad (52)$$

where  $C_x$ ,  $C_y$ , and  $C_z$  are the x, y, and z components of  $\mathbf{C}$ .

Cell latitudes and longitudes are found for every eighth scan position, i.e.,  $i = 1, 9, \dots, 121$ , and also for positions 123, 127, and 128. These 19 pairs of latitudes and longitudes are stored on the  $T_A$  tape. When reading the tape, subroutine DECODE interpolates to find the locations of the other cells. The reason for not storing all locations on the  $T_A$  tapes is to reduce the storage size. The interpolation used by DECODE is fast and is accurate to better than 2 km.

The F08 yaw correction done by DECODE is essentially the same as subtracting  $0.5^\circ$  from  $\omega_0$ . The F08 10-km along-track correction is done by adding 1.5 s to the ascending node times  $t_0$ . It should be noted that a  $0.2^\circ$  increase in  $\theta_n$  or a  $0.2^\circ$  decrease in the satellite pitch would also shift the location in the aft direction by about 10 km. It is difficult to determine which is the best type of correction: timing, boresight angle, or pitch.

## SECTION 7. ERRONEOUS DATA PERIODS

Occasionally the F08 SSM/I data are mislocated by thousands of kilometers. The problem was first revealed by global images of the SSM/I  $T_A$ 's that showed the continent of South America up where Greenland should have been. What appears to be happening is that a wrong time tag is applied to the data coming down from SSM/I. This wrong time is then used to locate the data. In some cases it is clear that the time tag is off by exactly one day. Another problem with the F08 SSM/I data is that the  $T_A$  values are sometimes completely unphysical, ranging from 0 K to 650 K. The cause for this is unclear, but we suspect telemetry errors.

We have not yet done an analysis of the F10 data and do not know if these two problems occur for F10.

Both the mislocation problem and the out-of-bounds (OOB) problem occur throughout a DEF data file. A DEF data file usually corresponds to approximately one orbit. When doing statistical analyses of the SSM/I data, it is very important to exclude these time periods of erroneous data. Otherwise, the statistics can be significantly distorted.

In order to detect periods of erroneous data, we compare the SSM/I  $T_A$  observations with a global  $1^\circ$  latitude by  $1^\circ$  longitude map of averaged  $T_A$ 's observed during the previous semimonthly period. A large and persistent discrepancy between the individual  $T_A$ 's and the map reveals the erroneous DEF data files.

Figure 5 shows the differences between the individual F08  $T_A$ 's and the average  $T_A$  map for the first half of September 1987. Each horizontal line corresponds to a Greenwich day, with the Julian day of year shown at the left. The horizontal scale is Greenwich hours in the day. The vertical scale in the figure is degrees Kelvin, with the distance between horizontal lines being 150 K.

Each point in the figure is the absolute value of a 90-second average of the difference between the 19-GHz h-pol  $T_A$  observations and the semimonthly map. The 19-GHz h-pol channel was used because it provides the greatest sensitivity to varying surface types (land, water, ice) and to the zonal water vapor signature over the world's oceans.

Under normal conditions, the points lie near the horizontal lines, with an occasional small outlier. Storms, coast lines, and varying sea ice can cause larger differences, but only for a short period of time. The periods of mislocated orbits and OOB  $T_A$ 's are shown as clusters of widely varying points. Figure 5 shows five periods of erroneous data on Julian days 246, 250, 252, 253, and 255.

Note that there are small, periodic features shown in the figure. These correspond to the SSM/I passing over coastlines and ice edges. The SSM/I revisits a particular feature every 14 orbits, which is 0.9912 days. Hence, as the Julian day increases the feature shifts to the left by 0.2 hours/day. Due to their periodicity, small size, and brief duration, these features can be distinguished from the mislocated orbits and OOB  $T_A$ 's.

Starting with the second half of May 1988, the procedure for generating the figures was modified. For the OOB problem, we sometimes found that the 19-GHz h-pol channel showed no anomalous behavior, while one or more of the other channels were erroneous. That is to say, the OOB problem does not necessarily affect all channels. Also, an rms  $T_A$  difference, rather than an absolute difference, proved to be a better discriminator of erroneous data. Accordingly, we updated the error detection algorithm.

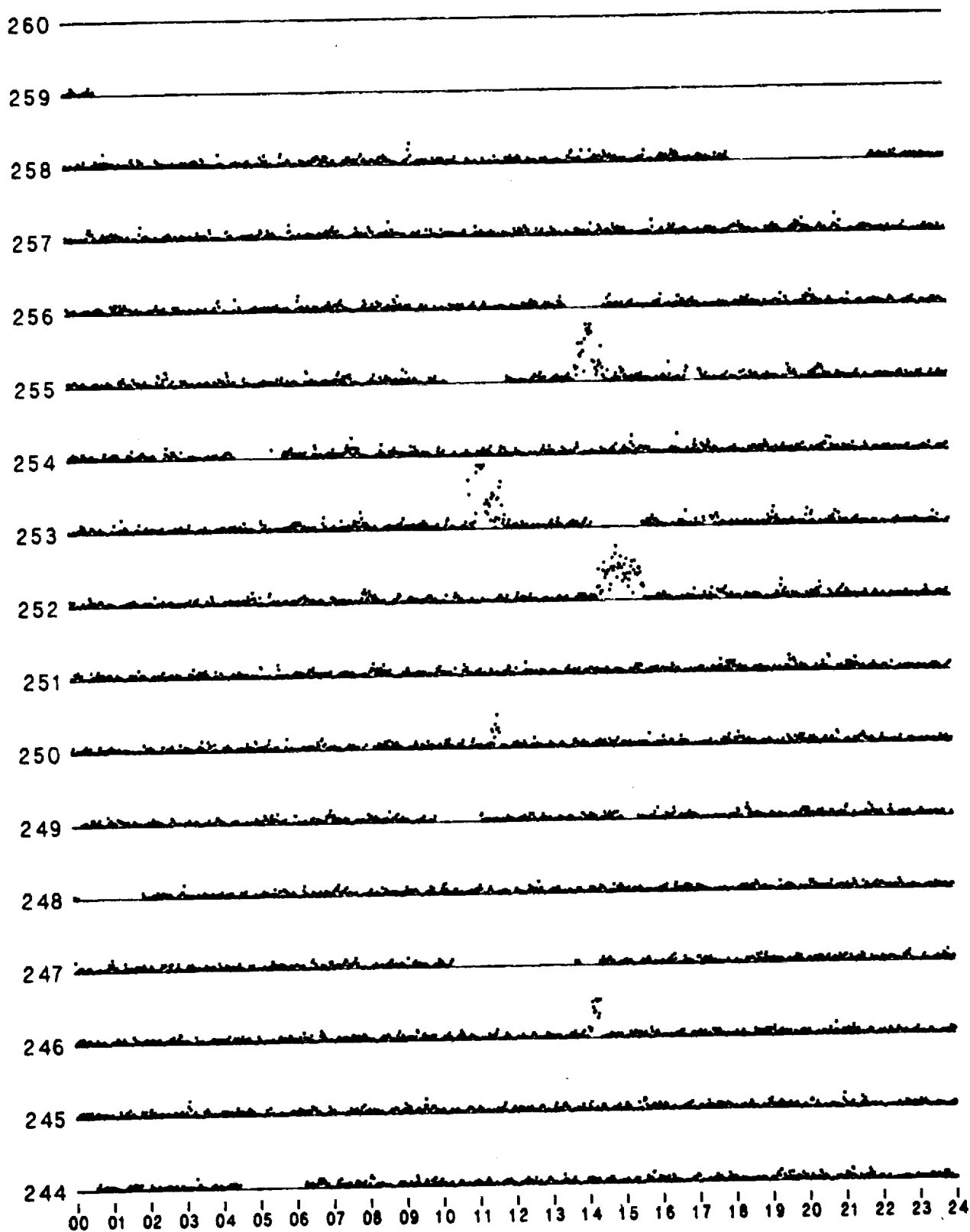


Fig. 5. Plot of erroneous and missing F08 data for the first half of September 1987.

For each scan, the new algorithm first computes the mean squared difference (msd) between the  $T_A$ 's and the semimonthly map. Five msd's are computed, corresponding to the SSM/I five lower frequency channels (i.e., 19V, 19H, 22V, 37V, and 37H). The maximum msd is then selected, and these maxima are averaged over 90 seconds (24 A-scans). Let  $Y$  denote the resulting 90-second average. Normally, the value of  $Y$  is about 20 K or less. Accordingly, for displaying anomalies, 20 K is subtracted from  $Y$ . The result,  $Y' = Y - 20$ , is then plotted as a single point in the figures. Note that if  $Y'$  is less than 0 K, it is set to 0 K; and if  $Y'$  is greater than 130 K, it is set to 130 K.

A complete set of figures showing erroneous data periods for F08 can be obtained from Remote Sensing Systems. In addition to revealing periods of erroneous data, the figures provide a complete inventory of the SSM/I data set. They can be used to find periods of missing data. These data gaps are shown by the absence of plotted points. There is one figure for each semimonthly period from July 1987 to the present. For example, the AAUG87 figure denotes the August 1 through 15, 1987 period, and BAUG87 figure denotes the August 16 through 31 period. We plan to produce similar figures for the F10 satellite.

We have visually inspected all of the F08 figures and have identified the begin and end times for the periods of erroneous data. A small ASCII data file called BADLOC containing these times is included on the enclosed 3.5" inch diskette. A listing of this data file is given in Appendix A. BADLOC is continually being updated. The enclosed version covers the first four years (July 1987 through June 1991) of F08 operation. Each record in the file contains 6 integers that specify the begin time and end time for the period of erroneous data. For example the first record is

```
1987 198 4.0 1987 198 5.0
```

The period of erroneous data begins in 1987 on Julian day 198 at Greenwich hour 4.0. The erroneous data ends one hour later at hour 5.0. These time windows are somewhat larger than the clusters of data outliers shown in the figures in order to ensure that all the erroneous data are excluded.

The problem of erroneous data was particularly bad during the second half of 1988. Then, in January 1989 and thereafter the occurrence of erroneous data greatly reduced. After 1988, there are, on the average, about one or two erroneous data periods each month.

## SECTION 8. TIME SERIES OF RADIOMETER PARAMETERS

The operation of the SSM/I is monitored by producing time series of various radiometer parameters. For example, Figure 6 shows the thermistor readings for three hardware components on the F08 SSM/I: the hot load, the top of the SSM/I drum, and the internal temperature of the electronics. Each of these component temperatures is shown as a different color in Figure 6 and is plotted versus time from July 1987 through June 1991. As can be seen, the temperatures go through a significant heating cycle every winter due to increase solar illumination. There is some concern that this large heating cycle may adversely affect the performance of the radiometers. The operation of the SSM/I radiometers is monitored by producing time series of the radiometer temperature resolution, noise temperature, and gain. The remainder of this section gives the formulation for computing these parameters and presents figures of the parameters plotted versus time for the first four years (July 1987 through June 1991) of the F08 operation. This type of analysis has not yet been done for the F10 satellite.

The rms temperature resolution of the SSM/I channels is computed as follows. The variation of the radiometer calibration counts  $C$  ( $C$  denotes either cold counts  $C_C$  or hot counts  $C_H$ ) for a single A-scan is first found:

$$\sigma_C = [\Sigma C^2 - (\Sigma C)^2/5]/4 \quad (53)$$

where  $\Sigma$  represents the sum over the five counts taken during an A-scan. The count variance is converted to a temperature variance by the following expression:

$$\sigma_T = A^2 \sigma_C \quad (54)$$

where the  $A$  coefficient is given by (4). The quantity  $\sigma_T$  is then averaged over a period of 3 or 4 days, and the rms temperature resolution is then given by

$$\Delta T = \langle \sigma_T \rangle^{1/2} \quad (55)$$

where  $\langle \rangle$  denotes the 3 or 4 day average. The temperature resolution found from the hot counts is slightly larger than that for the cold counts because the variation of the hot load emission is greater than the variation of the cold space emission.

Figures 7 and 8 show the temperature resolution for the seven F08 SSM/I channels as found from the cold counts and from the hot counts, respectively. Each color represents a different channel. The most striking feature in Figures 7 and 8 is the degradation of the 85V and 85H channels. Figure 9 is the same as Figure 7 except that the vertical scale has been compressed. Figure 9 can be used to determine those time periods for which the 85V and 85H channels are usable. The hash marks in these figures denote the beginning of the month. The horizontal axis goes from July 1, 1987 to July 1, 1991.

During the first heating cycle in December 1987, the 85V temperature resolution begins to degrade. After the heating cycle is over, the 85V channel continues to degrade. After April 1988, the noise in the 85V channel exceeds 20 K. Between May 1988 and January 1989, there are time windows in which the noise subsides. The possibility exists that useful information can be obtained from the 85V channel during these time windows. After January 1989, the noise becomes very large, and the channel is not usable.



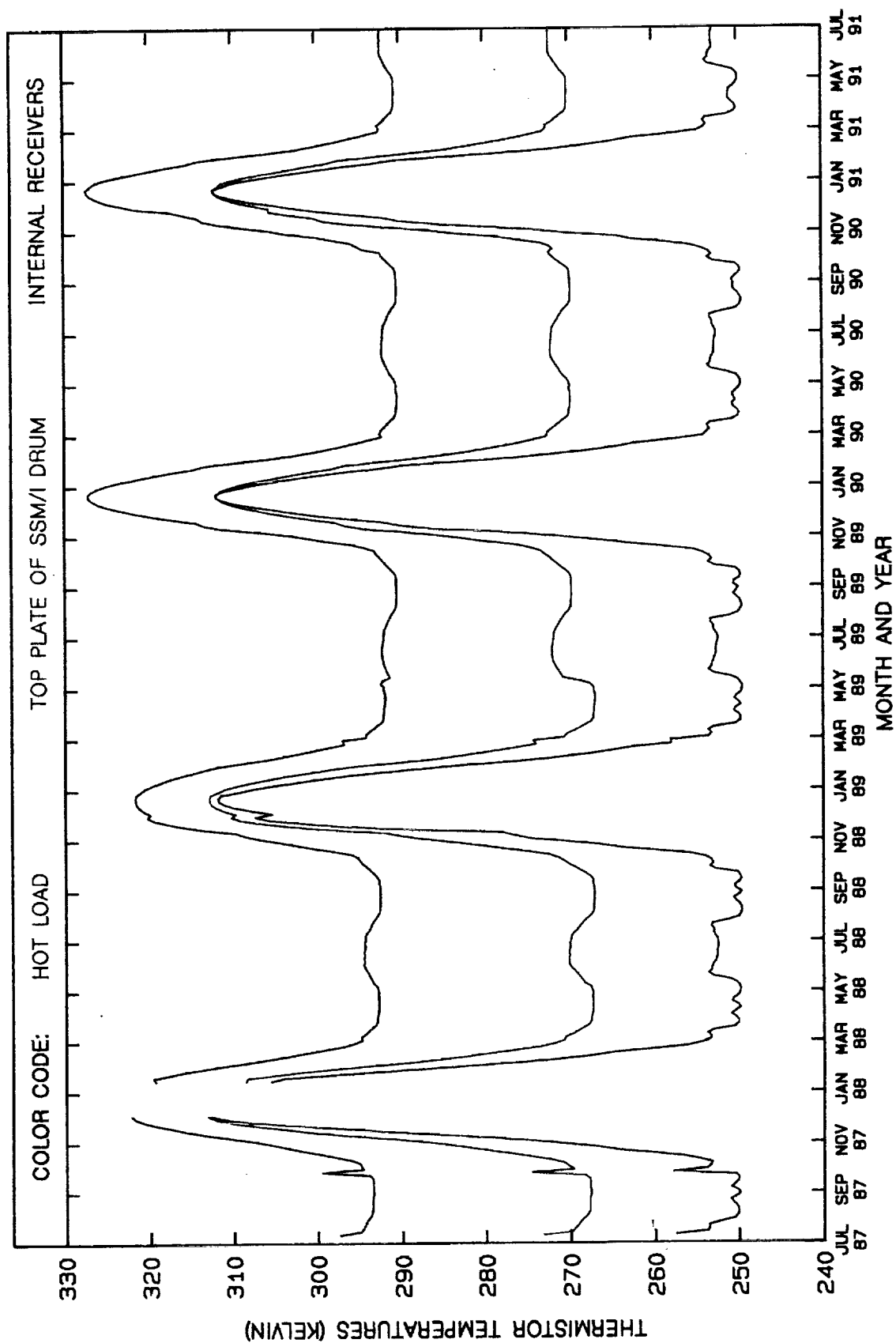


Fig. 6. F08 SSM/I thermistor readings for the hot load, top plate, and internal electronics.

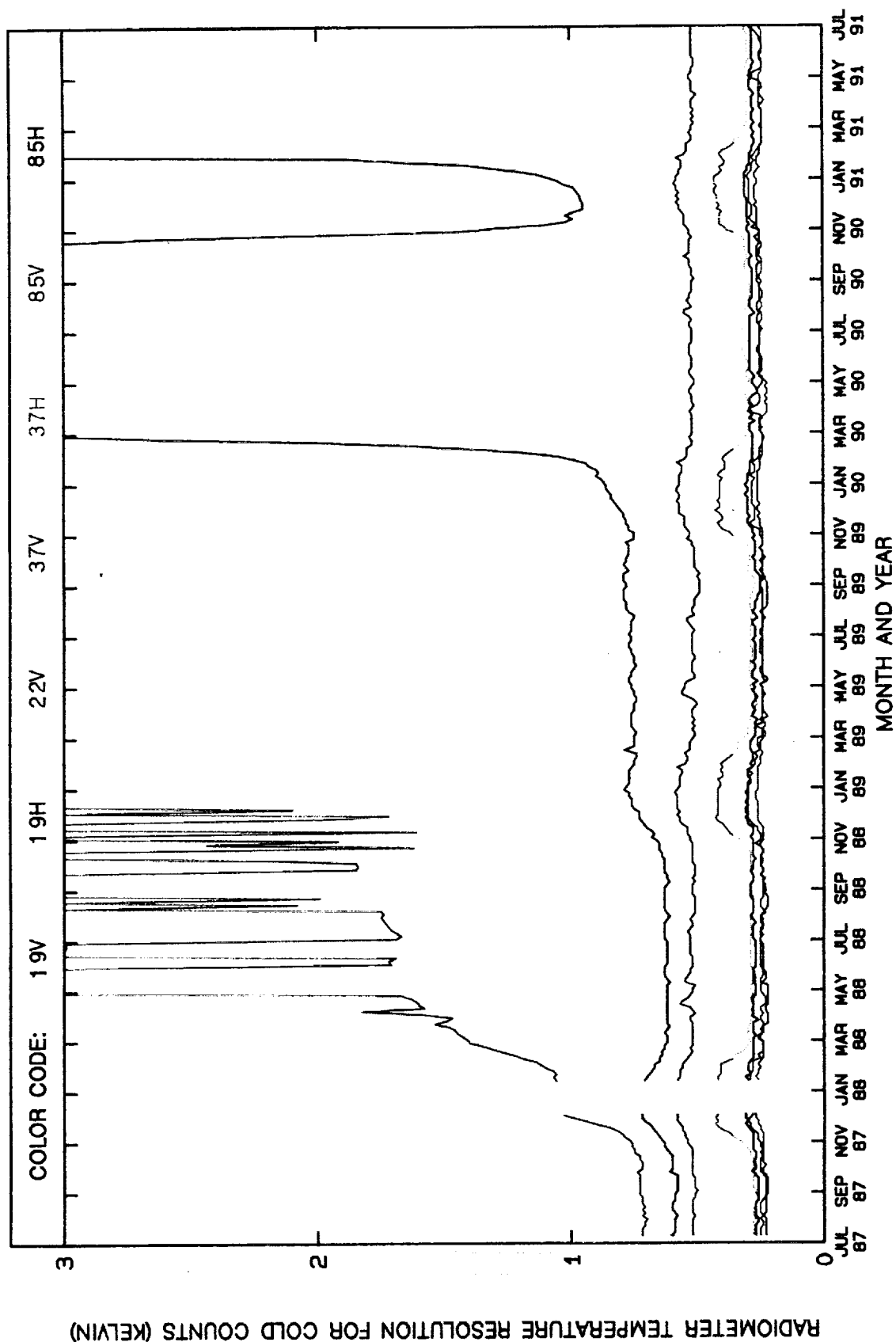


Fig. 7. F08 SSM/I radiometer temperature resolutions derived from the cold counts.

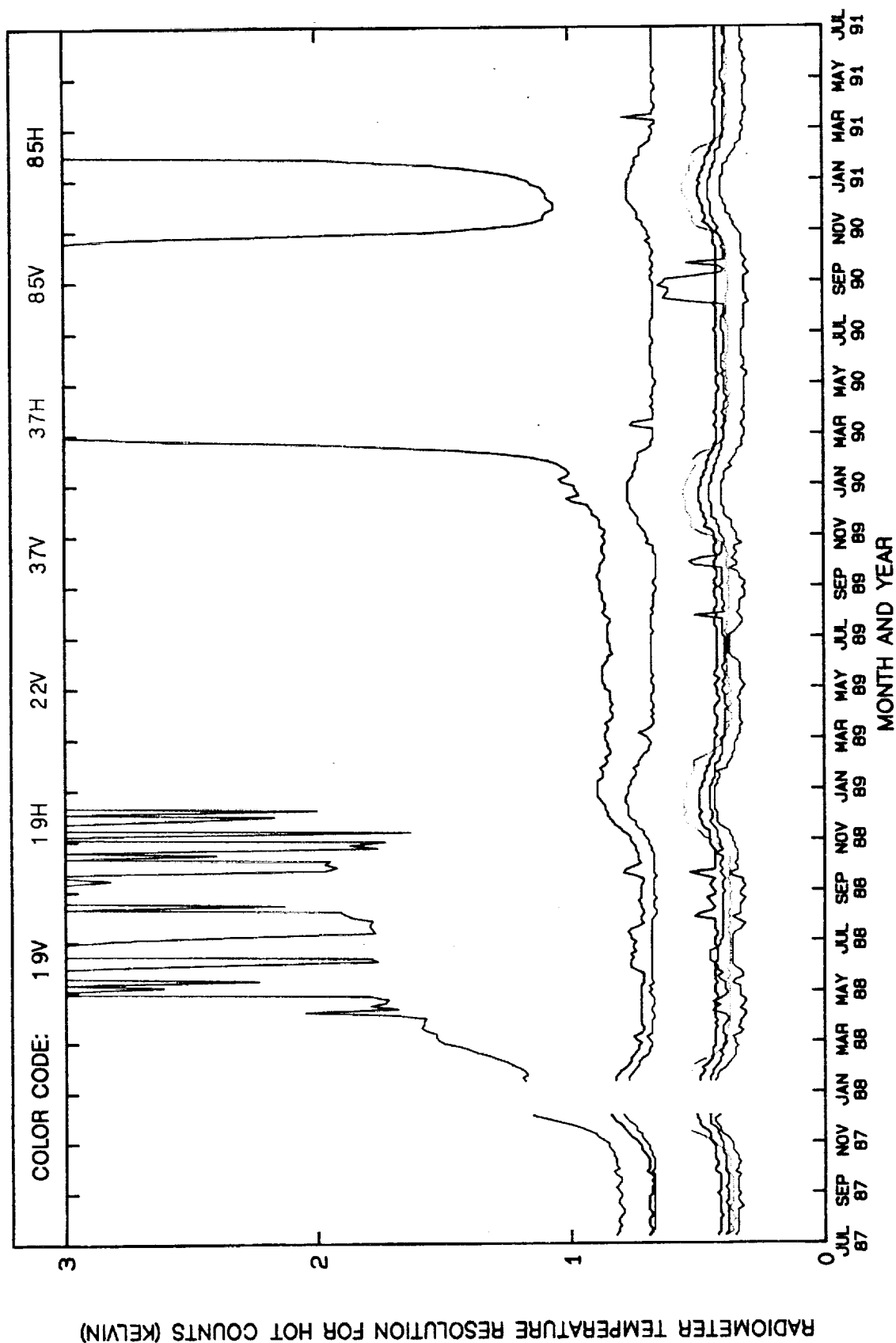


Fig. 8. F08 SSM/I radiometer temperature resolutions derived from the hot counts.

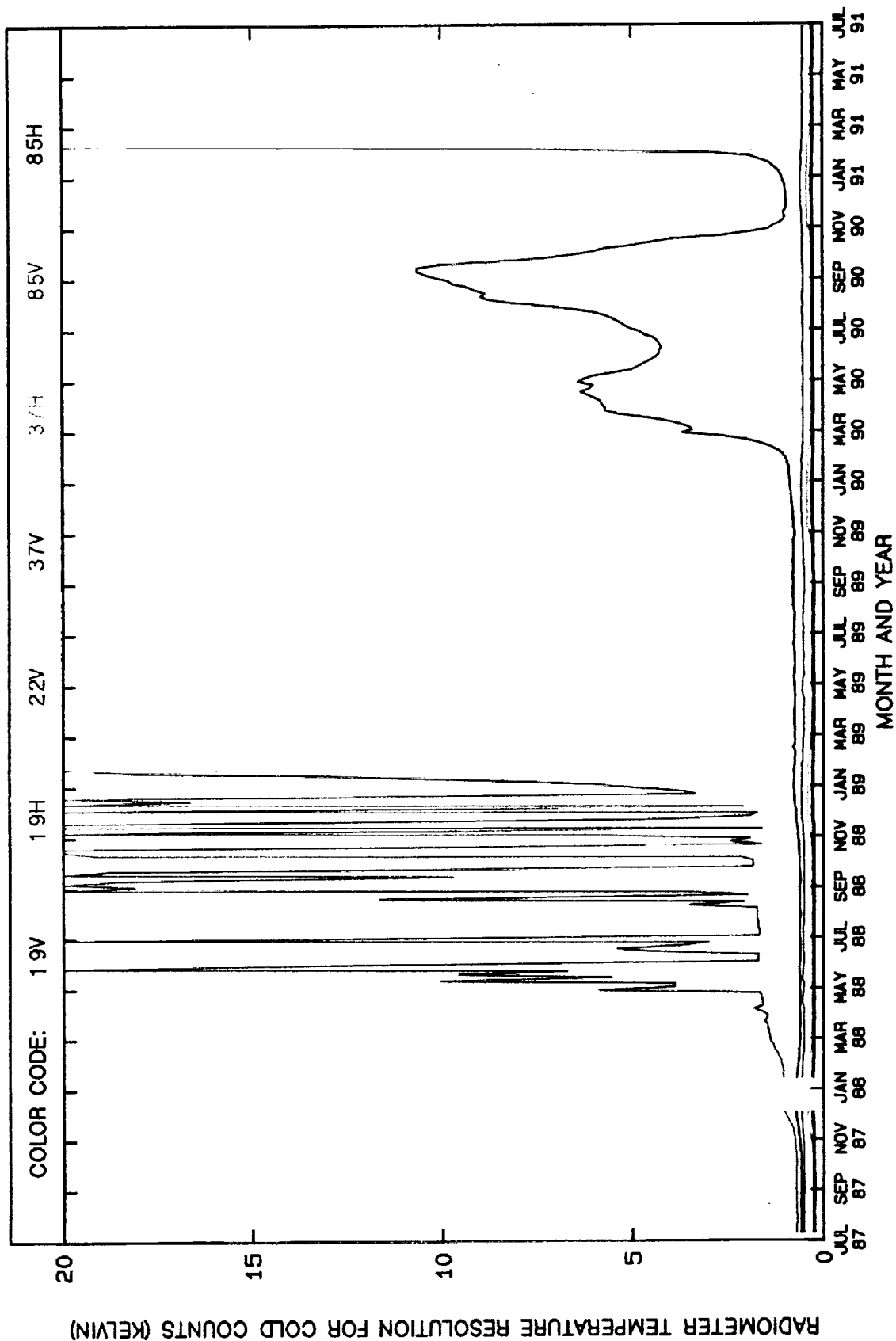


Fig. 9. Same as Figure 7 except vertical scale is compressed.

The 85H channel shows a slight degradation in the temperature resolution during the first heating cycle, but then recovers. The second heating cycle in December 1988 seems to cause a small but permanent degradation in the 85H channel. Then, the third heating cycle in December 1989 seriously damages the 85H channel, and the noise increases to between 5 and 10 K. Curiously, during the fourth heating cycle in December 1990, the 85H channel temporarily recovers, but after January 1991 the noise becomes very large, exceeding 20 K.

The other channels also experience a small increase in  $\Delta T$  during the heating cycles. Fortunately, the lower frequency channels are not permanently affected by the heating, and  $\Delta T$  returns to its normal level after the heating cycle is over.

The radiometer noise temperature is found from equations (1), (2), and (4) to be

$$T_N = (C_i + P)A - T_{Ai} \quad (56)$$

where the A coefficient is given by (4). Either the cold sky observations or the hot load observations can be used in (56) (i.e.,  $i = C$  or  $H$ ), with identical results. The offset P is 1782, 1796, 2835, 2614, 3178, 4167, and 4229 for the 19V, 19H, 22V, 37V, 37H, 85V, and 85H channels, respectively. The relationship between the noise temperature and the radiometer temperature resolution is

$$\Delta T = (T_{Ai} + T_N)/(\beta\tau)^{1/2} \quad (57)$$

where  $\beta$  is the effective bandwidth of the radiometer and  $\tau$  is the integration time. We have verified that the temperature resolution computed from (57) is in good agreement with that computed from (55). Figure 10 shows  $T_N$  for the seven channels. As expected from equation (57), this figure is very similar to Figures 7 and 8.

The system gain G is defined by the reciprocal of (4).

$$G = (C_H - C_C)/(T_{AH} - T_{AC}) \quad (58)$$

This gain is the product of two components:

$$G = G_r G_{agc} \quad (59)$$

where  $G_r$  is the gain of the radiometer front-end and receiver and  $G_{agc}$  is an attenuation applied by the automatic gain control (AGC) system. The variation in the receiver gain  $G_r$  is primarily due to changes in the temperature of the receiver. The purpose of the AGC is to compensate for the  $G_r$  variation such that the counts stay within the range of the digital converter. There are 16 AGC settings, and each setting adds 0.5 dB attenuation. When SSM/I was turned on (for the second time) in July 1987, the AGC system found initial settings for all channels. We denote these initial settings by  $G_o$ . Thereafter,  $G_{agc}$  was changed in steps of 0.5 dB in order to keep the counts within bounds.

$$G = G_r G_o \Delta G \quad (60)$$

where  $\Delta G$  is the AGC setting relative to the initial AGC setting. The term  $\Delta G$  is found from the AGC readings given on the  $T_A$  tapes. In order to monitor the variation in the receiver gain relative to its initial gain, we computed the quantity  $G_r G_o$  by first computing G from (58) and then divided by  $\Delta G$ .

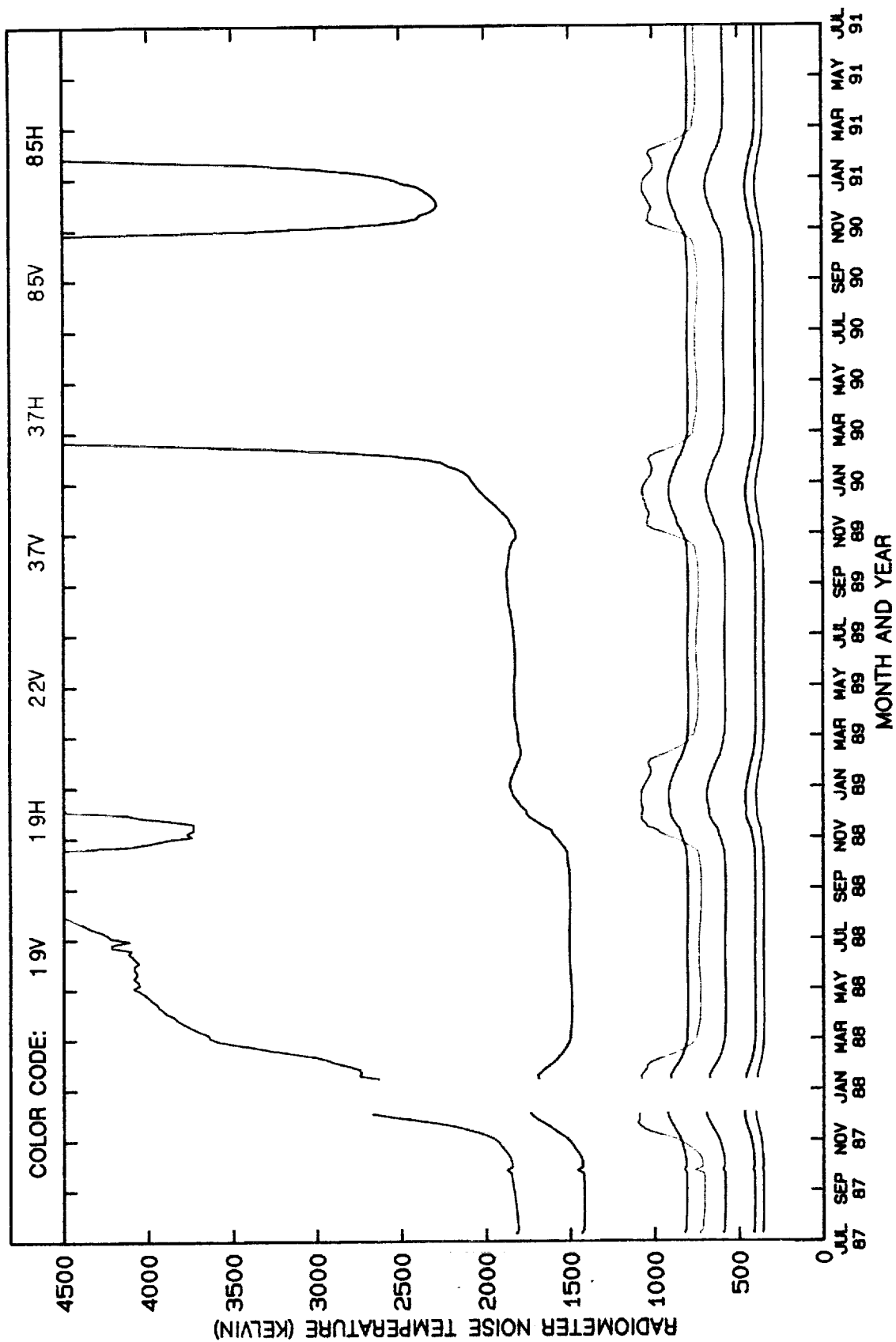


Fig. 10. F08 SSM/I radiometer noise temperatures.

Figure 11 shows  $G_r G_o$  for the seven SSM/I channels. The 85V and 85H gains decrease due to the heating cycles. The gain of the 37V and 37H channels also decreases with increasing temperature. In contrast, the gain of the 22V channel increases with increasing temperature. The gain of the 19V and 19H channels show little dependence on temperature.

The dependence of  $G_r$  on temperature is one of the primary reasons for doing an external calibration each scan. The temperature variation experience during a single orbit will produce changes in  $G_r$ . Unless frequent calibrations are performed, the changing gain will introduce errors in the computation of the antenna temperatures. We have verified that the derivative of  $G_r$  with respect to temperature displayed in Figure 11 is the same as that obtained from an analysis of the gain versus temperature variation for individual orbits.

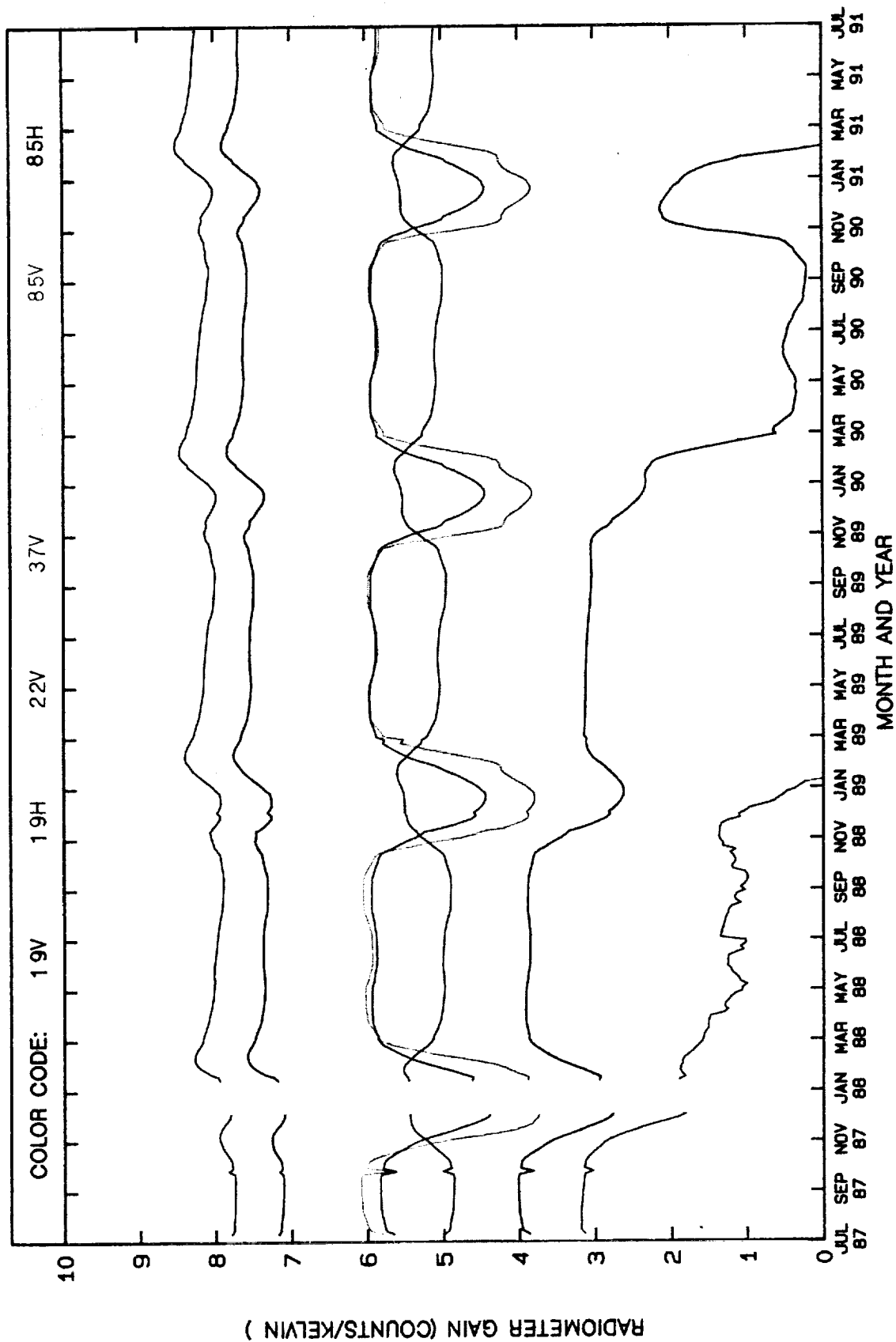


Fig. 11. F08 SSM/I radiometer gains.



## SECTION 9. ORGANIZATION OF ANTENNA TEMPERATURE TAPES

The SSM/I data reside on a series of 6250-bpi, 2400-ft magnetic tapes. A separate series of tapes is produced for each satellite. The first file on the tape is called the header file and contains general information about the tape. The remaining files are called data files and contain the SSM/I data. Each data file corresponds to a single SSM/I orbit. The beginning of an orbit is defined as the ascending equator crossing of the spacecraft (i.e., south-to-north crossing). The data files are chronologically ordered, and the last data file ends with a double end-of-file mark to specify the logical end of tape.

For each month and each satellite, eight  $T_A$  tapes are produced, except for a non-leap-year February for which there are only seven tapes. Table 3 shows the time periods corresponding to each of the tapes. A single tape contains either 3 or 4 days of data, except for February during a leap year, in which the eighth tape contains only 1 day of data. Each tape begins at the first ascending equator crossing for the Greenwich day specified in Table 3.

Table 3. The Eight SSM/I  $T_A$  Tapes per Month

Tape Number	Time Period (Day of Month)	
	Except February	February
1	1 through 4	1 through 4
2	5 through 8	5 through 8
3	9 through 12	9 through 12
4	13 through 15	13 through 16
5	16 through 19	17 through 20
6	20 through 23	21 through 24
7	24 through 27	25 through 28
8	28 through end of month	29 (for leap year)

The orbit period is approximately 102 minutes, and thus there are 14.1 orbits per day. A tape containing three (four) days of data will have either 42 or 43 (56 or 57) data files, if there are no data gaps. A four-day tape with no data gaps contains about 160 megabytes.

The header file contains 23192 bytes divided into 13 logical records, except for the F08 tapes prior to July 1, 1988, which contain only 21408 bytes divided into 12 logical records (see below). This record length of 1784 bytes is chosen to match the record length used for the data files.

The  $T_A$  data files consist of a series of chronologically-ordered logical records. Each record corresponds to a pair of A and B scans. The length of the logical record is 1784 bytes. The logical records are grouped into tape data blocks, which are separated by a 0.3 inch interblock gap. Each data block, except the last block in a file, contains 28544 bytes, which is 16 logical records. The last block in a file can contain any multiple of 1784 bytes, but not exceeding 28544 bytes. The logical record format for the  $T_A$  data is described in Section 10.

The remainder of this section discusses the contents of the header file. The first 12 records in the header file each contain 1784 ASCII characters. The following is an example of these 12 ASCII records

```
SSM/I F08 TAPE 1991_JUN_P2_A, 55 DATA FILES          -91129320242.0
SPEC. BEG DAY 156 Wed Jun 5, 1991 00:15:10
ACTUAL BEG DAY 156 Wed Jun 5, 1991 00:15:15
SPEC. END DAY 160 Sun Jun 9, 1991 01:00:43
ACTUAL END DAY 160 Sun Jun 9, 1991 01:00:42
SPECIFIED ORBITS: 020427 - 020483
ACTUAL ORBITS:    020427 - 020483
BEGIN GAP =      .08 MIN, END GAP =      .02 MIN
PERCENTAGE OF MISSING DATA = 16.389 %
PRODUCED BY REMOTE SENSING SYSTEMS
1101 COLLEGE AVE., SANTA ROSA, CA 95404
CONTACT FRANK WENTZ 707-545-2904 (F.WENTZ/OMNET)
```

The 12 records are padded on the right side with trailing ASCII blanks. This example is the header file for the second F08 T<sub>A</sub> tape in June 1991. The first line identifies the satellite and the time period according to year, month, and part of month (i.e., P1 through P8). The first line also gives the number of data files on the tape that follow the header file. The last number on the first line is a checksum. It is the sum of all 2-byte words in all data files on the tape. We use this number to verify tape copies.

There have been two changes to the first line in the header file. For the F08 tapes prior to 1991\_APR\_P7, the satellite number is not specified, and the format for the first line is

```
COMPACT TA TAPE 1991_APR_P6_A, 57 DATA FILES          -133747836598.0
```

The first header line for all F10 tapes specifies the satellite number. Thus if the satellite number is not specified, then the tape is an F08 tape. For the F08 tapes prior to 1989\_SEP\_P1, the checksum is not included, and the format is

```
COMPACT TA TAPE 1989_AUG_P8_A, 56 DATA FILES
```

The next four lines in the header file give the specified and actual begin and end times for the tape. The Julian day of year is given along with the date and time. The specified begin time is the time of the first ascending equator crossing specified for the T<sub>A</sub> tape. The specified end time is the time of the first ascending equator crossing specified for the next T<sub>A</sub> tape. The actual begin and end times are the first and last SSM/I scan times on the tape. Because of data gaps, the actual begin time may occur later than the specified begin time, and the actual end time may occur sooner than the specified end time. The next two lines in the header file give the specified and actual range of orbits. The differences (i.e., time gaps) between the specified and actual begin and end times are then given, and the following line shows the percentage of missing data for the specified time period. The remaining lines give the name and address of the organization responsible for producing the tape.

The 13th logical record is an inventory of the data files. Note that this inventory is not on the F08 tapes prior to 1988\_JUL\_P1. For these earlier tapes, there are only 12 records in the header file. The inventory record lists each orbit on the tape along with the times for the first and last scans in the orbit.

The following Fortran code can be used to print out the header file along with the tape inventory information.

```

      SUBROUTINE HEADER(LREC)
C
C   LREC IS THE ARRAY THAT CONTAINS THE BYTES IN THE TAPE BLOCK
C   THE USER MUST SUPPLY THE TAPE READ ROUTINE FOR FILLING LREC
C   BEFORE CALLING THIS ROUTINE
C
      CHARACTER*1 LREC(1784,16)
      INTEGER*2 IBUF(1784)
      DATA N1,N2,N3/256,65536,16777216/
C
C   PRINT OUT FIRST 12 LINES OF HEADER FILE
C
      DO 100 IREC=1,12
        WRITE(6,6001) (LREC(I,IREC),I=1,72)
6001  FORMAT(1X,72A1)
      100 CONTINUE
C
C   PRINT OUT INVENTORY FOR TAPE
C
      DO 200 I=1,1784
        IBUF(I)=ICHAR(LREC(I,13))
      200 CONTINUE
C
      N=-11
      DO 300 I=1,100
        N=N+12
C
C   IREV IS THE ORBIT NUMBER
C   ITIME1 IS THE TIME FOR THE FIRST SCAN IN ORBIT
C   ITIME2 IS THE TIME AT THE LAST SCAN IN THE ORBIT
C   ITIME1 AND ITIME2 ARE IN TERMS OF SECONDS FROM BEGIN OF 1987
C
      IREV= N3*IBUF(N) +N2*IBUF(N+1)+N1*IBUF(N+ 2)+IBUF(N+ 3)
      ITIME1= N3*IBUF(N+4)+N2*IBUF(N+5)+N1*IBUF(N+ 6)+IBUF(N+ 7)
      ITIME2= N3*IBUF(N+8)+N2*IBUF(N+9)+N1*IBUF(N+10)+IBUF(N+11)
C
C   IREV=0 MEANS YOU HAVE COME TO THE END OF THE INVENTORY
C
      IF(IREV.EQ.0) GO TO 310
      WRITE(6,6002) IREV,ITIME1,ITIME2
6002  FORMAT(1X,16,2I11)
      300 CONTINUE
      310 CONTINUE
      RETURN
      END

```

## SECTION 10. LOGICAL DATA RECORD FORMAT

The information in a logical data record is stored as a string of 1784 bytes, with each byte representing an integer ranging from 0 to 255. The subroutine DECODE converts this byte string to SSM/I sensor parameters (i.e., spacecraft and cell locations, calibration data, and antenna temperatures). The sensor data are stored in the common /OUTDAT/, which can be interfaced with the User's application program. A description of the DECODE calling procedure and the contents of /OUTDAT/ is given in Section 11.

We strongly recommend that DECODE be used to read the  $T_A$  tapes, rather than the User developing his/her own routine. The User does not need to know the logical record format for the  $T_A$  tapes because DECODE performs all the necessary conversions. The User only needs to call DECODE and then access the common /OUTDAT/. However, for some specialized applications, information on the record format may be useful. Accordingly, this section describes the data record format.

Table 4 shows the byte format for a logical record. The record is divided into 29 fields, with each field corresponding to a different set of data items. The table gives the number for the first byte in the field, the number of bytes in the field, the number of items in the field, the bias and scale factors to convert to the units specified, and a brief description of the data item. For example, Field 8 starts at byte 29, is 6 bytes long, and contains 3 hot load temperatures each stored as a 2-byte integer.

For Fields 1 and 2 and Fields 4 through 26, the conversion from tape bytes to the appropriate sensor parameter is simple. For these fields, each item corresponds to either 2 or 4 bytes, as indicated by Table 4. The bytes are first converted to a positive 16-bit or 32-bit integer  $I$ , where the first byte on the tape is the most significant. Letting  $S$  and  $B$  denote the scale and bias values given in Table 4, the sensor parameter  $P$  is given by

$$P = S (I - B) \quad (61)$$

where  $P$  is in terms of the units specified in Table 4.

The contents of Field 3 have undergone two changes. Originally, Field 3 was used to store the time for the spacecraft location, i.e., the time associated with the spacecraft latitude, longitude, and altitude. Beginning in 1989, the spacecraft location is computed at the scan time given in Field 1, hence it was not necessary to have a separate time for the spacecraft location. Thus, starting with the January 1, 1989  $T_A$  tape, Field 3 was used to store an orbit number that was more precise than the value stored in Field 2. Then starting with the September 1, 1989  $T_A$  tape the precise orbit number was stored in Field 2, thereby freeing Field 3. Finally, starting with the August 1, 1989  $T_A$  tapes for F08 and F10, Field 3 is used to store the satellite identification number and the incidence angle for the scan.

DECODE determines which  $T_A$  tape is being processed by looking at the scan time and then correctly interprets the contents of Field 3. Thus, the Field 3 format changes are transparent to the User.

The contents of Fields 13 through 19 have also undergone a change. Prior to September 1989, these fields contained various types of diagnostics data, which are of no use to the Users. Starting with the September 1, 1989  $T_A$  tape, these fields contain the SSM/I orbit parameters listed in Table 4. For the  $T_A$  tapes prior to September 1989, DECODE sets the seven orbit parameters to zero.

TABLE 4. DESCRIPTION OF LOGICAL DATA RECORDS ON SSM/ANTENNA TEMPERATURE TAPES

Field No.	First Byte	Field Bytes	Items	Bias	Scale	Units	Description
1	1	4	1	0	1.E0	seconds	integer time for scan from begin of 1987
2	5	4	1	0	1.E-4	none	orbit number
3	9	4	1	note 1	note 1	note 1	note 1
4	13	4	1	90000000	1.E-6	degrees	geodetic latitude of spacecraft
5	17	4	1	10000	1.E-4	seconds	fractional time for scan from begin of 1987
6	21	4	1	0	1.E-6	degrees	east longitude of spacecraft
7	25	4	1	0	1.E-3	km	altitude of spacecraft
8	29	6	3	0	1.E-2	kelvin	hot load temperatures
9	35	4	2	0	1.E0	counts	reference voltages
10	39	2	1	0	1.E-2	kelvin	r.f. mixer temperature
11	41	2	1	0	1.E-2	kelvin	forward radiator temperature
12	43	6	3	0	1.E0	counts	automatic gain control readings for A-scan
13 (note 2)	49	4	1	0	1.E0	seconds	spacecraft ascending node time from begin of 1987
14 (note 2)	53	4	1	0	1.E-4	seconds	period of spacecraft orbit
15 (note 2)	57	4	1	0	1.E-3	seconds	local time of spacecraft ascending node
16 (note 2)	61	4	1	0	1.E-6	degrees	180° minus inclination angle of spacecraft orbit
17 (note 2)	65	4	1	0	1.E-4	km	major semi-axis of spacecraft orbit
18 (note 2)	69	4	1	0	1.E-10	none	eccentricity of spacecraft orbit
19 (note 2)	73	4	1	0	1.E-5	degrees	angle of perigee of spacecraft orbit
20	77	70	35	0	1.E0	counts	cold counts for A-scan
21	147	70	35	0	1.E0	counts	hot counts for A-scan
22	217	6	3	0	1.E0	counts	automatic gain control readings for B-scan
23	223	20	10	0	1.E0	counts	cold counts for B-scan
24	243	20	10	0	1.E0	counts	hot counts for B-scan
25	263	38	19	9000	1.E-2	degrees	geodetic latitudes for A-scan
26	301	38	19	0	1.E-2	degrees	east longitudes for A-scan
27	339	38	19	packed	packed	degrees	B-scan minus A-scan latitude/longitude differences
28	377	640	576	packed	packed	kelvin	19, 22, 37 GHz T <sub>A</sub> 's and surface-type indices
29	1017	768	512	packed	packed	kelvin	85 GHz T <sub>A</sub> 's

Note 1: For T<sub>A</sub> tapes prior to January 1, 1989, Field 3 is the time for the spacecraft location. For T<sub>A</sub> tapes from January 1, 1989 through July 31, 1991, Field 3 is the precise orbit number. For the August 1, 1991 T<sub>A</sub> tape and thereafter, Field 3 contains the satellite identification number and the incidence angle.

Note 2: For T<sub>A</sub> tapes prior to September 1, 1989, Fields 13 through 19 contain diagnostic data. Thereafter, orbit parameters are stored in the fields.

For Fields 27, 28, and 29, the data are stored in special packed formats, and the above conversion (61) is not applicable. Each pair of latitude and longitude differences in Field 27 is stored as a single 2-byte integer, which must be decoded in a special way. The antenna temperatures in Fields 28 and 29 are stored as 12-bit integers, and the surface-type indices in Field 28 are stored as 3-bit integers. The procedure for unpacking these data is given in the listing of subroutine DECODE in Appendix B.

The T<sub>A</sub> tapes do not contain locations for all of the A-scan and B-scan cells. Rather, 19 pairs of latitudes and longitudes are stored for each scan. The subroutine DECODE interpolates these 19 locations to find the locations for the intermediate cells. The interpolation error is less than 2 km.

More information on the logical record format is given in Section 11, which provides a cross-reference between the fields shown in Table 4 and the SSM/I sensor parameters that are stored in common /OUTDAT/.

## SECTION 11. DESCRIPTION OF SUBROUTINE DECODE

A Fortran subroutine named DECODE is provided to the User for decoding the information on the  $T_A$  tapes. The subroutine is written in Fortran 77 and can be easily implemented on most computer systems. Before calling DECODE, the User must use his/her own routine to read from the tape. The bytes in a tape block must be read into the following array:

```
CHARACTER*1 LREC(1784,16)
```

The first dimension corresponds to the number of bytes in a logical record, and the second dimension corresponds to the maximum number of logical records in a tape block. See Sections 9 and 10 for further information on the tape format. Once LREC is filled, the User calls DECODE using the following statement:

```
CALL DECODE(185GHZ,ITB,IADJ,IREF,LREC)
```

The definitions of the User-defined arguments are given below. DECODE performs a number of functions. The bytes in LREC are converted to integers, which are then combined to compute values for the various SSM/I data items, including the spacecraft location, the calibration data, the cell locations, and the antenna temperatures. If ITB=1, then brightness temperatures are computed instead of antenna temperatures. These quantities are stored in a common area called /OUTDAT/, and program control is then returned to the User's program.

It is important for the User to understand the SSM/I sampling scheme. Each SSM/I scan is divided into 128 positions, with the distance between positions being 12.5 km. The along-track distance between scans is also 12.5 km. The 85 GHz channels are sampled at each scan position. Thus, the 85 GHz observations are available on a 12.5 km grid. A different sampling scheme is used for the five lower channels (i.e., 19V, 19H, 22V, 37V, and 37H). Observations of the lower channels are only taken every other scan. The scans during which the lower channels are sampled are called 'A-scans', and the scans during which only the 85 GHz channels are sampled are called 'B-scans' (see Figure 1). The distance between A-scans is then 25 km. The integration time for the five lower channels is twice that of the 85 GHz channels, and hence each lower channel is only sampled 64 times over the A-scan. Thus, the five lower channels are available on a 25 km grid. The phase of the integration time for the five lower channels is such that the locations of the 64 samples correspond to the locations of the odd 85 GHz scan positions. For example, the location of the 32<sup>th</sup> sample of the lower channels is the same as the location of the 63<sup>th</sup> sample of the 85 GHz channels. Each logical record on the  $T_A$  tape contains data for a single pair of A- and B-scans.

The remainder of this section is divided into three part. The first part discusses the specification of the arguments for DECODE. The second part is an overview of the execution of DECODE and the five subroutines called by DECODE. The third part is a detailed description of the common /OUTDAT/

Subroutine DECODE has five arguments that must be specified by the User. The definition of these arguments follows:

#### I85GHZ

This argument must be set to either 0 or 1. The User should set I85GHZ=0 if information on the two 85 GHz channels is not required. When I85GHZ=0, DECODE does not process the 85 GHz data, thereby substantially reducing the processing time. In this case, DECODE does not compute values for the B-scan arrays BLAT, BLON, BTAHI, and IBTOIL. Also, DECODE does not find values for the A-scan array ATAHI and for the even-numbered elements in the A-scan arrays ALAT, ALON, and IATOIL. These arrays are defined below. The even-numbered elements on the A-scan correspond to those cells for which only 85 GHz observations are taken. When I85GHZ is set to 1, all channels are processed.

#### ITB

This argument must be set to either 0 or 1. When ITB=0, the arrays TALO, ATAHI, and BTAHI are filled with the antenna temperatures computed from equation (3). When ITB=1, these arrays are filled with brightness temperatures computed from equations (19), (20), and (26). Also when ITB=1, the along-scan correction  $\eta$  specified by equation (16) is applied, but the offset correction  $\beta$  is set to zero. The offset correction removes small biases between the  $T_A$ 's and the Wentz [1991] radiative transfer model for the ocean. Along-scan and offset  $T_A$  corrections have not yet been found for the F10 SSM/I. If the User wants to implement the offset correction for F08, a simple change to the following two lines in subroutine FDTB08 is required. Comment out the first line and activate the second line.

```
DATA ABIAS/5*0./  
C DATA ABIAS/2.0,3.5,1.32,-1.57,-0.22/
```

For F08, if the User wants the 85H brightness temperatures for time periods when the 85V antenna temperatures are in error (see Section 8 and Figure 9), then a special change in subroutine FDTB08 is required to prevent the 85V  $T_A$  error for corrupting the 85H  $T_B$  computation. Set the 85H cross-polarization leakage term .01967 to 0. in the following line.

```
DATA CHI/.00379,.00525,.00983,0.0,.02136,.02664,.01387,.01967/
```

#### IADJ

This argument must be set to either 0 or 1. If IADJ=1, then DECODE does a 15-km along-track correction for the F08 tapes prior to 1989. No correction is done when IADJ=0. The setting of IADJ only affects the processing of F08 tapes prior to 1989. That is to say, for the F08  $T_A$  tapes after 1988 and for all F10 tapes, DECODE ignores the setting of IADJ because no along-track correction is needed for these tapes. Note that the along-track correction considerably slows down the processing speed, and hence IADJ should only be set to 1 if location accuracy is important. The correction translates the SSM/I imagery in the aft direction by 15 km.

#### IREC

This argument specifies which logical record is to be processed by DECODE. It must be set to a value between 1 and 16, and its value should not exceed the maximum number of logical records last read from the  $T_A$  tape. Note that the last block in a tape file can contain less than 16 logical records.

#### LREC

This is the character array described above. It contains the bytes that the User's program read from a data block on the  $T_A$  tape.



We now give an overview of the execution of DECODE and the five subroutines called by DECODE.

#### SUBROUTINE DECODE(I85GHZ, ITB, IADJ, IREC, LREC)

The arguments for this routine are described above. This routine begins by converting the specified logical record in the character array LREC to the integer array IBUF, which is used for all subsequent calculations. The routine then finds the spacecraft time, location, and orbit number. The satellite number ISAT (8=F08 and 10=F10) and incidence angle are next found. The calibration data and orbit parameters are then computed. DECODE next determines if an along-track adjustment is required. This adjustment is only required if the User has specified IADJ=1 and if the F08 scan time is before 1989 (i.e., IOLD=1). Note that the along-track correction requires the cell locations on both the A-scan and B-scan. Hence J85GHZ is set to 1 when the along-track correction is required. FDLTLN is then called to find the cell latitudes and longitudes. If the User has specified I85GHZ=1, then J85GHZ is set to 1 and FDLTLN finds locations for all cells on both scans. Otherwise, FDLTLN finds only the locations of the odd positions cells on the A-scan. The sub-routine FDTA is next called to compute the antenna temperatures. Finally, if the User has specified ITB=1, DECODE calls FDTB08 if the satellite is F08 or FDTB00 if the satellite is not F08 to convert the antenna temperatures to brightness temperatures.

#### SUBROUTINE FDLTLN(J85GHZ, IOLD, YAW)

This routine computes the latitudes and longitudes for the cells along the SSM/I scan. If the first argument J85GHZ=0, FDLTLN finds only the locations for the odd scan positions on the A-scan. If J85GHZ=1, then locations are found for all scan positions on both the A-scan and the B-scan. If the second argument IOLD=1, then a correction is applied to the location of scan position 128. This correction is only done for the F08 tapes prior to 1989. The third argument YAW specifies the yaw correction. This argument is scaled such that YAW=1 represents a 1.6° clockwise rotation (looking down on satellite) about nadir. The T<sub>A</sub> tapes do not contain locations for all cells. Rather, the latitudes and longitudes for 19 scan base positions are stored on tape, and the locations for the other cells are found by means of an interpolation. The error in the interpolation is less than 2 km. FDLTLN first finds the latitudes and longitudes for the 19 A-scan base positions. The remaining A-scan locations are then found by interpolating. If J85GHZ=0, the yaw correction is applied to the A-scan, and control returns to DECODE. If J85GHZ=1, the 19 B-scan base positions are found. The T<sub>A</sub> tapes contain the 19 differences of the B-scan latitudes and longitudes minus the A-scan latitudes and longitudes. Storing the differences requires less bytes than storing the full B-scan latitudes and longitudes. The 19 differences are added to the 19 A-scan base locations to obtain the 19 B-scan base locations. The interpolation is then done to obtain the locations at the other B-scan positions. The yaw correction is then applied to both the A-scan and B-scan locations, and control returns to DECODE.

#### SUBROUTINE ADJLOC(TRKADJ)

This routine shifts the cell locations in a direction parallel to the spacecraft velocity vector. The argument TRKADJ is scaled such that a value of TRKADJ=1 (-1) corresponds to a 12.5 km shift in the direction of (opposite to) the velocity vector.

#### SUBROUTINE FDTA(I85GHZ)

This routine computes the antenna temperatures. If the argument I85GHZ=0, then the 85 GHz antenna temperatures are not computed. Also if I85GHZ=0, the routine finds only the surface-type indices for the odd A-scan cells. If I85GHZ=1, then all antenna temperatures and surface-type indices are found. The antenna temperatures are stored on the  $T_A$  tapes as 12-bit words, and the surface-type indices are stored as 3-bit words. Most of the code in FDTA is for the unpacking of these bits. The precision of the  $T_A$ 's is 0.1 K except for anomalous values that exceed 380 K, for which the precision is 1.0 K.

#### SUBROUTINE FDTB08(I85GHZ)

This routine applies corrections to the F08 antenna temperatures and then converts the corrected antenna temperatures to brightness temperatures. If the argument I85GHZ=0, then the 85 GHz channels are not processed. The first time the routine is called, it computes the  $T_A$ -to- $T_B$  conversion coefficients and the along-scan correction arrays SBIAS1, SBIAS2, SBIAS3, SBIAS4, and SBIAS5. FDTB08 applies the along-scan correction  $\eta$  and the offset correction  $\beta$  to the  $T_A$ 's, except that no correction is applied to the 85 GHz channels. The corrected  $T_A$ 's are then converted to  $T_B$ 's and control returns to DECODE.

#### SUBROUTINE FDTB00(I85GHZ)

This routine is the same as FDTB08 except that the  $T_A$  correction arrays ABIAS, SBIAS1, SBIAS2, SBIAS3, SBIAS4, and SBIAS5 are set to zero. This routine is currently being used for the F10 and subsequent satellites until the  $T_A$  corrections are found.

The last part of this section gives a detailed description of the contents of the common /OUTDAT/. The form of /OUTDAT/ is:

```

C
  REAL*8 REV,XTIME
  INTEGER*4 ITIME,ITIMSC,IVOLT,IAGC,ICOLDA,IHOTA,ICOLDB,IHOTB,IASCTM
  INTEGER*4 IATOIL,IBTOIL,ISAT
  REAL*4 XLATSC,XLONSC,ALTSC,THT,HLTEMP,RFTMP,FRTEMP
  REAL*4 PERIOD,ASCLOC,ANGINC,AXIS,ECC,ANGPER,SPACER
  REAL*4 ALAT,ALON,BLAT,BLON,TALO,ATAHI,BTAHI
C
  COMMON/OUTDAT/ REV,XTIME,ITIME,ITIMSC,XLATSC,XLONSC,ALTSC,THT,
1 HLTEMP(3),IVOLT(2),RFTMP,FRTEMP,IAGC(6),
2 IASCTM,PERIOD,ASCLOC,ANGINC,AXIS,ECC,ANGPER,ISAT,SPACER(6),
3 ICOLDA(5,7),IHOTA(5,7),ICOLDB(5,2),IHOTB(5,2),
4 ALAT(128),ALON(128),BLAT(128),BLON(128),
5 TALO(5,64),ATAHI(2,128),BTAHI(2,128),IATOIL(128),IBTOIL(128)

```

The following is a description of each variable and array in /OUTDAT/. At the end of each description, we specify which field(s) in the Table 4 logical data record structure is used to compute the parameter.

#### REV

This 8-byte real variable is the orbit position of the spacecraft. Prior to 1989, the time corresponding to REV is given by ITIMSC. For 1989 and thereafter, the time corresponding to REV is given by XTIME. REV equals an integer value when the spacecraft is crossing the equator in the south-to-north direction (i.e., the ascending node). For example, REV=100.5 indicates that the spacecraft is halfway through orbit 100 and is crossing the equator in the descending, north-to-south direction. {Field 2 or Field 3}

#### XTIME

This 8-byte real variable is the Greenwich time at which the SSM/I B-scan begins. The time for the beginning of the A-scan is found by subtracting 1.9 s. This time is in terms of seconds from the beginning of 1987. Hence XTIME=0 denotes 00:00:00 Z, January 1, 1987. For the F08 T<sub>A</sub> tapes prior to 1987\_SEP\_P6, the fractional part of XTIME was not computed, and hence XTIME is the nearest integer to the actual time. That is to say, XTIME=ITIME for the early F08 T<sub>A</sub> tapes. {Fields 1 and 5}

#### ITIME

This 4-byte integer is the nearest integer to XTIME, i.e., ITIME=NINT(XTIME). {Field 1}

#### ITIMSC

This 4-byte integer is the nearest integer to the Greenwich time corresponding to the spacecraft location as specified by the spacecraft latitude XLATSC, longitude XLONSC, and altitude ALTSC. For T<sub>A</sub> tapes prior to 1989, this time is usually within 60 seconds of the scan time XTIME. Starting with the January 1, 1989 T<sub>A</sub> tape and thereafter, the spacecraft location is calculated at the scan time XTIME, and hence ITIMSC equals ITIME. This time is in terms of seconds from the beginning of 1987. {Field 3 for 1987 and 1988; Field 1 thereafter}

#### XLATSC

This 4-byte real variable is the spacecraft geodetic latitude in units of degrees. Negative latitudes correspond to south latitudes, and positive values correspond to north latitudes. This latitude corresponds to the location where a line from the Earth's center to the satellite intersects the Earth's surface. It is given by equation (36). Prior to 1989, the time corresponding to XLATSC is given by ITIMSC. For 1989 and thereafter, the time corresponding to XLATSC is given by XTIME. (Field 4)

#### XLONSC

This 4-byte real variable is the spacecraft east longitude in units of degrees. This longitude corresponds to the location where a line from the Earth's center to the satellite intersects the Earth's surface. It is given by equation (37). Prior to 1989, the time corresponding to XLONSC is given by ITIMSC. For 1989 and thereafter, the time corresponding to XLONSC is given by XTIME. (Field 6)

#### ALTSC

This 4-byte real variable is the spacecraft altitude in units of kilometers. It is the distance from the satellite to the location where a line from the Earth's center to the satellite intersects the Earth's surface. It is given by equation (38). Prior to 1989, the time corresponding to ALTSC is given by ITIMSC. For 1989 and thereafter, the time corresponding to ALTSC is given by XTIME. (Field 7)

#### THT

This 4-byte real variable is the incidence angle made by the antenna boresight vector and the vector normal to the Earth's surface at the point where the boresight vector intersects the Earth's surface. It is in units of degrees. It is computed as a function of the spacecraft altitude ALTSC and the Earth's radius of curvature at latitude XLATSC. The accuracy of the approximation being used is  $0.03^\circ$ . Prior to 1989, the time corresponding to THT is given by ITIMSC. For 1989 and thereafter, the time corresponding to THT is given by XTIME. (Fields 4 and 7 or Field 3)

#### HLTEMP(3)

This 4-byte real array contains the temperatures recorded by the three thermistors attached to the SSM/I external hot load. These temperatures are in units of Kelvin degrees. The average of these three temperatures is denoted by  $T_{OH}$  in equation (6). (Field 8)

#### IVOLT(2)

This 4-byte integer array contains two reference voltages for the SSM/I receiver. These voltages are in terms of counts and are not required by the calibration algorithm. (Field 9)

#### RFTEMP

This 4-byte real variable is the temperature recorded by the thermistor attached to the SSM/I R.F. mixer. It is in units of Kelvin degrees and is used to monitor the internal temperature of the receiver. It is not required by the calibration algorithm. (Field 10)

#### FRTEMP

This 4-byte real variable is the temperature recorded by the thermistor attached to the top plate of the rotating drum assembly which faces the hot load. It is in units of Kelvin degrees. FRTEMP is denoted by  $T_{OP}$  in equation (6). (Field 11)

### IAGC(6)

This 4-byte integer array contains the automatic gain control (AGC) readings in units of counts. The first three elements are the three reading for the A-scan, and the last three elements are the readings for the B-scan. For the A-scan, the AGC values for the individual channels are given by the following expressions:

```
IAGC85V = INT(IAGC(1)/256)
IAGC85H = INT((IAGC(1)-256*IAGC85V)/16)
IAGC37V = IAGC(1)-256*IAGC85V-16*IAGC85H
IAGC37H = INT(IAGC(2)/256)
IAGC19V = INT((IAGC(2)-256*IAGC37H)/16)
IAGC19H = IAGC(2)-256*IAGC37H-16*IAGC19V
IAGC22V = INT(IAGC(3)/256)
```

The B-scan values are also given by the above expressions, except that IAGC(4), IAGC(5), and IAGC(6) replace IAGC(1), IAGC(2), and IAGC(3), respectively. The AGC values are for diagnostic purposes only and are not required by the calibration algorithm. {Fields 12 and 22}

### IASCTM

This 4-byte integer is the Greenwich time of the ascending node for the current orbit. The ascending node time is defined as the time at which the satellite crosses the equator in the south-to-north direction. It is denoted by  $t_0$  in Section 6. This time is in terms of seconds from the beginning of 1987. For  $T_A$  tapes prior to September 1, 1989, this orbit parameter is not available and is set to zero. {Field 13}

### PERIOD

This 4-byte real variable is the period for the current orbit. The period is defined as the time between one ascending node and the next. It is denoted by  $P$  in Section 6. The period is in units of seconds. For  $T_A$  tapes prior to September 1, 1989, this orbit parameter is not available and is set to zero. {Field 14}

### ASCLOC

This 4-byte real variable is the local time of the ascending node for the current orbit. It is in terms of seconds in a day. It is denoted by  $t_L$  in Section 6. The east longitude of the ascending node is given by

```
XLONASC = 360.*(ASCLOC - MOD(IASCTM,86400))/86400.
IF(XLONASC.LT.0.) XLONASC=XLONASC+360.
```

For  $T_A$  tapes prior to September 1, 1989, this orbit parameter is not available and is set to zero. {Field 15}

### ANGINC

This 4-byte real variable is the inclination angle for the current orbit. It is in units of degrees and is denoted by  $\alpha$  in Section 6. For  $T_A$  tapes prior to September 1, 1989, this orbit parameter is not available and is set to zero. {Field 16}

### AXIS

This 4-byte real variable is the major semi-axis for the current orbit. It is in units of kilometers and is denoted by  $a$  in Section 6. For  $T_A$  tapes prior to September 1, 1989, this orbit parameter is not available and is set to zero. {Field 17}

#### ECC

This 4-byte real variable is the eccentricity for the current orbit. It is a pure number with no units and is denoted by  $\epsilon$  in Section 6. For  $T_A$  tapes prior to September 1, 1989, this orbit parameter is not available and is set to zero. (Field 18)

#### ANGPER

This 4-byte real variable is the angle of perigee for the current orbit. It is in units of degrees and is denoted by  $T_0$  in Section 6. For  $T_A$  tapes prior to September 1, 1989, this orbit parameter is not available and is set to zero. (Field 19)

#### ISAT

This 4-byte integer is the spacecraft identification number. For example, ISAT=8 denotes the F08 spacecraft, and ISAT=10 denotes the F10 spacecraft. (Field 3).

#### SPACER(6)

This 4-byte real array is filled with zeros. It is included in order to keep the size of the common /OUTDAT/ that same as for the first version of DECODE.

#### ICOLDA(5,7)

This 4-byte integer array contains the cold calibration counts  $C_C$  for the SSM/I A-scan. The first dimension of the array denotes the five samples of counts that are taken for each channel. The second dimension of the array denotes the channel, with the order being 19V, 19H, 22V, 37V, 37H, 85V and 85H. (Field 20)

#### IHOTA(5,7)

This 4-byte integer array contains the hot calibration counts  $C_H$  for the SSM/I A-scan. The first dimension of the array denotes the five samples of counts that are taken for each channel. The second dimension of the array denotes the channel, with the order being 19V, 19H, 22V, 37V, 37H, 85V, and 85H. (Field 21)

#### ICOLDB(5,2)

This 4-byte integer array contains the cold calibration counts  $C_C$  for the SSM/I B-scan. The first dimension of the array denotes the five samples of counts that are taken for each channel. The second dimension of the array denotes the channel, with the order being 85V and 85H. (Field 23)

#### IHOTB(5,2)

This 4-byte integer array contains the hot calibration counts  $C_H$  for the SSM/I B-scan. The first dimension of the array denotes the five samples of counts that are taken for each channel. The second dimension of the array denotes the channel, with the order being 85V and 85H. (Field 24)

#### ALAT(128)

This 4-byte real array contains the geodetic latitudes in units of degrees for the 128 cells in the SSM/I A-scan. Negative latitudes correspond to south latitudes, and positive values correspond to north latitudes. The odd elements in the array correspond to those cells for which observations are taken at all 7 SSM/I channels. The even elements correspond to those cells for which only the 85 GHz channels are sampled. The even elements are not compute if the User has selected I85GHZ=0. (Field 25)

#### ALON(128)

This 4-byte real array contains the longitudes for the 128 cells in the SSM/I A-scan. The longitudes are in units of degrees east of the prime meridian. The odd elements in this array correspond to those cells for which observations are taken at all 7 SSM/I channels. The even elements correspond to those cells for which only the 85 GHz channels are sampled. The even elements are not computed if the User has selected I85GHZ=0. (Field 26)

#### BLAT(128)

This 4-byte real array contains the geodetic latitudes in units of degrees for the 128 cells in the SSM/I B-scan. Negative latitudes correspond to south latitudes, and positive values correspond to north latitudes. On the B-scan, only the 85 GHz channels are sampled. This array is not computed if the User has selected I85GHZ=0. (Fields 25 and 27)

#### BLON(128)

This 4-byte real array contains the longitudes for the 128 cells in the SSM/I B-scan. The longitudes are in units of degrees east of the prime meridian. On the B-scan, only the 85 GHz channels are sampled. This array is not computed if the User has selected I85GHZ=0. (Fields 26 and 27)

#### TALO(5,64)

This 4-byte real array contains the antenna temperatures (or brightness temperatures if the User has selected ITB=1) in units of Kelvin for the SSM/I five lower channels. The first dimension *ich* denotes the channel, with the order being 19V, 19H, 22V, 37V, and 37H for *ich* = 1 to 5. The second dimension denotes the cell position on the A-scan. The 64 cell positions corresponds to the odd elements in the ALAT and ALON arrays. For example, the latitudes for TALO(*ich*,1), TALO(*ich*,32), and TALO(*ich*,64) are given by ALAT(1), ALAT(63), and ALAT(127), respectively. (Field 28)

#### ATAHI(2,128)

This 4-byte real array contains the antenna temperatures (or brightness temperatures if the User has selected ITB=1) in units of Kelvin for the 85 GHz channels on the A-scan. The first dimension denotes the 85V and 85H channel, respectively. The second dimension denotes the cell position. This array is not computed if the User has selected I85GHZ=0. (Field 29)

#### BTAHI(2,128)

This 4-byte real array contains the antenna temperatures (or brightness temperatures if the User has selected ITB=1) in units of Kelvin for the 85 GHz channels on the B-scan. The first dimension denotes the 85V and 85H channel, respectively. The second dimension denotes the cell position. This array is not computed if the User has selected I85GHZ=0. (Field 29)

#### IATOIL(128)

This 4-byte integer array contains the surface-type indices for the 128 cells in the SSM/I A-scan. Table 5 gives the definition of the surface-type indices. These indices are computed during the FNOC processing and correspond to the FNOC latitudes and longitudes rather than our recomputed latitudes and longitudes that are stored in ALAT and ALON. The difference between the FNOC locations and our locations rarely exceeds 25 km, and hence IATOIL will be correct except within 25 km of boundaries. The order of this array is the same as ALAT and ALON. The odd elements in this array correspond to those cells for which observations are taken at all 7 SSM/I channels. The even elements correspond to those cells for which only the 85 GHz channels are sampled. The even elements are not computed if the User has selected I85GHZ=0. (Field 28)

### IBTOIL(128)

This 4-byte integer array contains the surface-type indices for the 128 cells in the SSM/I B-scan. Table 5 gives the definition of the surface-type indices. These indices are computed during the FNOC processing and correspond to the FNOC latitudes and longitudes rather than our recomputed latitudes and longitudes that are stored in BLAT and BLON. The difference between the FNOC locations and our locations rarely exceeds 25 km, and hence IBTOIL will be correct except within 25 km of boundaries. The order of this array is the same as BLAT and BLON. This array is not computed if the User has selected I85GHZ=0. (Field 28)

Table 5. Definition of Surface-Type Index

surface-type index	definition
0	land
1	vegetal-covered land
2	not used
3	permanent sea ice
4	possible sea ice (note 1)
5	water
6	coast
7	index not available

Note 1. Possible sea ice is a climatology of regions where sea ice may occur.

Note 2. There can be a 25-km error in specifying surface type.

Note 3. The surface-type indices have no seasonal dependence.

Note 4. A value of 7 indicates that the FNOC surface index was out of bounds, and thus no surface index was available.



## SECTION 12. REFERENCES

Hollinger, J. P., DMSP Special Sensor Microwave/Imager Calibration/Validation, *NRL Final Report*, Naval Research Laboratory, Washington, DC, 1989.

Wentz, F. J., Measurement of Oceanic Wind Vector Using Satellite Microwave Radiometers, *RSS Tech. Rpt. 051591*, 33 pp, Remote Sensing Systems, Santa Rosa, CA, 1991.

**APPENDIX A. LIST OF ERRONEOUS DATA PERIODS  
FOR F08 SATELLITE FROM JULY 1987 THROUGH JUNE 1991**

(File BADLOC on enclosed 3.5" diskette)

1987	198	4.0	1987	198	5.0
1987	217	21.5	1987	217	23.5
1987	219	12.0	1987	219	14.0
1987	228	14.0	1987	228	16.0
1987	233	4.5	1987	233	6.5
1987	236	13.5	1987	239	15.0
1987	246	13.5	1987	246	14.5
1987	250	11.0	1987	250	12.0
1987	252	14.0	1987	252	16.0
1987	253	10.5	1987	253	12.5
1987	255	13.5	1987	255	15.0
1987	263	16.5	1987	263	18.0
1987	267	21.5	1987	267	23.0
1987	269	14.0	1987	269	16.0
1987	272	14.5	1987	272	16.0
1987	273	15.0	1987	273	15.5
1987	277	14.0	1987	277	15.5
1987	280	11.5	1987	280	13.0
1987	283	1.0	1987	283	3.0
1987	284	21.3	1987	284	23.0
1987	294	21.0	1987	294	22.0
1987	304	22.0	1987	304	23.7
1987	310	14.0	1987	310	15.0
1987	312	5.0	1987	312	5.7
1987	316	21.0	1987	316	23.5
1987	317	14.2	1987	317	16.0
1987	321	5.3	1987	321	7.8
1987	323	5.3	1987	323	6.0
1987	329	2.0	1987	329	3.7
1987	329	10.1	1987	329	10.8
1988	018	2.5	1988	018	4.5
1988	018	9.0	1988	018	10.3
1988	019	15.8	1988	019	17.5
1988	022	5.3	1988	022	8.6
1988	025	4.8	1988	025	7.2
1988	026	10.8	1988	026	12.6
1988	026	23.0	1988	027	1.0
1988	030	22.1	1988	030	23.5
1988	031	11.5	1988	031	13.3
1988	032	22.0	1988	032	23.3
1988	035	6.1	1988	035	6.8
1988	067	4.5	1988	067	5.1
1988	069	14.1	1988	069	15.8
1988	075	23.3	1988	076	0.2
1988	076	10.9	1988	076	13.1
1988	084	7.5	1988	084	9.8
1988	091	21.6	1988	092	1.1
1988	092	21.4	1988	092	23.5
1988	108	1.1	1988	108	2.0
1988	110	0.7	1988	110	3.3
1988	110	12.2	1988	110	16.0
1988	114	13.2	1988	114	15.2
1988	117	4.2	1988	117	7.5
1988	118	0.7	1988	118	2.3
1988	118	13.9	1988	118	16.0
1988	120	5.2	1988	120	6.9
1988	138	23.8	1988	139	1.0
1988	140	1.2	1988	140	3.6
1988	145	3.7	1988	145	5.6
1988	145	15.2	1988	145	18.0
1988	146	5.1	1988	146	7.5
1988	147	23.5	1988	148	2.0
1988	148	11.2	1988	148	12.5
1988	148	14.9	1988	148	16.4
1988	149	17.2	1988	149	21.1
1988	149	23.0	1988	150	0.5
1988	150	10.9	1988	150	11.8
1988	152	16.5	1988	152	17.9
1988	153	5.5	1988	153	9.1
1988	154	20.6	1988	154	22.4

1988	166	21.2	1988	166	22.9
1988	169	2.2	1988	169	4.2
1988	169	10.4	1988	169	11.0
1988	171	15.2	1988	171	15.4
1988	176	14.0	1988	176	15.7
1988	180	19.9	1988	180	21.0
1988	180	23.6	1988	181	0.6
1988	181	1.2	1988	181	1.6
1988	181	4.9	1988	181	6.1
1988	181	9.9	1988	181	11.2
1988	181	20.7	1988	181	21.0
1988	182	3.6	1988	182	4.0
1988	182	5.1	1988	182	5.3
1988	182	12.9	1988	182	13.5
1988	182	17.8	1988	182	19.7
1988	188	11.5	1988	188	13.2
1988	192	14.1	1988	192	16.0
1988	217	20.0	1988	217	21.0
1988	224	13.6	1988	224	15.3
1988	225	9.0	1988	225	11.4
1988	225	12.5	1988	225	13.1
1988	227	3.8	1988	227	5.2
1988	229	16.3	1988	229	16.8
1988	230	12.0	1988	230	13.7
1988	230	16.4	1988	230	19.5
1988	230	21.5	1988	230	22.8
1988	231	15.7	1988	231	16.1
1988	232	1.1	1988	232	3.3
1988	233	17.3	1988	233	21.3
1988	234	12.2	1988	234	12.8
1988	236	10.1	1988	236	11.2
1988	236	11.9	1988	236	12.6
1988	237	22.1	1988	237	22.8
1988	237	23.7	1988	238	0.9
1988	238	2.1	1988	238	2.6
1988	239	21.7	1988	239	23.6
1988	240	0.0	1988	240	0.5
1988	240	2.0	1988	240	4.0
1988	240	9.2	1988	240	10.0
1988	241	7.7	1988	241	8.0
1988	241	9.0	1988	241	12.2
1988	242	4.1	1988	242	6.2
1988	242	7.7	1988	242	8.0
1988	242	21.1	1988	242	22.4
1988	242	22.9	1988	242	23.3
1988	243	3.9	1988	243	4.6
1988	243	9.8	1988	243	10.0
1988	243	11.6	1988	243	12.6
1988	243	16.2	1988	243	19.1
1988	243	21.1	1988	243	21.4
1988	244	0.1	1988	244	1.0
1988	244	2.4	1988	244	5.5
1988	244	9.0	1988	244	9.8
1988	244	15.3	1988	244	16.6
1988	246	6.9	1988	246	8.0
1988	246	11.7	1988	246	12.2
1988	246	14.9	1988	246	16.4
1988	249	10.2	1988	249	12.0
1988	249	12.7	1988	249	13.6
1988	249	17.6	1988	249	20.3
1988	250	4.1	1988	250	7.6
1988	250	8.9	1988	250	9.6
1988	250	12.4	1988	250	13.2
1988	250	15.6	1988	250	15.8
1988	251	15.6	1988	251	16.1
1988	254	9.8	1988	254	15.8
1988	254	17.4	1988	254	18.6
1988	255	3.1	1988	255	4.1
1988	255	14.8	1988	255	15.4
1988	255	18.0	1988	255	21.9

1988	255	23.3	1988	255	23.5
1988	256	3.8	1988	256	4.1
1988	256	11.1	1988	256	12.7
1988	257	7.6	1988	257	9.1
1988	257	10.9	1988	257	14.4
1988	258	0.8	1988	258	2.2
1988	258	8.9	1988	258	10.0
1988	258	10.8	1988	258	11.9
1988	258	15.5	1988	258	15.7
1988	258	16.7	1988	258	19.8
1988	258	20.9	1988	258	21.1
1988	259	22.7	1988	259	23.7
1988	260	2.2	1988	260	3.3
1988	260	10.3	1988	260	10.6
1988	260	13.8	1988	260	14.2
1988	260	14.7	1988	260	14.9
1988	261	22.8	1988	261	23.0
1988	262	22.9	1988	262	23.4
1988	263	2.6	1988	263	3.4
1988	263	9.7	1988	263	10.4
1988	263	10.9	1988	263	11.4
1988	263	23.0	1988	263	23.2
1988	264	2.6	1988	264	2.8
1988	264	4.7	1988	264	6.6
1988	265	7.7	1988	265	8.3
1988	265	8.6	1988	265	9.1
1988	265	11.3	1988	265	12.7
1988	265	23.1	1988	266	0.8
1988	284	15.7	1988	284	15.9
1988	284	16.9	1988	284	20.2
1988	284	20.7	1988	284	20.9
1988	286	8.3	1988	286	8.9
1988	286	15.0	1988	286	16.2
1988	286	16.6	1988	286	21.2
1988	286	22.2	1988	286	23.4
1988	289	7.7	1988	289	8.3
1988	289	9.3	1988	289	11.0
1988	289	11.7	1988	289	12.0
1988	289	14.5	1988	289	15.2
1988	290	12.7	1988	290	15.1
1988	290	15.4	1988	290	16.0
1988	290	16.8	1988	290	17.3
1988	290	17.8	1988	290	22.3
1988	290	23.0	1988	290	23.2
1988	291	0.8	1988	291	1.6
1988	291	8.9	1988	291	12.0
1988	291	12.6	1988	291	13.5
1988	291	21.2	1988	291	22.5
1988	292	0.5	1988	292	0.9
1988	292	7.5	1988	292	8.5
1988	292	8.8	1988	292	10.1
1988	292	10.4	1988	292	11.5
1988	292	13.2	1988	292	13.5
1988	292	14.5	1988	292	15.2
1988	292	17.0	1988	292	17.3
1988	292	17.7	1988	292	18.3
1988	292	19.0	1988	292	19.8
1988	292	21.0	1988	292	22.6
1988	293	5.6	1988	293	7.5
1988	293	16.8	1988	293	18.4
1988	299	7.3	1988	299	7.8
1988	301	16.9	1988	301	18.8
1988	301	20.8	1988	301	21.5
1988	301	22.9	1988	301	23.5
1988	303	9.9	1988	303	10.1
1988	303	15.0	1988	303	16.6
1988	307	18.0	1988	307	18.3
1988	308	8.8	1988	308	10.6
1988	311	2.0	1988	311	3.7
1988	311	5.6	1988	311	5.8

1988 311	23.7	1988 312	0.0
1988 312	3.1	1988 312	5.1
1988 312	5.9	1988 312	7.5
1988 312	9.7	1988 312	10.0
1988 312	11.0	1988 312	11.6
1988 312	16.4	1988 312	17.3
1988 313	1.3	1988 313	1.5
1988 313	4.7	1988 313	6.2
1988 313	6.5	1988 313	7.7
1988 313	9.5	1988 313	9.8
1988 314	15.5	1988 314	15.8
1988 315	14.0	1988 315	15.8
1988 320	17.6	1988 320	17.9
1988 321	3.2	1988 321	4.7
1988 321	8.9	1988 321	13.5
1988 321	14.3	1988 321	14.8
1988 322	9.3	1988 322	10.4
1988 322	12.8	1988 322	14.3
1988 325	16.9	1988 325	18.1
1988 326	2.0	1988 326	3.2
1988 326	4.9	1988 326	5.2
1988 326	22.4	1988 326	22.9
1988 327	0.0	1988 327	1.8
1988 327	5.3	1988 327	6.1
1988 327	11.8	1988 327	12.8
1988 327	20.7	1988 327	21.9
1988 328	2.0	1988 328	3.1
1988 328	18.3	1988 328	18.9
1988 329	17.9	1988 329	20.0
1988 330	23.1	1988 331	1.0
1988 331	9.1	1988 331	10.8
1988 332	12.4	1988 332	13.8
1988 332	14.1	1988 332	15.2
1988 332	18.9	1988 332	19.9
1988 334	5.6	1988 334	7.8
1988 335	20.7	1988 335	21.3
1988 336	5.1	1988 336	7.4
1988 336	8.0	1988 336	9.1
1988 336	16.5	1988 336	17.9
1988 337	11.8	1988 337	12.8
1988 338	7.7	1988 338	9.2
1988 338	11.1	1988 338	11.7
1988 338	18.1	1988 338	19.5
1988 338	20.0	1988 338	20.8
1988 338	21.9	1988 338	22.3
1988 339	0.4	1988 339	1.4
1988 339	2.7	1988 339	3.8
1988 339	4.3	1988 339	4.9
1988 339	14.3	1988 339	15.0
1988 349	3.9	1988 349	4.6
1988 349	9.4	1988 349	10.9
1988 349	12.3	1988 349	12.5
1988 349	12.8	1988 349	14.9
1988 349	15.6	1988 349	16.8
1988 349	17.0	1988 349	18.1
1988 349	18.5	1988 349	20.7
1988 349	21.0	1988 349	22.5
1988 349	22.7	1988 349	23.4
1988 350	3.9	1988 350	5.2
1988 350	5.4	1988 350	5.7
1988 350	6.0	1988 350	8.1
1988 350	8.6	1988 350	9.9
1988 350	10.2	1988 350	11.5
1988 350	12.0	1988 350	12.4
1988 350	16.8	1988 350	18.0
1988 351	16.6	1988 351	19.7
1988 351	20.0	1988 351	20.3
1988 351	21.6	1988 351	21.8
1988 351	23.8	1988 352	0.7
1988 352	1.6	1988 352	2.3

1988	352	2.9	1988	352	3.1
1988	352	4.8	1988	352	5.3
1988	352	5.6	1988	352	7.1
1988	352	8.1	1988	352	8.9
1988	352	9.8	1988	352	10.6
1988	354	9.8	1988	354	11.0
1988	354	11.2	1988	354	11.9
1988	354	16.2	1988	354	17.5
1988	356	6.0	1988	356	6.6
1988	357	2.7	1988	357	3.0
1989	7	5.8	1989	7	8.8
1989	30	14.1	1989	30	15.8
1989	46	14.2	1989	46	15.8
1989	56	3.2	1989	56	4.2
1989	56	4.8	1989	56	7.4
1989	92	1.4	1989	92	2.0
1989	130	23.5	1989	131	0.0
1989	155	23.7	1989	156	0.0
1989	156	23.4	1989	157	0.0
1989	163	23.6	1989	164	0.0
1989	164	23.3	1989	165	0.0
1989	169	22.2	1989	170	0.0
1989	173	23.1	1989	174	0.0
1989	179	23.6	1989	180	0.0
1989	182	22.9	1989	183	0.0
1989	186	23.7	1989	187	0.0
1989	187	23.5	1989	188	0.0
1989	195	23.6	1989	196	0.0
1989	207	22.7	1989	208	0.0
1989	234	23.6	1989	235	0.0
1989	271	20.8	1989	271	22.5
1989	276	23.0	1989	277	1.0
1990	019	16.6	1990	019	17.0
1990	065	23.9	1990	066	0.0
1990	169	3.1	1990	169	5.0
1990	216	14.2	1990	216	16.2
1990	243	9.9	1990	243	11.4
1990	272	22.1	1990	273	0.1
1990	282	9.7	1990	282	10.4
1990	294	0.0	1990	294	3.0
1990	300	20.5	1990	300	21.5
1990	301	6.0	1990	301	7.5
1990	307	18.7	1990	307	19.8
1990	308	0.0	1990	308	1.0
1990	309	0.0	1990	309	1.0
1991	74	0.0	1991	74	0.8
1991	98	18.5	1991	98	19.3
1991	134	15.0	1991	134	16.0
1991	181	22.1	1991	181	22.6

**APPENDIX B. LISTING OF SUBROUTINE DECODE, REVISION 1**

(File DECODE.FOR on the enclosed 3.5" diskette)



```

C      SUBROUTINE DECODE(185GHZ,ITB,IADJ,IREC,LREC)
C ***** DESCRIPTION OF ARGUMENTS *****
C      185GHZ=0 PROCESSES ONLY THE 19, 22, AND 37 GHZ OBS.
C      185GHZ=1 PROCESSES ALL CHANNELS
C
C      ITB=0 COMPUTES TA'S
C      ITB=1 COMPUTES TB'S
C
C      IADJ=0 DOES NO ALONGTRACK LOCATION CORRECTION
C      IADJ=1 DOES AN ALONGTRACK LOCATION CORRECTION
C
C      IREC DENOTES LOGICAL RECORD NUMBER (1 THROUGH 16)
C
C      LREC IS THE ARRAY THAT CONTAINS THE BYTES IN THE TAPE BLOCK
C      THE USER MUST SUPPLY THE TAPE READ ROUTINE FOR FILLING LREC
C      BEFORE CALLING THIS ROUTINE
C ***** DECLARATION OF VARIABLES, ARRAYS, AND COMMONS *****
C
C      CHARACTER*1 LREC(1784,16)
C
C      INTEGER*2 IBUF
C      COMMON /INDATA/ IBUF(1784)
C
C      REAL*8 REV,XTIME
C      INTEGER*4 ITIME,ITIMSC,IVOLT,IAGC,ICOLDA,IHOTA,ICOLDB,IHOTB,IASCTM
C      INTEGER*4 IATOIL,IBTOIL,ISAT
C      REAL*4 XLATSC,XLONSC,ALTSC,THT,HLTEMP,RFTEMP,FRTEMP
C      REAL*4 PERIOD,ASCLOC,ANGINC,AXIS,ECC,ANGPER,SPACER
C      REAL*4 ALAT,ALON,BLAT,BLON,TALO,ATAHI,BTAHI
C      COMMON/OUTDAT/ REV,XTIME,ITIME,ITIMSC,XLATSC,XLONSC,ALTSC,THT,
C      1 HLTEMP(3),IVOLT(2),RFTEMP,FRTEMP,IAGC(6),
C      2 IASCTM,PERIOD,ASCLOC,ANGINC,AXIS,ECC,ANGPER,ISAT,SPACER(6),
C      2 ICOLDA(5,7),IHOTA(5,7),ICOLDB(5,2),IHOTB(5,2),
C      3 ALAT(128),ALON(128),BLAT(128),BLON(128),
C      4 TALO(5,64),ATAHI(2,128),BTAHI(2,128),IATOIL(128),IBTOIL(128)
C
C      ***** DATA INITIALIZATION *****
C
C      DATA N1,N2,N3/256,65536,16777216/
C      DATA RAD/0.017453293/
C ***** BEGIN EXECUTION *****
C
C      TRANSFER TAPE BYTES IN IREC LOGICAL RECORD TO ARRAY IBUF
C
C      DO 100 I=1,1784
C      IBUF(I)=ICHAR(LREC(I,IREC))
C 100 CONTINUE

```

```

C
C FIND SCAN TIME
C
  ITIME= N3*IBUF( 1)+N2*IBUF( 2)+N1*IBUF( 3)+IBUF( 4)
  IFRCTM=N3*IBUF(17)+N2*IBUF(18)+N1*IBUF(19)+IBUF(20)
  IF(IFRCTM.EQ.0) XTIME=ITIME
  IF(IFRCTM.NE.0) XTIME=ITIME+1.D-4*(IFRCTM-10000)

C
C FIND SPACECRAFT TIME AND ORBIT NUMBER
C
  IOLD=1 FOR ALL SCANS BEFORE 1989
C
  IF(ITIME.LT.63163966) THEN
    IOLD=1
    ITIMSC= N3*IBUF( 9)+N2*IBUF(10)+N1*IBUF(11)+IBUF(12)
  ELSE
    IOLD=0
    ITIMSC=ITIME
  ENDIF

C
  IF(ITIME.GE.63163966.AND.ITIME.LT.84156110) THEN
    REV=1.D-4*(N3*IBUF( 9)+N2*IBUF(10)+N1*IBUF(11)+IBUF(12))
  ELSE
    REV=1.D-4*(N3*IBUF( 5)+N2*IBUF( 6)+N1*IBUF( 7)+IBUF( 8))
  ENDIF

C
C FIND SPACECRAFT LATITUDE, LONGITUDE, AND ALTITUDE
C
  XLATSC=1.D-6*(N3*IBUF(13)+N2*IBUF(14)+N1*IBUF(15)+IBUF(16))-90.
  XLONSC=1.D-6*(N3*IBUF(21)+N2*IBUF(22)+N1*IBUF(23)+IBUF(24))
  ALTSC= 1.D-3*(N3*IBUF(25)+N2*IBUF(26)+N1*IBUF(27)+IBUF(28))

C
C DETERMINE SATELLITE NUMBER AND INCIDENCE ANGLE
C
  FACTOR OF .7040147 = SIN(44.75 DEG)
  FACTOR OF .7116583 = SIN(45.37 DEG)
C
  IF(ITIME.GT.144554200) THEN
    ITERM=N3*IBUF( 9)+N2*IBUF(10)+N1*IBUF(11)+IBUF(12)
    THT=0.001*INT(ITERM/1000)
    ISAT=ITERM-1000*INT(ITERM/1000)
  ELSE
    EARTH=RADIUS OF CURVATURE OF EARTH'S SURFACE
    EARTH=6345.7+55.0*SIN(RAD*XLATSC)**2
    DIFREV=DABS(REV-300-(XTIME-16530609)/6118.)
    IF(DIFREV.LT.100.) THEN
      ISAT=8
      THT=ASIN(0.7040147*(EARTH+ALTSC)/EARTH)/RAD
    ELSE
      ISAT=10
      THT=ASIN(0.7116583*(EARTH+ALTSC)/EARTH)/RAD
    ENDIF
  ENDIF

C
C FIND RADIOMETER CALIBRATION DATA
C
  HLTEMP(3)=0.01*(N1*IBUF(29)+IBUF(30))
  HLTEMP(2)=0.01*(N1*IBUF(31)+IBUF(32))
  HLTEMP(1)=0.01*(N1*IBUF(33)+IBUF(34))
  RFTEMP= 0.01*(N1*IBUF(39)+IBUF(40))
  FRTEMP= 0.01*(N1*IBUF(41)+IBUF(42))
  IVOLT(2)= N1*IBUF(35)+IBUF(36)
  IVOLT(1)= N1*IBUF(37)+IBUF(38)
  IAGC(3)= N1*IBUF(43)+IBUF(44)
  IAGC(2)= N1*IBUF(45)+IBUF(46)
  IAGC(1)= N1*IBUF(47)+IBUF(48)

```

```

C
  N=-2
  DO 200 ICH=1,7
    IF(ICH.NE.7) SPACER(ICH)=0.
    DO 200 IP=1,5
      N=N+2
      ICOLDA(IP,ICH)=N1*IBUF(N + 77)+IBUF(N + 78)
      IHOTA(IP,ICH)= N1*IBUF(N +147)+IBUF(N +148)
200 CONTINUE
C
  IAGC(6)=N1*IBUF(217)+IBUF(218)
  IAGC(5)=N1*IBUF(219)+IBUF(220)
  IAGC(4)=N1*IBUF(221)+IBUF(222)
C
  N=-2
  DO 300 ICH=1,2
    DO 300 IP=1,5
      N=N+2
      ICOLDB(IP,ICH)=N1*IBUF(N +223)+IBUF(N +224)
      IHOTB(IP,ICH)= N1*IBUF(N +243)+IBUF(N +244)
300 CONTINUE
C
  FIND ORBIT PARAMETERS
C
  IF(ITIME.LT.84156110) THEN
    IASCTM=0
    PERIOD=0.
    ASCLOC=0.
    ANGINC=0.
    AXIS=0.
    ECC=0.
    ANGPER=0.
C
  ELSE
    IASCTM=      N3*IBUF(49)+N2*IBUF(50)+N1*IBUF(51)+IBUF(52)
    PERIOD= 1.D-4*(N3*IBUF(53)+N2*IBUF(54)+N1*IBUF(55)+IBUF(56))
    ASCLOC= 1.D-3*(N3*IBUF(57)+N2*IBUF(58)+N1*IBUF(59)+IBUF(60))
    ANGINC= 1.D-6*(N3*IBUF(61)+N2*IBUF(62)+N1*IBUF(63)+IBUF(64))
    ANGINC=180.-ANGINC
    AXIS= 1.D-4*(N3*IBUF(65)+N2*IBUF(66)+N1*IBUF(67)+IBUF(68))
    ECC= 1.D-10*(N3*IBUF(69)+N2*IBUF(70)+N1*IBUF(71)+IBUF(72))
    ANGPER= 1.D-5*(N3*IBUF(73)+N2*IBUF(74)+N1*IBUF(75)+IBUF(76))
    ENDIF
C
  DETERMINE IF ALONGTRACK AND YAW ADJUSTMENT IS NEEDED
C
  TRKADJ=-1.2 CORRESPONDS TO A 15 KM ALONGTRACK ADJUSTMENT
C
  YAW=.3125 CORRESPONDS TO A 0.5 DEG. YAW ROTATION
C
  TRKADJ=0.
  IF(IOLD.EQ.1.AND.IADJ.EQ.1) TRKADJ=-1.2
  YAW=0.
  IF(ISAT.EQ.8) YAW=.3125
C
  FIND CELL LATITUDES AND LONGITUDES
C
  J85GHZ=I85GHZ
  IF(TRKADJ.NE.0.) J85GHZ=1
  CALL FDLTLN(J85GHZ,IOLD,YAW)
  IF(TRKADJ.NE.0.) CALL ADJLOC(TRKADJ)
C
  FIND EITHER TA'S OR TB'S
C
  CALL FDTA(I85GHZ)
  IF(ITB.EQ.1.AND.ISAT.EQ. 8) CALL FDTB08(I85GHZ)
  IF(ITB.EQ.1.AND.ISAT.NE. 8) CALL FDTB00(I85GHZ)
C
  RETURN
C
  END

```

```

SUBROUTINE FDLTLN(J85GHZ,IOLD,YAW)
C
C   THIS SUBROUTINE FINDS THE LATS AND LONS FOR THE SSMI CELLS
C   J85GHZ=0 DOES NOT DO 85 GHZ LAT/LOW, J85GHZ=1 DOES 85 GHZ LAT LOW
C
C   INTEGER*4 INDEX(19),JINDEX(3,109)
C
C   SPECIFY COMMON /INDATA/
C
C   INTEGER*2 IBUF
C   COMMON /INDATA/ IBUF(1784)
C
C   SPECIFY COMMON /OUTDAT/
C
C   REAL*8 REV,XTIME
C   INTEGER*4 ITIME,ITIMSC,IVOLT,IAGC,ICOLDA,IHOTA,ICOLDB,IHOTB,IASCTM
C   INTEGER*4 IATOIL,IBTOIL,ISAT
C   REAL*4 XLATSC,XLONSC,ALTSC,THT,HLTEMP,RFTEMP,FRTEMP
C   REAL*4 PERIOD,ASCLOC,ANGINC,AXIS,ECC,ANGPER,SPACER
C   REAL*4 ALAT,ALON,BLAT,BLON,TALO,ATAHI,BTAHI
C   COMMON/OUTDAT/ REV,XTIME,ITIME,ITIMSC,XLATSC,XLONSC,ALTSC,THT,
1  HLTEMP(3),IVOLT(2),RFTEMP,FRTEMP,IAGC(6),
2  IASCTM,PERIOD,ASCLOC,ANGINC,AXIS,ECC,ANGPER,ISAT,SPACER(6),
3  ICOLDA(5,7),IHOTA(5,7),ICOLDB(5,2),IHOTB(5,2),
4  ALAT(128),ALON(128),BLAT(128),BLON(128),
5  TALO(5,64),ATAHI(2,128),BTAHI(2,128),IATOIL(128),IBTOIL(128)
C
C   DATA INITIALIZATION
C
C   DATA N1/256/
C   DATA RAD/0.017453293/
C   DATA INDEX/1,9,17,25,33,41,49,57,65,73,81,89,97,105,113,121,123,
1  127,128/
C   DATA JINDEX/
1  5, 1, 9, 13, 9, 17, 21, 17, 25, 29, 25, 33, 37, 33, 41,
1  45, 41, 49, 53, 49, 57, 61, 57, 65, 69, 65, 73, 77, 73, 81,
1  85, 81, 89, 93, 89, 97, 101, 97, 105, 109, 105, 113, 117, 113, 121,
1  3, 1, 5, 7, 5, 9, 11, 9, 13, 15, 13, 17, 19, 17, 21,
1  23, 21, 25, 27, 25, 29, 31, 29, 33, 35, 33, 37, 39, 37, 41,
1  43, 41, 45, 47, 45, 49, 51, 49, 53, 55, 53, 57, 59, 57, 61,
1  63, 61, 65, 67, 65, 69, 71, 69, 73, 75, 73, 77, 79, 77, 81,
1  83, 81, 85, 87, 85, 89, 91, 89, 93, 95, 93, 97, 99, 97, 101,
1  103, 101, 105, 107, 105, 109, 111, 109, 113, 115, 113, 117, 119, 117, 121,
1  125, 123, 127, 2, 1, 3, 4, 3, 5, 6, 5, 7, 8, 7, 9,
1  10, 9, 11, 12, 11, 13, 14, 13, 15, 16, 15, 17, 18, 17, 19,
1  20, 19, 21, 22, 21, 23, 24, 23, 25, 26, 25, 27, 28, 27, 29,
1  30, 29, 31, 32, 31, 33, 34, 33, 35, 36, 35, 37, 38, 37, 39,
1  40, 39, 41, 42, 41, 43, 44, 43, 45, 46, 45, 47, 48, 47, 49,
1  50, 49, 51, 52, 51, 53, 54, 53, 55, 56, 55, 57, 58, 57, 59,
1  60, 59, 61, 62, 61, 63, 64, 63, 65, 66, 65, 67, 68, 67, 69,
1  70, 69, 71, 72, 71, 73, 74, 73, 75, 76, 75, 77, 78, 77, 79,
1  80, 79, 81, 82, 81, 83, 84, 83, 85, 86, 85, 87, 88, 87, 89,
1  90, 89, 91, 92, 91, 93, 94, 93, 95, 96, 95, 97, 98, 97, 99,
1  100, 99, 101, 102, 101, 103, 104, 103, 105, 106, 105, 107, 108, 107, 109,
1  110, 109, 111, 112, 111, 113, 114, 113, 115, 116, 115, 117, 118, 117, 119,
1  120, 119, 121, 122, 121, 123, 124, 123, 125, 126, 125, 127/
C
C   BEGIN EXECUTION
C
C   SET TABLE LAT/LOW FOR A-SCAN
C
C   N=-2
C   DO 100 JCEL=1,19
C   N=N+2
C   ICEL=INDEX(JCEL)
C   ALAT(ICEL)=0.01*(N1*IBUF(N +263)+IBUF(N +264)-9000)
C   ALON(ICEL)=0.01*(N1*IBUF(N +301)+IBUF(N +302))
C   IF(ALON(ICEL).GE.360.) ALON(ICEL)=ALON(ICEL)-360.
100 CONTINUE
C

```

```

C   SET MID-POINTS FOR A-SCAN
C
  NCEL=46
  IF(J85GHZ.EQ.1) NCEL=109
  DO 200 JCEL=1,NCEL
    ICEL=JNDEX(1,JCEL)
    I1=JNDEX(2,JCEL)
    I2=JNDEX(3,JCEL)
    DIFLAT=ALAT(I2)-ALAT(I1)
    AVGLAT=0.5*(ALAT(I1)+ALAT(I2))
    DIFLON=ALON(I2)-ALON(I1)
    IF(DIFLON.GT. 180.) DIFLON=DIFLON-360.
    IF(DIFLON.LT.-180.) DIFLON=DIFLON+360.
    AVGLON=ALON(I1)+0.5*DIFLON
    XSQ=(2.*RAD*AVGLAT)**2
    XFAC=1.-0.16627142*XSQ+0.00807934*XSQ*XSQ-0.000151880*XSQ*XSQ*XSQ
    ALAT(ICEL)=AVGLAT*(1.+0.125*(RAD*DIFLON)**2*XFAC)
    X=RAD*(90.-ABS(AVGLAT))
    TANLAT=1./(X+X*X*X/3.)
    IF(AVGLAT.LT.0.) TANLAT=-TANLAT
    ALON(ICEL)=AVGLON-0.2500*RAD*DIFLAT*DIFLON*TANLAT
    IF(ALON(ICEL).LT. 0.) ALON(ICEL)=ALON(ICEL)+360.
    IF(ALON(ICEL).GE.360.) ALON(ICEL)=ALON(ICEL)-360.
200 CONTINUE
C
C   DO YAW CORRECTION
C
  IF(J85GHZ.EQ.0) THEN
    IF(YAW.EQ.0.) RETURN
  C
    DO 260 ICEL=1,127,2
      IF(ICEL.EQ.127) GO TO 250
      DIFLAT=ALAT(ICEL+2)-ALAT(ICEL)
      DIFLON=ALON(ICEL+2)-ALON(ICEL)
      IF(DIFLON.LT.-180.) DIFLON=DIFLON+360.
      IF(DIFLON.GT. 180.) DIFLON=DIFLON-360.
250 CONTINUE
      ALAT(ICEL)=ALAT(ICEL)+YAW*DIFLAT
      ALON(ICEL)=ALON(ICEL)+YAW*DIFLON
      IF(ALON(ICEL).LT. 0.) ALON(ICEL)=ALON(ICEL)+360.
      IF(ALON(ICEL).GE.360.) ALON(ICEL)=ALON(ICEL)-360.
260 CONTINUE
      RETURN
    ENDIF
  C
  C   SET TABLE LAT/LON FOR B-SCAN
  C
    N=-2
    DO 300 JCEL=1,19
      N=N+2
      ICEL=INDEX(JCEL)
      IDEL=N1*IBUF(N +339)+IBUF(N +340)
      IF(IDEL.GT.32767) IDEL=IDEL-65536
      LATDEL=(IDEL+30000)/1000-30
      LONDEL=IDEL+29100-1000*(LATDEL+30)
      BLAT(ICEL)=ALAT(ICEL)+0.01*LATDEL
      BLON(ICEL)=ALON(ICEL)+0.01*LONDEL
      IF(BLON(ICEL).LT. 0.) BLON(ICEL)=BLON(ICEL)+360.
      IF(BLON(ICEL).GE.360.) BLON(ICEL)=BLON(ICEL)-360.
300 CONTINUE
  C

```

```

C      SET MID-POINTS FOR B-SCAN
C
DO 400 JCEL=1,109
ICEL=JNDEX(1,JCEL)
I1=JNDEX(2,JCEL)
I2=JNDEX(3,JCEL)
DIFLAT=BLAT(I2)-BLAT(I1)
AVGLAT=0.5*(BLAT(I1)+BLAT(I2))
DIFLON=BLON(I2)-BLON(I1)
IF(DIFLON.GT. 180.) DIFLON=DIFLON-360.
IF(DIFLON.LT.-180.) DIFLON=DIFLON+360.
AVGLON=BLON(I1)+0.5*DIFLON
XSQ=(2.*RAD*AVGLAT)**2
XFAC=1.-0.16627142*XSQ+0.00807934*XSQ*XSQ-0.000151880*XSQ*XSQ*XSQ
BLAT(ICEL)=AVGLAT*(1.+0.125*(RAD*DIFLON)**2*XFAC)
X=RAD*(90.-ABS(AVGLAT))
TANLAT=1./(X+X*X*X/3.)
IF(AVGLAT.LT.0.) TANLAT=-TANLAT
BLON(ICEL)=AVGLON-0.2500*RAD*DIFLAT*DIFLON*TANLAT
IF(BLON(ICEL).LT. 0.) BLON(ICEL)=BLON(ICEL)+360.
IF(BLON(ICEL).GE.360.) BLON(ICEL)=BLON(ICEL)-360.
400 CONTINUE
C
C      CORRECT CELL 128 FOR DATA BEFORE 1989
C
IF(IOLD.EQ.1) THEN
DIFLAT=ALAT(127)-ALAT(126)
DIFLON=ALON(127)-ALON(126)
IF(DIFLON.LT.-180.) DIFLON=DIFLON+360.
IF(DIFLON.GT. 180.) DIFLON=DIFLON-360.
ALAT(128)=ALAT(127)+DIFLAT
ALON(128)=ALON(127)+DIFLON
IF(ALON(128).LT. 0.) ALON(128)=ALON(128)+360.
IF(ALON(128).GE.360.) ALON(128)=ALON(128)-360.
C
DIFLAT=BLAT(127)-BLAT(126)
DIFLON=BLON(127)-BLON(126)
IF(DIFLON.LT.-180.) DIFLON=DIFLON+360.
IF(DIFLON.GT. 180.) DIFLON=DIFLON-360.
BLAT(128)=BLAT(127)+DIFLAT
BLON(128)=BLON(127)+DIFLON
IF(BLON(128).LT. 0.) BLON(128)=BLON(128)+360.
IF(BLON(128).GE.360.) BLON(128)=BLON(128)-360.
ENDIF
C
C      DO YAW CORRECTION
C
IF(YAW.EQ.0.) RETURN
DO 600 ICEL=1,128
IF(ICEL.EQ.128) GO TO 580
DIFLAT1=ALAT(ICEL+1)-ALAT(ICEL)
DIFLON1=ALON(ICEL+1)-ALON(ICEL)
IF(DIFLON1.LT.-180.) DIFLON1=DIFLON1+360.
IF(DIFLON1.GT. 180.) DIFLON1=DIFLON1-360.
DIFLAT2=BLAT(ICEL+1)-BLAT(ICEL)
DIFLON2=BLON(ICEL+1)-BLON(ICEL)
IF(DIFLON2.LT.-180.) DIFLON2=DIFLON2+360.
IF(DIFLON2.GT. 180.) DIFLON2=DIFLON2-360.
580 CONTINUE
ALAT(ICEL)=ALAT(ICEL)+2.*YAW*DIFLAT1
ALON(ICEL)=ALON(ICEL)+2.*YAW*DIFLON1
IF(ALON(ICEL).LT. 0.) ALON(ICEL)=ALON(ICEL)+360.
IF(ALON(ICEL).GE.360.) ALON(ICEL)=ALON(ICEL)-360.
BLAT(ICEL)=BLAT(ICEL)+2.*YAW*DIFLAT2
BLON(ICEL)=BLON(ICEL)+2.*YAW*DIFLON2
IF(BLON(ICEL).LT. 0.) BLON(ICEL)=BLON(ICEL)+360.
IF(BLON(ICEL).GE.360.) BLON(ICEL)=BLON(ICEL)-360.
600 CONTINUE
RETURN
END

```

```

C      SUBROUTINE ADJLOC(TRKADJ)
C
C      CORRECT FOR ALONGTRACK ERROR
C
C      SPECIFY COMMON /OUTDAT/
C
      REAL*8 REV,XTIME
      INTEGER*4 ITIME,ITIMSC,IVOLT,IAGC,ICOLDA,IHOTA,ICOLDB,IHOTB,IASCTM
      INTEGER*4 IATOIL,IBTOIL,ISAT
      REAL*4 XLATSC,XLONSC,ALTSC,THT,HLTEMP,RFTMP,FRTEMP
      REAL*4 PERIOD,ASCLOC,ANGINC,AXIS,ECC,ANGPER,SPACER
      REAL*4 ALAT,ALON,BLAT,BLON,TALO,ATAHI,BTAHI
      COMMON/OUTDAT/ REV,XTIME,ITIME,ITIMSC,XLATSC,XLONSC,ALTSC,THT,
1 HLTEMP(3),IVOLT(2),RFTMP,FRTEMP,IAGC(6),
2 IASCTM,PERIOD,ASCLOC,ANGINC,AXIS,ECC,ANGPER,ISAT,SPACER(6),
2 ICOLDA(5,7),IHOTA(5,7),ICOLDB(5,2),IHOTB(5,2),
3 ALAT(128),ALON(128),BLAT(128),BLON(128),
4 TALO(5,64),ATAHI(2,128),BTAHI(2,128),IATOIL(128),IBTOIL(128)
C
C      BEGIN EXECUTION
C
      DO 100 ICEL=1,128
      DIFLAT=BLAT(ICEL)-ALAT(ICEL)
      ALAT(ICEL)=ALAT(ICEL)+TRKADJ*DIFLAT
      BLAT(ICEL)=BLAT(ICEL)+TRKADJ*DIFLAT
C
      DIFLON=BLON(ICEL)-ALON(ICEL)
      IF(DIFLON.LT.-180.) DIFLON=DIFLON+360.
      IF(DIFLON.GT. 180.) DIFLON=DIFLON-360.
C
      ALON(ICEL)=ALON(ICEL)+TRKADJ*DIFLON
      IF(ALON(ICEL).LT. 0.) ALON(ICEL)=ALON(ICEL)+360.
      IF(ALON(ICEL).GE.360.) ALON(ICEL)=ALON(ICEL)-360.
C
      BLON(ICEL)=BLON(ICEL)+TRKADJ*DIFLON
      IF(BLON(ICEL).LT. 0.) BLON(ICEL)=BLON(ICEL)+360.
      IF(BLON(ICEL).GE.360.) BLON(ICEL)=BLON(ICEL)-360.
100 CONTINUE
      RETURN
      END
C

```

```

SUBROUTINE FDTA(185GHZ)
C
C THIS SUBROUTINE FINDS THE ANTENNA TEMPERATURES AND SURFACE TYPES
C
C INTEGER*4 ITALO(5),ITAH1(8)
C
C SPECIFY COMMON /INDATA/
C
C INTEGER*2 IBUF
C COMMON /INDATA/ IBUF(1784)
C
C SPECIFY COMMON /OUTDAT/
C
C REAL*8 REV,XTIME
C INTEGER*4 ITIME,ITIMSC,IVOLT,IAGC,ICOLDA,IHOTA,ICOLDB,IHOTB,IASCTM
C INTEGER*4 IATOIL,IBTOIL,ISAT
C REAL*4 XLATSC,XLONSC,ALTSC,THT,HLTEMP,RFTEMP,FRTEMP
C REAL*4 PERIOD,ASCLOC,ANGINC,AXIS,ECC,ANGPER,SPACER
C REAL*4 ALAT,ALON,BLAT,BLON,TALO,ATAH1,BTAH1
C COMMON/OUTDAT/ REV,XTIME,ITIME,ITIMSC,XLATSC,XLONSC,ALTSC,THT,
1 HLTEMP(3),IVOLT(2),RFTEMP,FRTEMP,IAGC(6),
2 IASCTM,PERIOD,ASCLOC,ANGINC,AXIS,ECC,ANGPER,ISAT,SPACER(6),
2 ICOLDA(5,7),IHOTA(5,7),ICOLDB(5,2),IHOTB(5,2),
3 ALAT(128),ALON(128),BLAT(128),BLON(128),
4 TALO(5,64),ATAH1(2,128),BTAH1(2,128),IATOIL(128),IBTOIL(128)
C
C DATA N1,N2/256,65536/
C
C BEGIN EXECUTION
C
C N=-10
C M=-12
C
C DO 100 ICEL=1,64
C JCEL=2*ICEL-1
C
C FIND THE TA'S FOR THE 3 LOWER FREQUENCIES
C
C N=N+10
C
C IWORK4=N2*IBUF(N +377)+N1*IBUF(N+378)+IBUF(N+379)
C ITAV=INT(IWORK4/4096)
C ITALO(1)=ITAV
C ITALO(2)=IWORK4-4096*ITAV
C
C IWORK4=N2*IBUF(N +380)+N1*IBUF(N+381)+IBUF(N+382)
C ITAV=INT(IWORK4/4096)
C ITALO(4)=ITAV
C ITALO(5)=IWORK4-4096*ITAV
C
C IWORK4=N2*IBUF(N +383)+N1*IBUF(N+384)+IBUF(N+385)
C ITAV=INT(IWORK4/4096)
C ITALO(3)=ITAV
C
C SCALE THE TA'S
C
C DO 20 ICH=1,5
C IF(ITALO(ICH).LE.3800) THEN
C TALO(ICH,ICEL)=0.1*ITALO(ICH)
C ELSE
C TALO(ICH,ICEL)=ITALO(ICH)-3420
C ENDIF
20 CONTINUE
C
C FIND THE TOIL FLAGS
C
C IRES=IWORK4-4096*ITAV
C ITOIL1=INT(IRES/512)
C IATOIL(JCEL)=ITOIL1
C

```



```

      IF(185GHZ.EQ.0) GO TO 100
C
C      FIND 85 GHZ TOILS'S AND TA'S
C
      M=M+12
C
      IRES=IRES-ITOIL1*512
      ITOIL2=INT(IRES/64)
      IRES=IRES-ITOIL2*64
      ITOIL3=INT(IRES/8)
      ITOIL4=IRES-ITOIL3*8
      IBTOIL(JCEL)=ITOIL2
      IATOIL(JCEL+1)=ITOIL3
      IBTOIL(JCEL+1)=ITOIL4
C
      IWORK4=N2*IBUF(M+1017)+N1*IBUF(M+1018)+IBUF(M+1019)
      ITAV=INT(IWORK4/4096)
      ITAHI(1)=ITAV
      ITAHI(3)=IWORK4-4096*ITAV
C
      IWORK4=N2*IBUF(M+1020)+N1*IBUF(M+1021)+IBUF(M+1022)
      ITAV=INT(IWORK4/4096)
      ITAHI(2)=ITAV
      ITAHI(4)=IWORK4-4096*ITAV
C
      IWORK4=N2*IBUF(M+1023)+N1*IBUF(M+1024)+IBUF(M+1025)
      ITAV=INT(IWORK4/4096)
      ITAHI(5)=ITAV
      ITAHI(7)=IWORK4-4096*ITAV
C
      IWORK4=N2*IBUF(M+1026)+N1*IBUF(M+1027)+IBUF(M+1028)
      ITAV=INT(IWORK4/4096)
      ITAHI(6)=ITAV
      ITAHI(8)=IWORK4-4096*ITAV
C
C      SCALE THE TA'S
C
      K=0
      DO 40 KCEL=JCEL,JCEL+1
      DO 40 ICH=1,2
      K=K+1
      IF(ITAHI(K).LE.3800) THEN
      ATAHI(ICH,KCEL)=0.1*ITAHI(K)
      ELSE
      ATAHI(ICH,KCEL)=ITAHI(K)-3420
      ENDIF
C
      K=K+1
C
      IF(ITAHI(K).LE.3800) THEN
      BTAHI(ICH,KCEL)=0.1*ITAHI(K)
      ELSE
      BTAHI(ICH,KCEL)=ITAHI(K)-3420
      ENDIF
C
      40 CONTINUE
C
      100 CONTINUE
      RETURN
      END
C

```

```

SUBROUTINE FDT808(185GHZ)
C
C THIS SUBROUTINE CONVERTS ANTENNA TEMPS. TO BRIGHTNESS TEMPS.
C F08 ALONG-SCAN AND OFFSET CORRECTIONS
C
REAL*4 DELTA(4),CHI(2,4),AVGTA(5),ABIAS(5)
REAL*4 SBIAS1(64),SBIAS2(64),SBIAS3(64),SBIAS4(64),SBIAS5(64)
REAL*4 AVV(4),AHV(4),AOV(4),AHH(4),AVH(4),AOH(4)
C
C SPECIFY COMMON /OUTDAT/
C
REAL*8 REV,XTIME
INTEGER*4 ITIME,ITIMSC,IVOLT,IAGC,ICOLDA,IHOTA,ICOLDB,IHOTB,IASCTM
INTEGER*4 IATOIL,IBTOIL,ISAT
REAL*4 XLATSC,XLONSC,ALTSC,THT,HLTEMP,RFTEMP,FRTEMP
REAL*4 PERIOD,ASCLOC,ANGINC,AXIS,ECC,ANGPER,SPACER
REAL*4 ALAT,ALON,BLAT,BLON,TALO,ATAHI,BTAHI
COMMON/OUTDAT/ REV,XTIME,ITIME,ITIMSC,XLATSC,XLONSC,ALTSC,THT,
1 HLTEMP(3),IVOLT(2),RFTEMP,FRTEMP,IAGC(6),
2 IASCTM,PERIOD,ASCLOC,ANGINC,AXIS,ECC,ANGPER,ISAT,SPACER(6),
2 ICOLDA(5,7),IHOTA(5,7),ICOLDB(5,2),IHOTB(5,2),
3 ALAT(128),ALON(128),BLAT(128),BLON(128),
4 TALO(5,64),ATAHI(2,128),BTAHI(2,128),IATOIL(128),IBTOIL(128)
C
C DATA INITIALIZATION
C
DATA ISTART/1/
DATA DELTA/0.03199,0.02685,0.01434,0.01186/
DATA CHI/.00379,.00525,.00983,0.0,.02136,.02664,.01387,.01967/
DATA AVGTA/190.93,130.14,215.42,211.39,158.16/
C
C *****
C DATA ABIAS/5*0./
C IN ORDER TO APPLY WENTZ [1992] OFFSET TO TB'S,
C ACTIVATE NEXT STATEMENT AND COMMENT OUT PREVIOUS STATEMENT
C DATA ABIAS/2.0,3.5,1.32,-1.57,-0.22/
C *****
C
DATA SBIAS1/
+ .09, .10, .12, .12, .13, .13, .13, .13, .13, .14,
+ .14, .14, .14, .14, .15, .15, .14, .14, .13, .12,
+ .12, .11, .11, .11, .11, .11, .12, .11, .10, .10,
+ .09, .07, .06, .05, .05, .04, .03, .03, .02, .01,
+ -.01, -.02, -.04, -.05, -.06, -.08, -.09, -.09, -.11, -.12,
+ -.14, -.18, -.21, -.26, -.30, -.36, -.43, -.52, -.63, -.75/
DATA SBIAS2/
+ .01, .01, .01, .01, .01, .01, .01, .02, .03, .04,
+ .04, .05, .05, .05, .05, .05, .04, .04, .04, .04,
+ .04, .04, .04, .04, .04, .05, .06, .07, .07, .08,
+ .07, .07, .06, .07, .07, .06, .06, .06, .06, .06,
+ .05, .04, .04, .04, .04, .02, .00, -.01, -.02, -.03,
+ -.04, -.06, -.09, -.12, -.16, -.20, -.26, -.32, -.39, -.48/
DATA SBIAS3/
+ .08, .09, .10, .11, .11, .12, .12, .13, .14, .14,
+ .15, .15, .17, .17, .16, .16, .15, .14, .14, .14,
+ .13, .13, .13, .13, .13, .13, .14, .13, .14, .13,
+ .12, .11, .10, .09, .09, .08, .07, .05, .04, .03,
+ .02, .00, -.01, -.02, -.04, -.05, -.07, -.10, -.12, -.14,
+ -.17, -.20, -.25, -.31, -.36, -.42, -.50, -.63, -.79, -.97/
DATA SBIAS4/
+ .03, .04, .05, .06, .06, .07, .09, .10, .11, .13,
+ .14, .15, .15, .16, .16, .16, .16, .16, .16, .15,
+ .14, .14, .14, .13, .13, .13, .14, .13, .13, .13,
+ .12, .11, .10, .10, .09, .08, .08, .06, .06, .05,
+ .04, .03, .02, .01, .00, -.02, -.05, -.07, -.09, -.12,
+ -.16, -.18, -.22, -.27, -.33, -.42, -.50, -.60, -.74, -.90/

```

```

DATA SBIAS5/
+ -.14, -.13, -.12, -.10, -.09, -.10, -.09, -.07, -.05, -.04,
+ -.03, .00, .01, .03, .04, .04, .04, .05, .05, .05,
+ .04, .04, .04, .05, .05, .07, .08, .09, .10, .11,
+ .10, .10, .09, .10, .10, .09, .09, .09, .09, .08,
+ .07, .07, .07, .09, .09, .08, .08, .08, .08, .08,
+ .06, .04, .00, -.03, -.07, -.11, -.16, -.22, -.29, -.41/

C
C BEGIN EXECUTION
C
IF(ISTART.EQ.0) GO TO 30
ISTART=0
DO 10 IFREQ=1,4
IF(IFREQ.EQ.2) GO TO 10
XFAC=(1.-CHI(1,IFREQ)*CHI(2,IFREQ))*(1.-DELTA(IFREQ))
AVV(IFREQ)=(1.+CHI(1,IFREQ))/XFAC
AHV(IFREQ)=-CHI(1,IFREQ)*(1.+CHI(2,IFREQ))/XFAC
AOV(IFREQ)=(1.-AVV(IFREQ)-AHV(IFREQ))*2.7
AHH(IFREQ)=(1.+CHI(2,IFREQ))/XFAC
AVH(IFREQ)=-CHI(2,IFREQ)*(1.+CHI(1,IFREQ))/XFAC
AOH(IFREQ)=(1.-AHH(IFREQ)-AVH(IFREQ))*2.7
10 CONTINUE
C
DO 20 ICEL=1,64
SBIAS1(ICEL)=1.-SBIAS1(ICEL)/AVGTA(1)
SBIAS2(ICEL)=1.-SBIAS2(ICEL)/AVGTA(2)
SBIAS3(ICEL)=1.-SBIAS3(ICEL)/AVGTA(3)
SBIAS4(ICEL)=1.-SBIAS4(ICEL)/AVGTA(4)
SBIAS5(ICEL)=1.-SBIAS5(ICEL)/AVGTA(5)
20 CONTINUE
C
30 CONTINUE
C
DO 100 ICEL=1,64
TA19V=TALO(1,ICEL)*SBIAS1(ICEL)-ABIAS(1)
TA19H=TALO(2,ICEL)*SBIAS2(ICEL)-ABIAS(2)
TA22V=TALO(3,ICEL)*SBIAS3(ICEL)-ABIAS(3)
TA37V=TALO(4,ICEL)*SBIAS4(ICEL)-ABIAS(4)
TA37H=TALO(5,ICEL)*SBIAS5(ICEL)-ABIAS(5)
C
TALO(1,ICEL)=AVV(1)*TA19V+AHV(1)*TA19H+AOV(1)
TALO(2,ICEL)=AHH(1)*TA19H+AVH(1)*TA19V+AOH(1)
TALO(3,ICEL)=1.01993*TA22V+1.994
TALO(4,ICEL)=AVV(3)*TA37V+AHV(3)*TA37H+AOV(3)
TALO(5,ICEL)=AHH(3)*TA37H+AVH(3)*TA37V+AOH(3)
100 CONTINUE
C
IF(185GHZ.EQ.0) RETURN
C
DO 200 ICEL=1,128
TB85V=AVV(4)*ATAHI(1,ICEL)+AHV(4)*ATAHI(2,ICEL)+AOV(4)
TB85H=AHH(4)*ATAHI(2,ICEL)+AVH(4)*ATAHI(1,ICEL)+AOH(4)
ATAHI(1,ICEL)=TB85V
ATAHI(2,ICEL)=TB85H
TB85V=AVV(4)*BTAHI(1,ICEL)+AHV(4)*BTAHI(2,ICEL)+AOV(4)
TB85H=AHH(4)*BTAHI(2,ICEL)+AVH(4)*BTAHI(1,ICEL)+AOH(4)
BTAHI(1,ICEL)=TB85V
BTAHI(2,ICEL)=TB85H
200 CONTINUE
RETURN
END
C

```

```

SUBROUTINE FDTB00(185GHZ)
C
C THIS SUBROUTINE CONVERTS ANTENNA TEMPS. TO BRIGHTNESS TEMPS.
C ALONG-SCAN AND OFFSET CORRECTIONS SET TO ZERO
C
REAL*4 DELTA(4),CHI(2,4),AVGTA(5),ABIAS(5)
REAL*4 SBIAS1(64),SBIAS2(64),SBIAS3(64),SBIAS4(64),SBIAS5(64)
REAL*4 AVV(4),AHV(4),AOV(4),AHH(4),AVH(4),AOH(4)
C
C SPECIFY COMMON /OUTDAT/
C
REAL*8 REV,XTIME
INTEGER*4 ITIME,ITIMSC,IVOLT,IAGC,ICOLDA,IHOTA,ICOLDB,IHOTB,IASCTM
INTEGER*4 IATOIL,IBTOIL,ISAT
REAL*4 XLATSC,XLONSC,ALTSC,THT,HLTEMP,RFTEMP,FRTEMP
REAL*4 PERIOD,ASCLOC,ANGINC,AXIS,ECC,ANGPER,SPACER
REAL*4 ALAT,ALON,BLAT,BLON,TALO,ATAHI,BTAHI
COMMON/OUTDAT/ REV,XTIME,ITIME,ITIMSC,XLATSC,XLONSC,ALTSC,THT,
1 HLTEMP(3),IVOLT(2),RFTEMP,FRTEMP,IAGC(6),
2 IASCTM,PERIOD,ASCLOC,ANGINC,AXIS,ECC,ANGPER,ISAT,SPACER(6),
2 ICOLDA(5,7),IHOTA(5,7),ICOLDB(5,2),IHOTB(5,2),
3 ALAT(128),ALON(128),BLAT(128),BLON(128),
4 TALO(5,64),ATAHI(2,128),BTAHI(2,128),IATOIL(128),IBTOIL(128)
C
C DATA INITIALIZATION
C
DATA ISTART/1/
DATA DELTA/0.03199,0.02685,0.01434,0.01186/
DATA CHI/.00379,.00525,.00983,0.0,.02136,.02664,.01387,.01967/
DATA AVGTA/190.93,130.14,215.42,211.39,158.16/
DATA ABIAS/5*0./
DATA SBIAS1/64*0./
DATA SBIAS2/64*0./
DATA SBIAS3/64*0./
DATA SBIAS4/64*0./
DATA SBIAS5/64*0./
C
C BEGIN EXECUTION
C
IF(ISTART.EQ.0) GO TO 30
ISTART=0
DO 10 IFREQ=1,4
IF(IFREQ.EQ.2) GO TO 10
XFAC=(1.-CHI(1,IFREQ)*CHI(2,IFREQ))*(1.-DELTA(IFREQ))
AVV(IFREQ)=(1.+CHI(1,IFREQ))/XFAC
AHV(IFREQ)=-CHI(1,IFREQ)*(1.+CHI(2,IFREQ))/XFAC
AOV(IFREQ)=(1.-AVV(IFREQ)-AHV(IFREQ))*2.7
AHH(IFREQ)=(1.+CHI(2,IFREQ))/XFAC
AVH(IFREQ)=-CHI(2,IFREQ)*(1.+CHI(1,IFREQ))/XFAC
AOH(IFREQ)=(1.-AHH(IFREQ)-AVH(IFREQ))*2.7
10 CONTINUE
C
DO 20 ICEL=1,64
SBIAS1(ICEL)=1.-SBIAS1(ICEL)/AVGTA(1)
SBIAS2(ICEL)=1.-SBIAS2(ICEL)/AVGTA(2)
SBIAS3(ICEL)=1.-SBIAS3(ICEL)/AVGTA(3)
SBIAS4(ICEL)=1.-SBIAS4(ICEL)/AVGTA(4)
SBIAS5(ICEL)=1.-SBIAS5(ICEL)/AVGTA(5)
20 CONTINUE
C
30 CONTINUE
C

```

```

DO 100 ICEL=1,64
TA19V=TALO(1,ICEL)*SBIAS1(ICEL)-ABIAS(1)
TA19H=TALO(2,ICEL)*SBIAS2(ICEL)-ABIAS(2)
TA22V=TALO(3,ICEL)*SBIAS3(ICEL)-ABIAS(3)
TA37V=TALO(4,ICEL)*SBIAS4(ICEL)-ABIAS(4)
TA37H=TALO(5,ICEL)*SBIAS5(ICEL)-ABIAS(5)
C
TALO(1,ICEL)=AVV(1)*TA19V+AHV(1)*TA19H+AOV(1)
TALO(2,ICEL)=AHH(1)*TA19H+AVH(1)*TA19V+AOH(1)
TALO(3,ICEL)=1.01993*TA22V+1.994
TALO(4,ICEL)=AVV(3)*TA37V+AHV(3)*TA37H+AOV(3)
TALO(5,ICEL)=AHH(3)*TA37H+AVH(3)*TA37V+AOH(3)
100 CONTINUE
C
IF(I85GHZ.EQ.0) RETURN
C
DO 200 ICEL=1,128
TB85V=AVV(4)*ATAHI(1,ICEL)+AHV(4)*ATAHI(2,ICEL)+AOV(4)
TB85H=AHH(4)*ATAHI(2,ICEL)+AVH(4)*ATAHI(1,ICEL)+AOH(4)
ATAHI(1,ICEL)=TB85V
ATAHI(2,ICEL)=TB85H
TB85V=AVV(4)*BTAHI(1,ICEL)+AHV(4)*BTAHI(2,ICEL)+AOV(4)
TB85H=AHH(4)*BTAHI(2,ICEL)+AVH(4)*BTAHI(1,ICEL)+AOH(4)
BTAHI(1,ICEL)=TB85V
BTAHI(2,ICEL)=TB85H
200 CONTINUE
RETURN
END

```

# Report Documentation Page

1. Report No.		2. Government Accession No.		3. Recipient's Catalog No.	
4. Title and Subtitle  FINAL REPORT  PRODUCTION OF SSM/I DATA SETS				5. Report Date  September 1, 1992	
				6. Performing Organization Code	
7. Author(s)  Frank J. Wentz				8. Performing Organization Report No.  RSS Tech. Report 090192	
				10. Work Unit No.	
9. Performing Organization Name and Address Remote Sensing Systems 1101 College Avenue, Suite 220 Santa Rosa, California 95404				11. Contract or Grant No.  NAS8-38075	
				13. Type of Report and Period Covered FINAL 09/01/89 through 09/01/92	
12. Sponsoring Agency Name and Address National Aeronautics and Space Administration Marshall Space Flight Center Huntsville, Alabama				14. Sponsoring Agency Code	
15. Supplementary Notes					
16. Abstract  <p>This Final Report is a summary of the work that was performed under Contract NAS8-38075 between NASA Marshall Space Flight Center and Remote Sensing Systems from September 1989 to September 1992. The primary accomplishment was the delivery of SSM/I data tapes containing sensor and geophysical products. In all, 515 tapes (80 gigabytes) were delivered. These tapes contained the F08 SSM/I data for the period from July 1988 through December 1991 and the F10 SSM/I data for the period from December 1990 through December 1991. For the F08 SSM/I, a data inventory was compiled and an engineering assessment was done. Ephemeris tables for the F08 and F10 spacecrafts were computed. Scientific studies on the oceanic wind vector and water vapor field were published, and color atlases of monthly ocean products were produced. This investigation was part of NASA's WETNET program.</p>					
17. Key Words (Suggested by Author(s))  SSM/I, microwave radiometer, ocean wind, water vapor, remote sensing			18. Distribution Statement  Unclassified-Unlimited		
19. Security Classif. (of this report)  Unclassified		20. Security Classif. (of this page)  Unclassified		21. No. of pages  87	
				22. Price	